DESIGN OF A HIGH-SPEED CYLINDRICAL GRINDING MACHINE

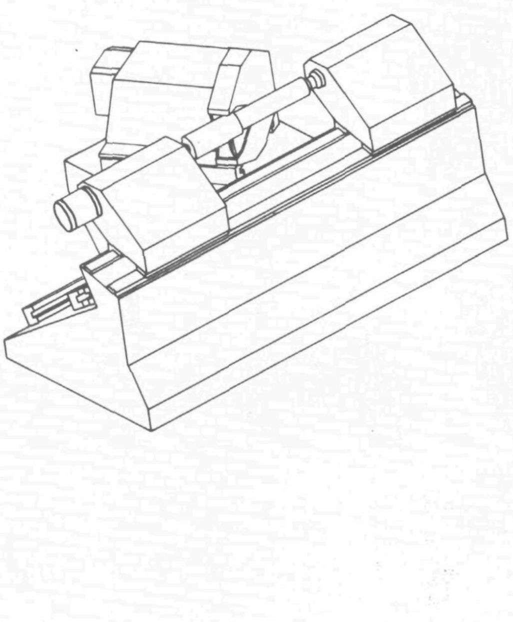

T. STORM

DESIGN OF A HIGH-SPEED CYLINDRICAL GRINDING MACHINE

PROEFONTWERP

TER VERKRIJGING VAN DE GRAAD VAN DOCTOR IN DE TECHNISCHE WETENSCHAPPEN AAN DE TECHNISCHE HOGESCHOOL DELFT, OP GEZAG VAN DE RECTOR MAGNIFICUS PROF. DR. IR. H. VAN BEKKUM, VOOR EEN COMMISSIE, AANGEWEZEN DOOR HET COLLEGE VAN DEKANEN, TE VERDEDIGEN OP DONDERDAG 10 JUNI 1976 TE 16.00 UUR

DOOR

TONNY STORM

werktuigkundig ingenieur

geboren te Ede

Dit proefschrift is goedgekeurd door de promotor
PROF. IR. D. A. A. KOOLEN

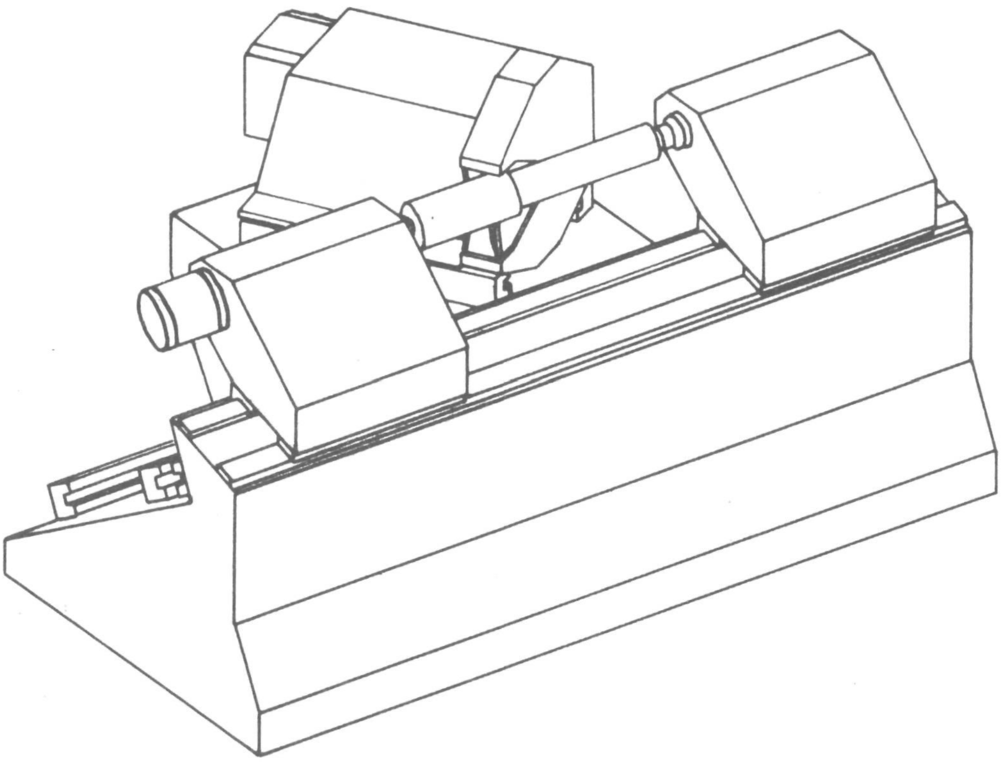

CONTENTS

		Page
List of symbols		1
Summary		4
1.	Introduction	9
2.	Basic starting points for the design	10
	2.1. The product	10
	2.2. The process	10
	2.3. The machine	10
3.	Basic calculations	12
	3.1. Grinding power and forces	12
	3.2. Speeds of grinding wheel and workpiece	13
	3.3. The grinding wheel	17
4.	The wheel head	19
	4.1. The grinding spindle	19
	4.2. The spindle drive	21
5.	The hydraulic motor	22
	5.1. Basic concept	22
	5.2. Geometrical design	27
	5.3. The manufacture	29
	5.4. Conclusion	35
6.	The construction of the machine	36
	6.1. General design	36
	6.2. Deformation of the machine structure	45
	6.2.1. Method of calculation	45
	6.2.2. Execution of the calculations	46
	6.3. Design of the work heads	61
7.	Drive of wheel head, slide and workpiece	62
8.	Apparatus for dressing of the grinding wheel	69
	8.1. Wheel wear and dressing conditions	69
	8.2. Design of the dressing apparatus	71
9.	The control of the grinding machine	73
	9.1. Control of the grinding process	73
	9.2. Control of the grinding wheel position	74
10.	The power supply of the grinding machine	78
11.	Secondary aspects of the design	81
	11.1. Safety	81
	11.1. Coolant-supply	82

		Page
12.	Drawings of the machine	84
13.	Conclusion	105
Appendix A	Deformation of the grinding spindle	106
Appendix B	Calculation of the hydrostatic bearings	109
Appendix C	Contact of rotor circumference	113
Appendix D	Leakage and mechanical losses in the hydraulic motor	114
References		117
Curriculum Vitae		120

LIST OF SYMBOLS

Symbol		Unit
A	area	m^2
a	depth of cut	mm
a	difference of maximum and minimum rotor radius	mm
a	length of spindle part between front bearing and grinding wheel	mm
a_d	infeed of dressing wheel	mm/rev
α	angle between the axes of grinding wheel and workpiece	degree
b	width of the rotors of hydraulic motor	mm
b	length of spindle part between spindle bearings	mm
b	width of bearing gap	mm
b_s	width of grinding wheel	mm
c	stiffness	N/mm
c_w	specific heat	W/kg ^{o}C
D	spindle diameter	mm
d_s	diameter of grinding wheel	mm
d_w	diameter of workpiece	mm
d_{ws}	diameter of work head spindle	mm
ΔT	temperature rise	^{o}C
e	excentricity	mm
ε	efficiency	
η	dynamic viscosity	kg/m.s
F_{dt}	tangential dressing force	N
F'_{dt}	specific tangential dressing force	N/mm
F_{dr}	radial dressing force	N
F'_{dr}	specific radial dressing force	N/mm

Symbol		Unit
F_t	tangential grinding force	N
F_n	normal grinding force	N
f_P	displacement of a point P caused by deformation	mm
ϕ	angle, polar co-ordinate	degree
ϕ	angle between plane of the grinding wheel and the workpiece axis	degree
G	grinding ratio	
γ	angle between radius vector and tangent	degree
h	height of gap	mm
I	moment of inertia	kgm^2
i	transmission ratio	
L_e	effective length of hydrostatic bearing	mm
l_x	length of travel in x-direction	mm
l_y	length of travel in y-direction	mm
M	torque	Nm
M_a	torque related to inertia forces	Nm
M_{dw}	torque at dressing wheel	Nm
M_g	torque related to grinding forces	Nm
m	mass	kg
n	number	
n_{dw}	r.p.m. of dressing wheel	rev./min
n_s	r.p.m. of grinding wheel	rev./min
n_w	r.p.m. of workpiece	rev./min
ω	angular velocity	rad/s
$\dot{\omega}$	angular acceleration	rad/s^2
P	grinding power	kW
P'	specific grinding power	$W/mm^3/s$
P_{dw}	dressing power	kW

Symbol		Unit
P_p	pump power	kW
P_w	friction power	kW
p	pressure	N/m^2
Q	oil flow	m^3/s
R	radius, polar co-ordinate	mm
ρ	density	kg/m^3
s	feed	mm/rev.
t	acceleration time	s
v_a	feed rate	mm/s
v_{dr}	speed of dressing head	mm/s
v_f	infeed rate	mm/s
v_h	relative speed of bearing surfaces	m/s
v_s	peripheral speed of the grinding wheel	m/s
v_w	peripheral speed of the workpiece	m/s
w'	specific wheel wear	$mm^3/mm.s$
z	metal removal rate	mm^3/s
z'	specific metal removal rate	$mm^3/mm.s$

SUMMARY

The thesis describes the design of a high speed cylindrical grinding machine. From research in a number of institutes it appeared that an increase of the wheel speed offers the possibility to obtain a high metal removal rate at a good surface quality and a high geometrical accuracy of the workpiece. Besides the investigations concerning the cut-off grinding process at the University of Delft showed that specific metal removal rates up to 1600 $mm^3/mm.s$ at a wheel speed of 100 m/s can be realized.
Starting from these facts a high speed cylindrical grinding machine is designed capable of machining shafts with a maximum length of 750 mm and a maximum diameter of 250 mm at a metal removal rate of 20.000 mm^3/s and a wheel speed of 150 m/s. The grinding process will be realized according to the figure that shows the relative movements of the grinding wheel and the workpiece.

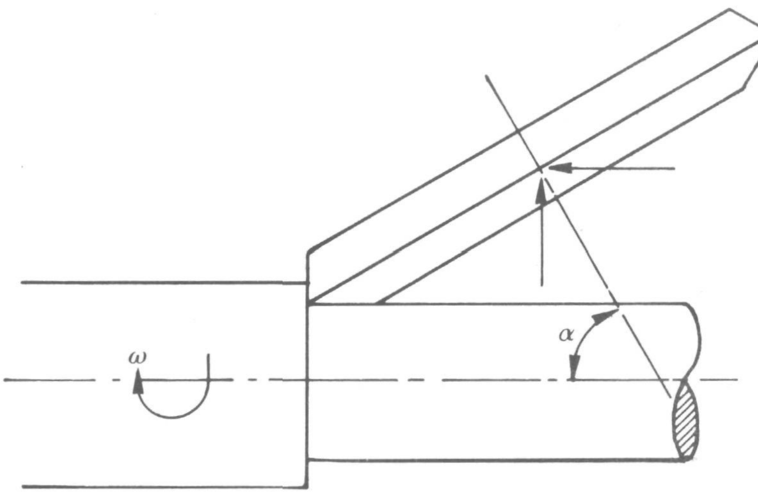

Schematic view of workpiece and grinding wheel.

The first part of the design concerns the drive of the grinding wheel. It is decided to drive the grinding spindle directly without any transmission. This demand leads to the design of a special hydraulic motor with a maximum power of 150 kW at a speed of 10.000 r.p.m.
The second part of the design applies to the machine structure. This structure supports the grinding spindle and the workpiece. The main requirement for the structure concerns the maximum deformation that is allowed with regard to the accuracy of the workpiece. In order to calculate the deformation of the structure a "finite element" program is applied.
The third part is related to the drives of the slide, the wheel head and the workpiece and the control of the machine. The drive motors that are applied are electrical stepping motors, which results in a relative simple control system. This control system achieves in the first place the movements of the grinding wheel relative to the workpiece according to the workpiece geometry. Secondly the control system provides the correct conditions for the grinding process.
Finally some secondary aspects of the design are discussed. These aspects concern in the first place the dressing of the grinding wheel, which will be

realized by means of a diamond wheel. Secondly the safety of the machine in the event of a wheel bursting is considered.
At last the supply of coolant both to the grinding zone and the dressing zone is regarded.
The final design is shown in the drawings that form part of this thesis.

SAMENVATTING

Het proefontwerp heeft betrekking op een rondslijpmachine voor hoge snelheden. Uit onderzoek in een aantal instituten is gebleken dat een verhoging van de slijpsnelheid een grote verspaningscapaciteit mogelijk maakt bij een goede oppervlaktekwaliteit en een grote nauwkeurigheid van de werkstukgeometrie. Bovendien is door onderzoek van het doorslijpproces aan de Technische Hogeschool in Delft aangetoond dat een specifieke verspaningscapaciteit van 1600 $mm^3/mm.s$ bij een slijpsnelheid van 100 m/s gerealiseerd kan worden. Uitgaande van deze feiten wordt een rondslijpmachine ontworpen die in staat is assen met een maximale lengte van 750 mm en een maximale diameter van 250 mm te bewerken bij een verspaningscapaciteit van 20.000 mm^3/s en een slijpsnelheid van 150 m/s. Het slijpproces zal worden gerealiseerd volgens onderstaande figuur, waarin de relatieve bewegingen van de slijpschijf ten opzichte van het werkstuk zijn aangegeven.

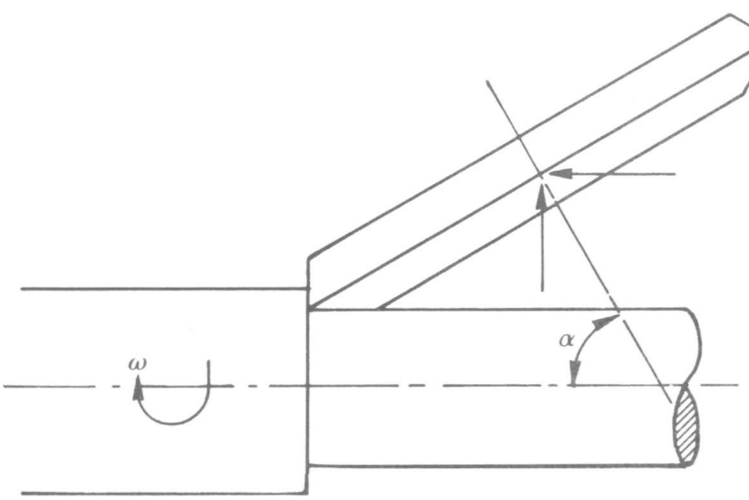

Schematische voorstelling van werkstuk en slijpschijf.

Het eerste deel van het ontwerp betreft de aandrijving van de slijpsteen. De slijpspil zal direkt worden aangedreven zonder overbrenging. Deze eis is aanleiding tot het ontwerp van een speciale hydromotor met een maximum vermogen van 150 kW bij een maximale snelheid van 10.000 omw./min.
Het tweede deel van het ontwerp heeft betrekking op het gestel van de machine. Dit machinegestel vormt de ondersteuning van slijpspil en werkstuk. De voornaamste eis die aan dit deel van de machine wordt gesteld betreft de maximale vervorming ten gevolge van de slijpkrachten die met betrekking tot de nauwkeurigheid van het werkstuk is toegestaan. Voor de berekening van deze vervormingen wordt gebruik gemaakt van de "eindige elementen methode".
Het derde deel wordt gevormd door het ontwerp van de aandrijvingen van de slede, de slijpkop en het werkstuk en de besturing van de machine. De aandrijfmotoren die worden toegepast zijn electrische stappenmotoren, waardoor het besturingssysteem betrekkelijk eenvoudig wordt. Dit besturingssysteem bewerkstelligt in de eerste plaats de bewegingen van de slijpschijf ten opzichte van het werkstuk overeenkomstig de geometrie van het werkstuk. In de tweede plaats worden door het besturingssysteem de juiste procesomstandigheden tot stand gebracht.
Het laatste deel behandelt enkele nevenaspecten van het ontwerp. In de eerste

plaats betreft dit het afdraaien van de slijpschijf, waarvoor een diamantschijf wordt toegepast. Vervolgens wordt aandacht besteed aan de veiligheid van de machine in het geval van een slijpschijfexplosie.
Tenslotte komt de toevoer van koelmiddel, zowel bij het slijpen als bij het afdraaien, aan de orde.
Het ontwerp van de slijpmachine is weergegeven in een aantal tekeningen.

1. INTRODUCTION

Grinding was probably the first metal cutting process in the world. The ability of abrasive grains to remove particles of metal has been used during many centuries and for a long time it was the only possible way to remove metal. Since the use of tool steel, highspeed steel, carbide and aluminium oxyde for metal cutting the application of grinding is mainly restricted to finishing operations and the machining of hard materials. The main reason for this is the fact that the use of the materials mentioned above made it possible to realize an optimal tool geometry and, on account of the large dimensions of the cutting edge, a high metal removal rate. Besides the cutting process using tools of wellknown shape and dimensions is better predictable and also more reliable than the use of a grinding wheel with an unknown number of cutting edges with unknown shapes and unknown cutting conditions.

However, during the last ten years there has been a large increase in research concerning grinding all over the world. One of the main aspects of this research was the effect of an increase of the wheel speed on both the metal removal rate and the surface quality. From this research it appeared that an increase of the wheel speed results in a substantial decrease of the grinding forces and besides in an improvement of the surface quality [1, 2, 3, 4]. This decrease of the cutting forces offered the possibility to raise the metal removal rate to very high values. This way of grinding became known as abrasive machining. The application of abrasive machining or high-speed grinding in industry followed, mainly in mass production like the motor-car and ballbearing industry. In these industries many products are manufactured by forging followed by grinding. The turning process can be eliminated in many cases. At this moment wheel speeds of 80 m/s and even higher are used in industry resulting in a specific metal removal rate of about 50 $mm^3/mm.s$, while in laboratories much higher values have been reached.

Besides the development described above there has been another application of the grinding process that is of great interest, namely cut-off grinding. This process has often been considered as different from other grinding processes, but apart from the wheel width no fundamental distinction can be proved.

Cut-off grinding has been subject of research in many research institutes [5, 6] and also in the laboratory for machine tool design of the University of Technology in Delft, Netherlands. In this laboratory a special cut-off grinding machine has been designed and built [7]. The results of the research carried out on this machine have considerably contributed to the design of the grinding machine described in this thesis. One of the main results concerned the high metal removal rate that was reached on this cut-off grinding machine. At a wheel speed of 100 m/s a specific metal removal rate of 1600 $mm^3/mm.s$ has been realized.

The development described above leads to the conclusion that in the near future grinding will become a process for high-metal removal and will compete with first-operation processes such as turning and milling. This prediction was also part of the outcome of a survey commissioned by the Science Research Council in England [8, 9]. This survey showed besides that it will be necessary to use greater inputs of power than those used at present, thereby leading to the development of more rigid machine structures to accommodate high powers without sacrificing the work surface and geometrical accuracies. Another conclusion of this report is that external cylindrical grinding is expected to be the most important area of grinding. However, the design of a machine capable of realizing an optimal grinding process is a prerequisite. Starting from the above this thesis describes the design of a high-speed cylindrical grinding machine.

2. BASIC STARTING POINTS FOR THE DESIGN

2.1. The product

The design of a machine tool has to be based on the manufacture of a well-defined type of product. If the design concerns a cylindrical grinding machine at least the maximum diameter and the maximum length of the workpieces have to be known. The grinding machine described in this thesis shall be suited to grind workpieces with a maximum diameter of 250 mm and a maximum length of 750 mm. Although this choice is rather arbitrary the area of application has to be of such importance that it justifies the development of a totally new type of grinding machine. In the range of dimensions mentioned above many products can be found. Typical examples are machine tool spindles, shafts of electric motors and gearboxes and so on. Generally these products are manufactured from cylindrical bars or from semi-manufactured products obtained by forging.

2.2. The process

The basic idea for the design is to provide a grinding machine capable of removing metal at a rate comparable with that of modern turning machines. So, if compared with a heavy-duty lathe with a maximum power of about 50 kW, using carbide or aluminium oxyde tool material, the maximum metal removal rate has to be about 20.000 mm^3/s. Just like the choice of the type of product that will be manufactured the determination of the metal removal rate cannot be based on accurate data concerning a well-known production of certain workpieces. In consequence the metal removal rate will be chosen according to the data that may be expected. It has already been assumed that the workpieces that will be machined are mainly shafts of different types. These products have usually in common that metal removal represents an important part of the cost of manufacturing. So, in order to reduce this cost the rate of metal removal should be high. For this reason the maximum metal removal rate shall be 20.000 mm^3/s according to a high production turning machine for the same type of product.
Until now the maximum value of the specific metal removal rate that has been achieved in grinding is about 1600 mm^3/mm.s, while wheelspeeds of 125 m/s have been applied. The fast development in grinding makes it likely that within a few years higher values will be possible. In consequence the design of the grinding machine will be based on a specific metal removal rate of 2000 mm^3/mm.s at a wheelspeed v_s = 150 m/s. This means that under these conditions the effective wheelwidth is 10 mm.

2.3. The machine

Starting from the data concerning both the kind of workpiece and the grinding process it has to be decided in what way the process will be realized. The two major points are the shape of the grinding wheel and the movement of the grinding wheel relative to the workpiece. As mentioned before the width of the wheel is small compared with the length of the workpiece. This means that the grinding wheel has to move both in radial and axial direction of the workpiece. In this way the wheel has to be able to generate at least cylindrical surfaces and planes perpendicular to the center line of the workpiece. So the grinding wheel needs two surfaces touching the workpiece in two straight lines that are perpendicular to each other. This requirement is met by two conical surfaces with axes that coincide and of which the sum of the vertical angles is 180° (see figure 1). The value

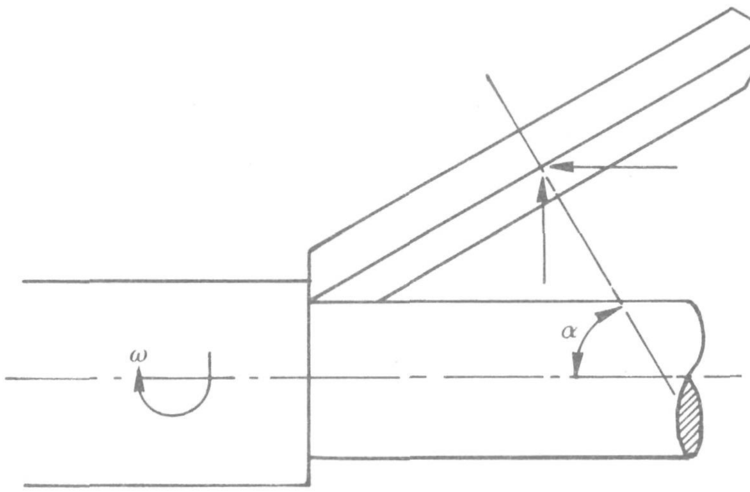

FIGURE 1.

Schematic view of workpiece and grinding wheel.

of the angle α between the axis of the cones and the center line of the workpiece has to be determined, based on the following considerations. Consequent on the high speed of the grinding wheel the internal stress in the wheel is very high. For this reason it is important to avoid an increase of this stress caused by the grinding process. This means that the conditions concerning the grinding process have to be such as to eliminate forces perpendicular to the plane of the grinding wheel. As the stiffness of the wheel in this direction is small the elimination of these forces results besides in a smaller wheel deformation and hence in a higher accuracy of the workpiece. Based on these facts the value of α has to be determined such as to cause the smallest deformation of the workpiece by the grinding forces. As this deformation is mainly determined by that component of the grinding force that is perpendicular to the surface of the workpiece the value of α has to be chosen as near as possible to 90° in order to reduce this force. However, it will appear from the design that it is not possible to realize a value of α greater than about 60°. Another point that is of importance to the design of the grinding machine is the maximum wheel diameter that will be applied. On the one hand there are a number of factors that tend to a small wheel diameter. In the first place the stiffness of the system "grinding wheel - machine - workpiece" increases with a decrease of the wheel diameter. Secondly the kinetic energy of a rotating grinding wheel is smaller, at the same circumferential speed, when using a smaller wheel diameter. This fact and the wheel diameter itself simplify an effective protection against the consequences of a possible explosion of the grinding wheel. On the other hand a large diameter of the wheel results in a longer wheel life. Besides the problems of the design of a proper drive for the grinding wheel at high speeds become more difficult at a smaller diameter. At last it is very important to be sure that a grinding wheel according to the demands can be manufactured. Based on these considerations a maximum of 500 mm shall be applied. A grinding wheel of these dimensions has already been applied in industry at a wheel speed of 125 m/s and this application got the approval of the German D.S.A. The minimum diameter depends on the dimensions of the flanges that hold the grinding wheel and shall be 300 mm. This means that the speed of rotation of the grinding wheel n_s varies from 5730 to 9550 r.p.m.

3. BASIC CALCULATIONS

3.1. Grinding power and forces

It has been mentioned before that cut-off grinding is the only grinding process until now where a specific metal removal rate exceeding 1000 $mm^3/mm.s$ has been realized. As this grinding process and the grinding process that will be applied on the machine that is designed differ substantially from conventional grinding processes, even in the case of so called "high-speed grinding", it may lead to errors if the results of these processes should be extrapolated and applied to the design without further consideration. For this reason primarily the data concerning the cut-off grinding process will be used for the design calculations of the grinding machine. In the laboratory for machine tool design of the University of Technology in Delft an extensive research concerning cut-off grinding has been carried out [7, 10]. From this research and research in other laboratories [5, 6, 11] the data are derived.
At first it is necessary to know the power that is required for a metal removal rate of 20.000 mm^3/s. From figure 2 it appears that at high metal removal rates the specific power P' varies between 6 and 7.5 $W/mm^3/s$ for different materials. The values of the specific power, shown in this figure,

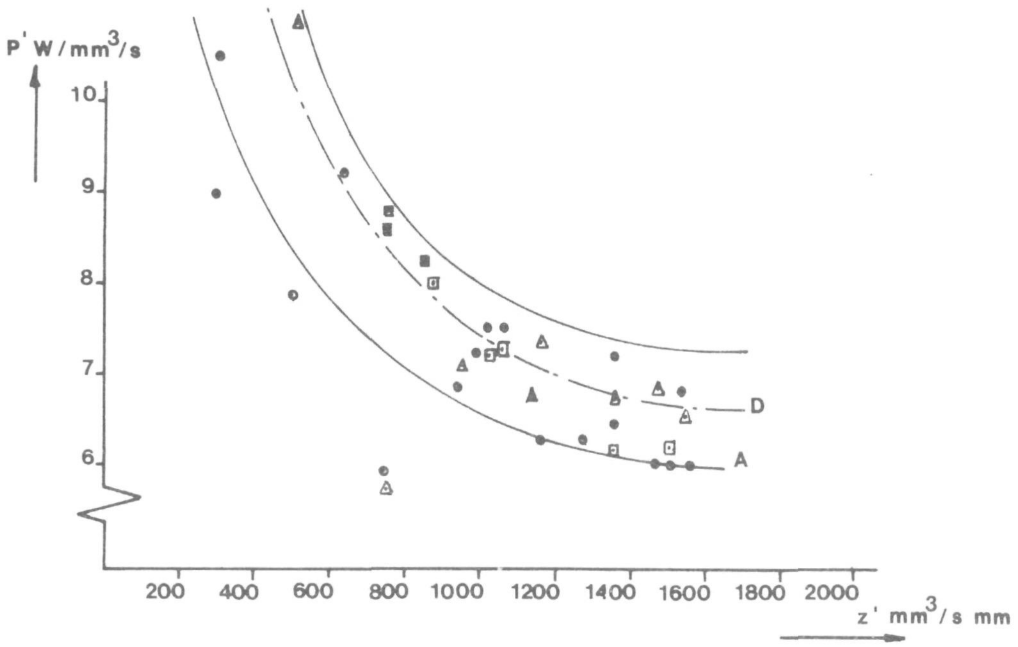

FIGURE 2.

Specific power P' at cut-off grinding.

concern the power input at the grinding spindle. This means that these values include losses due to friction in the spindle bearings and air friction at the grinding wheel surface. As the research concerning the grinding power was carried out at a wheel speed v_s = 100 m/s and specific metal removal rates smaller than 1600 $mm^3/mm.s$ it is necessary to determine what the specific power is expected to be at 150 m/s and a specific metal removal rate of 2000 $mm^3/mm.s$ On the one side the power will increase at higher wheel speeds due to an increase of the friction. On the other side the grinding forces and hence the grinding power decrease at higher wheel speeds as a result of a decrease of the chip thickness at each grain of the wheel. Based on these considerations the specific power P' at a wheel speed v_s = 150 m/s and a specific metal removal of 2000 mm^3/mm.s is assumed to be 7.5 W/mm^3/s at maximum for the materials that will be ground on this machine. In this value only the air friction at the wheel surface is included. As the maximum metal removal rate amounts to 20.000 mm^3/s the maximum power for this process P_{max} = 150 kW. From this value it follows that the maximum grinding force tangential to the wheel circumference

$$F_{t\ max} = \frac{P_{max}}{v_s} = 1000 \text{ N.}$$

From the research mentioned above it appeared that the grinding force perpendicular to the active wheel surface F_n is about three times the force in tangential direction F_t. So $F_{n\ max}$ = 3000 N. In chapter 2.3 it is noticed that the direction of this force is perpendicular to the axis of rotation of the grinding wheel.

3.2. Speeds of grinding wheel and workpiece

The movement of the grinding wheel with regard to the workpiece can be separated in a rotation of the workpiece and a linear movement of the grinding wheel parallel to the center line of the workpiece or a movement of the workpiece parallel to its center line. The ratio of these two speeds determines the direction of the force F_n as will be shown in the following.

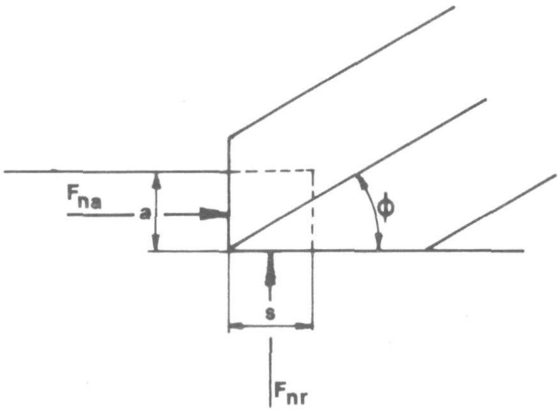

FIGURE 3.

Schematic representation of workpiece and grinding wheel.

From figure 3 it appears that the force F_n is perpendicular to the axis of rotation of the grinding wheel if:

$$F_{na} \cdot \sin\phi = F_{nr} \cdot \cos\phi \qquad (3.1)$$

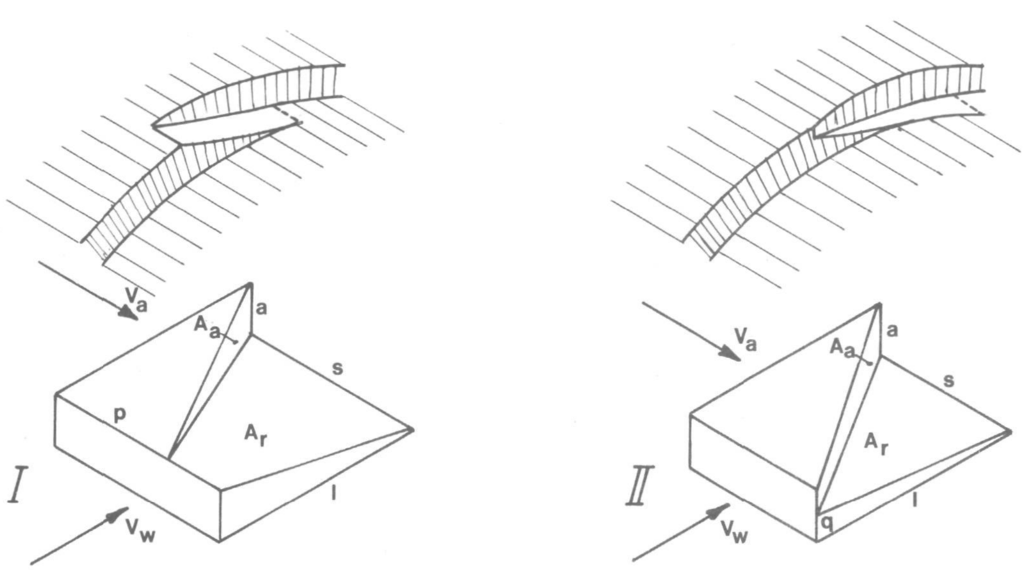

FIGURE 4.

Workpiece, showing the areas of contact of the grinding wheel.

In figure 4 the areas of contact of workpiece and grinding wheel are shown. From this figure it appears that there are two different situations concerning the intersection of the surface of the workpiece and the surface of the grinding wheel. Which situation will appear depends on the dimensions of the workpiece and the grinding wheel and on the relation between the depth of cut a and the feed s. The relation between these data can be calculated as follows: At first it is assumed that the forces perpendicular to the wheel surface are proportional to the metal removal rate achieved by this wheel surface. This means that the equation (3.1) can be written as:

$$z_a \cdot \sin\phi = z_r \cdot \cos\phi \qquad (3.2)$$

In this equation z_a and z_r are the metal removal rates achieved at the areas A_a and A_r. Corresponding to figure 4-I the values of z_a and z_r can be calculated from

$$z_a = 0.5 \cdot a \cdot l \cdot v_a + 0.5 \cdot a \cdot p \cdot v_w \qquad (3.3)$$

$$z_r = (a \cdot s - 0.5 \cdot a \cdot p) \qquad (3.4)$$

In these equations v_a and v_n represent the speed of the grinding wheel parallel to the centerline of the workpiece and the peripheral speed of the workpiece; l and p represent geometrical data of the linearized representation of the areas of contact, on which the equations (3.3) and (3.4) are based. As

$$\frac{v_a}{v_w} = \frac{s}{\pi \cdot d_w}$$

in which d_w is the diameter of the workpiece, the equation (3.2) changes into:

$$a \cdot v_w \left(\frac{0.5 \cdot l \cdot s}{\pi \cdot d_w} + 0.5 \cdot p\right) \cdot tg\phi = a \cdot v_w (s - 0.5 \cdot p)$$

from which:

$$s = \frac{0.5 \cdot p(1 + tg\phi)}{1 - \dfrac{0.5 \cdot l \cdot tg\phi}{\pi \cdot d_w}} \qquad (3.5)$$

As, at the chosen value of $\phi = 30^{o}$, it appears that in all cases the value of p exceeds the value of s, it is not possible that the workpiece and the grinding wheel intersect according to figure 4-I and at the same time the grinding process meets the equation (3.2).
If the intersection of grinding wheel and workpiece corresponds to figure 4-II the metal removal rates z_a and z_r can be calculated from:

$$z_a = (a \cdot l - 0.5 \cdot q \cdot l) \cdot v_a + (a \cdot s - 0.5 \cdot s \cdot q) \cdot v_w \qquad (3.6)$$

$$z_r = 0.5 \cdot q \cdot s \cdot v_w \qquad (3.7)$$

In these equations l and q represent geometrical data of the linearized representation of the areas of contact as shown in figure 4-II. The equations (3.6) and (3.7) are derived from this representation. In the same way as before these equations lead to:

$$a = 0.5 \cdot q \cdot \left(1 + \frac{1}{\frac{l \, tg\phi}{\pi \cdot d_w} + tg\phi}\right) \qquad (3.8)$$

From this equation it appears that at a value of $\phi = 30^{o}$ and a workpiece diameter and a grinding wheel diameter within the limits assumed before the intersection of the workpiece and the grinding wheel corresponds to the representation of figure 4-II. This means that at any value of a there is a value of s at which the forces perpendicular to the plane of the grinding wheel are eliminated. The ratio of a and s depends on the value of a, the diameter of the workpiece and the diameter of the grinding wheel as shown in figure 5.

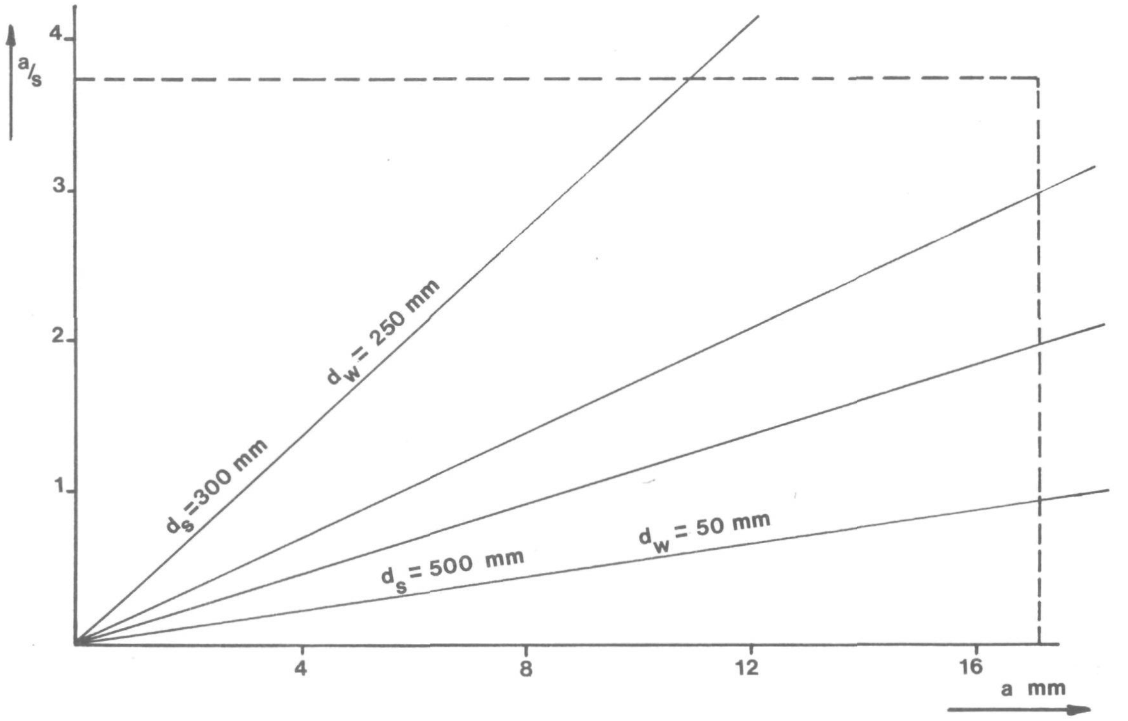

FIGURE 5.

The ratio a/s at various grinding conditions.

From calculations concerning the geometry of the intersection of the grinding wheel and the workpiece it appears that the value of q in figure 4-II can be approximated by

$$q = 0.74 \cdot a$$

Besides, as the value of v_a is very small if compared with the value of v_w, the equations (3.6) and (3.7) can be approximated by

$$z_a = 0.63 \cdot a \cdot s \cdot v_w \qquad (3.9)$$

and

$$z_r = 0.37 \cdot a \cdot s \cdot v_w \qquad (3.10)$$

The values of z_a and z_r can also be calculated from:

$$z_a = a \cdot z'_a \qquad (3.11)$$

and

$$z_r = s \cdot z'_r \qquad (3.12)$$

The maximum value of v_w will be necessary at the maximum metal removal rate and at the same time at the maximum value of z'_a and z'_r. From the ratio of a and s and the ratio of z_a and z_r it appears that z'_a is always less than z'_r. This means that only the value of z'_r can reach its maximum of 2000 $mm^3/mm.s$.
As the maximum metal removal rate z_{max} = 20000 mm^3/s:

$$z_{r\ max} = 0.37 \cdot 20000 = 7400\ mm^3/s$$

and hence:

$$s_{max} = z_r/z'_r = \underline{3.7\ mm}$$

The corresponding value of a depends on the diameter of the workpiece and the diameter of the grinding wheel. At the maximum workpiece diameter of 250 mm and the minimum grinding wheel diameter of 300 mm a = 9.5 mm. At small workpiece diameters it is not possible to reach the maximum metal removal rate as the value of a exceeds half the diameter of the workpiece. So the maximum value of a that will be applied shall be limited to <u>16 mm.</u> The corresponding value of s at a workpiece diameter of 50 mm and a grinding wheel diameter of 500 mm is 1.2 mm. Consequently the metal removal rate decreases proportionally to s.
From the above it follows that at a workpiece diameter of 250 mm and a grinding wheel diameter of 300 mm the equation (3.10) leads to:

$$7400 = 0.37 \cdot 9.5 \cdot 3.7 \cdot v_{w\ max}$$

from which

$$\underline{v_{w\ max} = 569\ mm/s}$$

At a workpiece diameter of 50 mm and a grinding wheel diameter of 500 mm

$$z_r = 7400 \cdot \frac{1.2}{3.7} = 2400\ mm^3/s$$

so:

$$2400 = 0.37 \cdot 16 \cdot 1.2 \cdot v_w$$

from which

$$v_w = 338 \text{ mm/s}$$

Assuming that workpiece diameters smaller than 50 mm will not be taken into consideration the maximum speed of rotation of the workpiece

$$\underline{n_{w\ max} = 130 \text{ r.p.m.}}$$

The minimum value of n_w is determined by the desired speed v_w at the maximum workpiece diameter and the possibility to apply specific metal removal rates smaller than 2000 mm^3/mm.s.
If the minimum value of z' that will be applied is 1000 mm^3/mm.s the speed v_w at a workpiece diameter of 250 mm will be 285 mm/s. So:

$$\underline{n_{w\ min} = 21 \text{ r.p.m.}}$$

From the speed of rotation of the workpiece and the value of s the relative speed of the grinding wheel with regard to the workpiece in axial direction v_a can be calculated. It is obvious that v_a reaches its maximum value at the smallest workpiece diameter that allows the maximum value of s. From figure 5 and the calculations before it follows that this diameter is about 100 mm. This means that

$$v_{a\ max} = \frac{v_{w\ max} \cdot s_{max}}{\pi \cdot 100} = \underline{6.7 \text{ mm/s}}$$

In order to position the grinding wheel with regard to the workpiece in a short time a "rapid travel" speed $\underline{v_{a\ r} = 50 \text{ mm/s}}$ will be realized.
Besides a movement in axial direction will be necessary in order to move the grinding wheel or the workpiece in a direction perpendicular to the center line of the workpiece. Although the grinding process allows an infeed of 16 mm/rev., corresponding with the depth of cut a in the foregoing, it has not much sense to apply such high values. So a maximum infeed rate $v_{f\ max}$ = 5 mm/s has been chosen. The "rapid travel" speed in this direction will be $\underline{v_{f\ r} = 25 \text{ mm/s}}$.

3.3. The grinding wheel

In chapter 2 it has already been assumed that the maximum diameter of the grinding wheel will be 500 mm and the minimum diameter 300 mm. Besides the diameter the width of the grinding wheel is of interest. From figure 6 it can be seen that the width of the grinding wheel can be devided in two parts b_{s1} and b_{s2} that are in relation with the value of a and s. The

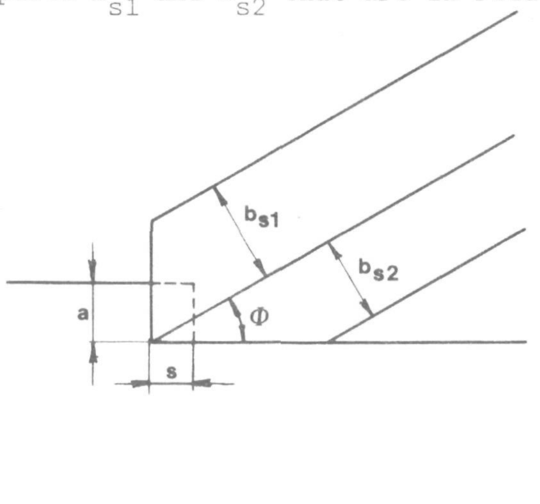

FIGURE 6.

The width of cut at the grinding wheel.

minimum value of b_{s1} has to exceed at least the value $a_{max} \cdot \cos\phi$ and $b_{s2\,min}$ has to be greater than $s_{max} \cdot \sin\phi$. The choice of the wheel width is based on the following considerations. If the value of b_{s2} equals exactly the value of $s_{max} \cdot \sin\phi$ the wear of the grinding wheel will cause an error in the workpiece diameter. There are two possibilities to avoid this error. At first the wheel wear can be eliminated by adapting the position of the grinding wheel in such a way that the distance between the workpiece and the wheel surface is kept constant. It may be necessary to dress the grinding wheel continuously or intermittend in order to restore the geometry of the grinding wheel. Secondly the value of b_{s2} can be chosen two or more times the value of $s_{max} \cdot \sin\phi$. In this case the error caused by the wear of the grinding wheel can be corrected by that part of the grinding wheel that did not participate in the grinding process before. However, after some time the total width of the grinding wheel will be involved in the process and the wear of the grinding wheel will also cause an error in the diameter of the workpiece. In consequence the grinding wheel needs to be dressed and its position has to be corrected. The first method requires a continuous measuring of the workpiece diameter in order to obtain a reasonable accuracy. The second method, however, results in an increase of the wheel width and hence an increase of the damage that can be caused by an explosion of the grinding wheel. Based on these considerations the following values are chosen: b_{s1} = 14 mm and b_{s2} = 6 mm. So the total wheel width $\underline{b_s = 20\ \text{mm}}$.

4. THE WHEEL HEAD

The central part of the grinding machine is the wheel head comprising the grinding wheel, the spindle, the bearings and the drive. From the foregoing the dimensions of the grinding wheel, the required speeds and power and the forces at the wheel circumference are known. The first point to determine is in what way the grinding wheel, the grinding spindle and the bearings will be set up. It is most obvious to mount the grinding wheel at the end of a rotating spindle and to arrange the drive at the other end of the spindle. Other solutions, such as the application of bearings at both sides of the grinding wheel or a fixed spindle and a bearing in the center of the grinding wheel are not considered because they do not allow a practical and fast change of the grinding wheel and besides the space between the grinding wheel and the workpiece is too small to accommodate any bearing construction. Both the design of the grinding spindle and the design of the spindle drive will be discussed in the following.

4.1. The grinding spindle

The most important factor that determines the design of the grinding spindle concerns the deformation, caused by the grinding forces, that is allowable with regard to the workpiece accuracy. It is assumed that the error in the diameter of the workpiece caused by the deformation of the grinding machine, including the spindle and the bearings, shall not exceed a value of 0.025 mm at the maximum grinding forces. This means that at an average workpiece diameter of 125 mm and an average length of 500 mm the error in the diameter of the workpiece, including the deformation of the workpiece itself, corresponds to the tolerance according to an ISO-tolerance quality 6. In this consideration the radial deformation of the grinding wheel is not taken into account. This deformation and the errors in the positioning of the workpiece with regard to the grinding wheel may result in the possibility to reach an ISO-tolerance quality 7 at maximum grinding power, with the exception of small workpiece diameters. As it is not possible to determine an optimal distribution of the deformations for all the machine parts it is assumed that the deformation of the grinding spindle and the spindle bearings shall not cause an error in the diameter of the workpiece that exceeds 0.01 mm. Besides the error in axial direction of the workpiece shall be smaller than 0.01 mm. Starting from the above it is necessary to determine what factors are of importance with regard to the deformation of the grinding spindle. In the first place the forces that cause a deformation that is important with regard to the workpiece accuracy have to be known. In figure 7 the grinding spindle is

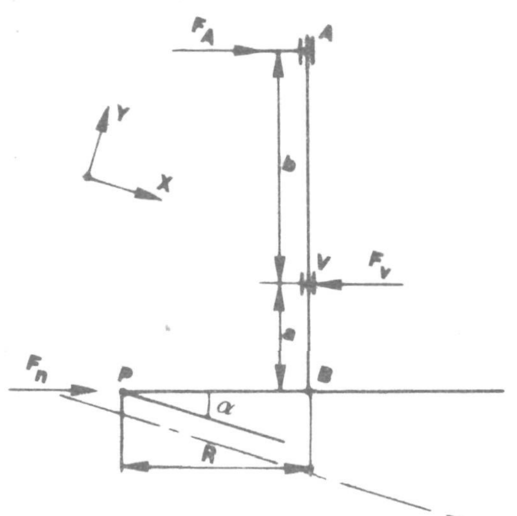

FIGURE 7.

Schematic representation of the grinding spindle.

drawn schematically. From this figure it appears that only the deformations in x- and y-direction have an influence on the workpiece accuracy. A deformation in z-direction has only a negligible influence on the dimensions of the workpiece. This means that only the force F_n has to be taken into account for the calculations of the spindle data. The second important factor is the grinding spindle itself. The deformations depend on the diameter of the spindle D, the distance of the bearings b and the point of application of the force F_n, determined by the distance a from the front bearing to the center of the grinding wheel. At last the deformation of the spindle bearings forms part of the total deformation. In order to know this deformation it is necessary to choose the type of bearings that will be applied. It follows from a rough calculation that the application of ball- or roller bearings is not possible because of the high speed of the spindle. So the only solution is to apply hydrodynamic or hydrostatic bearings. As the thickness of the oil film in hydrodynamic bearings at the desired stiffness of the bearings is very small the generation of heat in the bearings may cause severe problems. For this reason hydrostatic bearings will be applied, using one pump for each pocket, in order to reduce the heat generation as much as possible.

Starting from the above the design data both for the spindle and the bearings will be calculated. The main requirement that has to be met concerns the maximum deformation of the spindle and the bearings as a result of the normal grinding force F_n. This requirement means that in the point P of the grinding wheel (see figure 7) the displacement in y-direction f_y caused by the maximum force $F_{n\ max}$ is not allowed to exceed a value of 5 µm. At the same time the displacement in x-direction f_x has to be smaller than 10 µm. Besides this requirement there are some other factors that are of interest for the design of the spindle. At first the diameter of the spindle determines not only the deformation of the spindle but also the heat generation in the bearings. Secondly the position of the bearings relative to the spindle has a great influence on the stiffness of the total system. At last the demands for maximum stiffness of the bearing and minimum heat generation are contradictory. It is obvious that it is not possible to design a grinding spindle that meets all the demands mentioned above. For this reason a choice will be made based on a calculation of the influence of the various parameters on the stiffness of the spindle, the temperature rise in the bearings and the power needed for the oil supply to the bearings. At first it is assumed that the temperature rise in the bearings shall not exceed 15° C. At this value cooling can be realized without expensive and complicated cooling systems. Secondly the design of the wheel head does not allow a distance between the centers of the grinding wheel and the front bearing smaller than 100 mm. It appears that at a stiffness of the front bearing $C_V = 15 \cdot 10^5$ N/mm, a stiffness of the rear bearing $C_A = 7.5 \cdot 10^5$ N/mm, a spindle diameter D = 120 mm and a distance between the bearings b = 250 to 325 mm the deformation of the spindle does not exceed the values mentioned before. The calculations on which these values are based are written down in Appendix A. These calculations are rather simplified, as the exact geometrical data of the spindle are not known at this stage. When these data are known a more precise calculation will be carried out. In Appendix B the calculation of the data for the hydrostatic bearings is carried out. Besides the data mentioned before the design is based on the following considerations. At first the minimum value of the oil viscosity is determined by the fact that standard hydraulic components will be applied. This means that the oil viscosity is at least 5 cSt. Secondly the total area of the oil film is kept as small as possible in order to reduce the friction losses. At last the length of the front bearing is mainly determined by the demand to reduce the distance between the centers of the grinding wheel and the front bearing. The main results from this calculation are as follows:

	Front bearing	Rear bearing
Bearing diameter	$D_v = 120$ mm	$D_A = 80$ mm
Oilfilm thickness	$h_o = 30 \cdot 10^{-6}$ mm	$h_o = 30 \cdot 10^{-6}$ mm
Bearing length	$Le_v = 90$ mm	$Le_A = 80$ mm
Total oil flow	$Q_v = 16 \cdot 10^{-5}\ m^3/s$	$Q_A = 12 \cdot 10^{-5}\ m^3/s$
Oil pressure	$P_v = 16.4 \cdot 10^5\ N/m^2$	$P_A = 18.5 \cdot 10^5\ N/m^2$

The geometrical data concerning the detailed design of the bearings are described in Appendix B.

4.2. The spindle drive

From chapter 3.1 it appears that the drive of the grinding wheel has to meet the following requirements. At first the power needed for the grinding process has to be 150 kW over a speed range from 5730 to 9550 r.p.m. This means that the maximum torque at the grinding spindle comes to 250 Nm. Secondly the speed of the spindle has to be controlled continuously in order to keep the speed at the wheel circumference at a constant value of 150 m/s. The most common way to drive machine tool spindles is the use of electric motors in many cases together with mechanical drives. An important disadvantage of these drives is the fact that both the weight and the dimensions are of such a kind that practical application in this case is almost impossible. The only way to keep the dimensions of the drive within acceptable limits is the application of a hydraulic drive, as the ratio of power to weight is much higher than ever can be obtained at electric motors. Looking at the hydraulic motors that are available it appears that it is not possible to get a hydraulic motor with a power of 150 kW and a maximum speed of 9550 r.p.m. This would mean that it will be necessary to apply a mechanical transmission between the motor and the grinding spindle. This mechanical transmission, however, presents severe difficulties. At first the transmission causes a static load on the spindle and hence an undesirable deformation. Another objection is the fact that it is very difficult to avoid vibrations when using mechanical transmissions at high speeds. These vibrations cause a disturbance of the surface quality of the workpiece and in some cases inadmissible forces in the grinding wheel. Based on these considerations it has been decided to design a new hydraulic motor that is suited to drive the grinding spindle directly at the required speed and the required power. The design of this hydraulic motor will be described in the following chapter.

5. THE HYDRAULIC MOTOR

5.1. Basic concept

It is obvious that the principle of the motor has to be based on the method of positive-displacement, as a fixed relation between speed and flow rate, independent of load, is essential for the drive. Starting from this it has to be determined in what way the displacement of oil from inlet to outlet will be transformed in a rotation of the shaft of the motor. At first reciprocating pistons or even vanes should be avoided. At the high speeds that are applied these movements may cause problems as a result of high inertia-forces or may cause inadmissable vibrations. This means that only rotating parts should be used, preferably at a constant speed of rotation. In order to achieve a rotary movement of the shaft of the motor as a result of a displacement of a certain oil-volume there has to be at least one chamber of which the volume changes as a result of a rotation of the motorshaft. One possibility to realize this change of volume is to apply one rotor that rotates on an axis that is also rotating, in a non-cylindrical housing. On this application the well-known Wankel-combustion-engine is based. Because of the complexity and the difficulties concerning the balancing of the rotor this solution is not considered. The other possibility is to use at least two non-cylindrical rotors, each of which is rotating in a cylindrical boring, in such a way that the external surfaces of the rotors together with the internal surfaces of the housing form at least two chambers of which the volume changes as a result of a rotation of the rotors. The design of the motor will be based on this solution. Figure 8 shows a

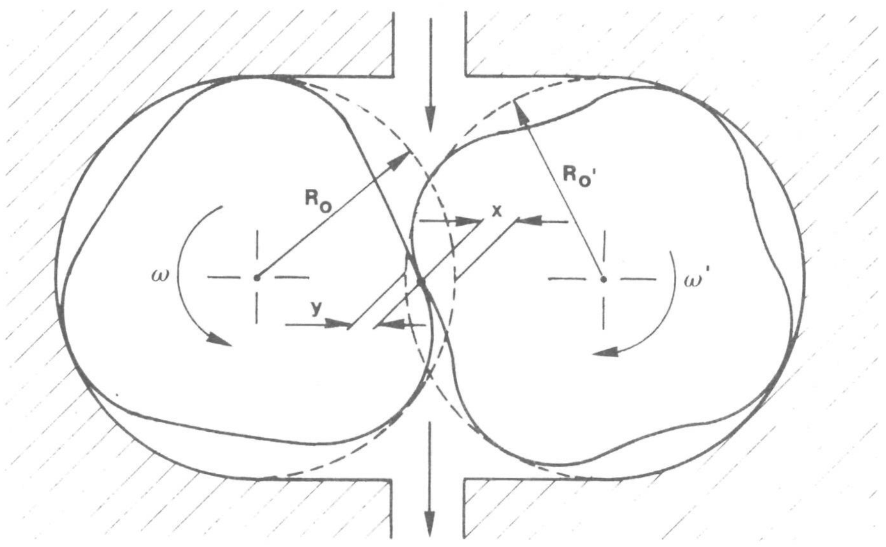

FIGURE 8.

Schematic representation of a hydraulic motor with two rotors.

cross-section of this system. Both rotors are supposed to be disc-shaped and to rotate between two planes perpendicular to the axes of rotation of the rotors. From the figure it appears that the rotors separate the inlet-chamber from the outlet-chamber. This means that the circumference of each rotor has to touch the cylindrical boring of the housing in which it is rotating at least in one place. Besides the circumferences of the rotors

have to touch each other continuously. These requirements and the demand that there has to be a linear relationship between the change of the volume of the inlet- and outlet chamber and the rotation of the rotors determine the shape of the rotors. It appears to be very complicated to translate these requirements into mathematical relations and to derive from these relations the correct shape of the rotors. For this reason a rotor shape will be chosen and calculations will be carried out in order to check if the requirements mentioned above can be met.
The shape of the rotor can be described by

$$R = R_o - x \tag{5.1}$$

where R is the radius of the rotor, R_o the maximum value of R and x a function of the angle ϕ as shown in figure 8. If a second rotor is suited to act together with this rotor, according to the requirements described before, and if the shape of this rotor meets the equation

$$R' = R_o' - y \tag{5.2}$$

it is obvious that there has to be a relation between x and y in those points where the rotor circumferences touch each other. If it is assumed that these points lie in a plane through the axes of the rotors, the sum of x and y has to be constant. The first demand for the motor concerns the relation between the speed and the oil flow of the motor. This relation has to be linear, which means that at constant speeds of rotation ω and ω' of the rotors the oil flow Q has to be constant. From figure 8 the following equation can be derived:

$$Q = \omega \cdot b(R_o - \tfrac{1}{2} \cdot x) \cdot x + \omega' \cdot b(R_o' - \tfrac{1}{2} \cdot y) \cdot y \tag{5.3}$$

where b is the width of the rotors.
As the sum of x and y equals a constant value a, this equation can be written as follows:

$$(\omega \cdot R_o - \omega' \cdot R_o + \omega' \cdot a) \cdot x - \tfrac{1}{2} (\omega + \omega') \cdot x^2 = \text{constant} \tag{5.4}$$

As the above equation is not true for each value of x the demands for the motor cannot be met by this system. For this reason a system with two inlet- respectively two outlet chambers of which the total oil flow is constant at constant rotor speed will be considered. This system can be realized by using three rotors, one rotor being the central rotor acting together with two identical secondary rotors.

In figure 9 a system with three rotors is shown. As the value of R in the relation between the polar co-ordinates of the rotorcircumference has to vary from

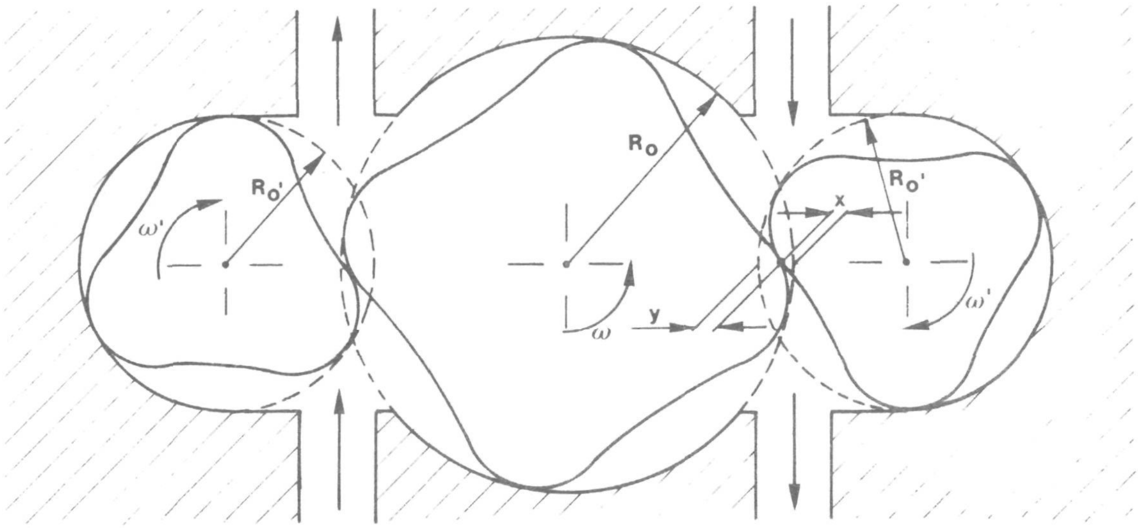

FIGURE 9.

Hydraulic motor with three rotors.

a minimum to a maximum it is obvious to choose a sinusoidal variation. The most simple relation is represented by:

$$R = R_o - a \sin^2 (n \cdot \phi) \qquad (5.5)$$

If the circumference of the central rotor meets this equation the secondary rotors have to meet the following relations:

$$R' = R_o' - a \cdot \cos^2 (n' \cdot \phi') \qquad (5.6)$$

and:

$$R'' = R_o' - a \cdot \cos^2 (n' \cdot \phi'') \qquad (5.7)$$

If the secondary rotors touch the central rotor in lines at the angles ϕ and $\phi + \alpha$ the position of the lines of contact on the secondary rotors is determined by an angle ϕ' that equals $\frac{n}{n'} \cdot \phi$ and an angle $\phi'' = \frac{n}{n'} \cdot (\phi+\alpha)$.
In this case it is also assumed that the lines of contact lie in the planes through the axes of each two rotors that act together. If the oil flow through the motor is calculated, based on a value of

$$\alpha = \frac{\pi}{2n} + i \cdot \frac{2\pi}{n}$$

where i may equal any whole number:

$$\begin{aligned} Q = {} & \omega \cdot b(R_o - \tfrac{1}{2} \cdot a \cdot \cos^2(n \cdot \phi)) \cdot a \cdot \cos^2(n \cdot \phi) + \\ & \omega . b(R_o - \tfrac{1}{2} \cdot a \cdot \sin^2(n \cdot \phi)) \cdot a \cdot \sin^2(n \cdot \phi) + \\ & \omega' \cdot b(Ro' - \tfrac{1}{2} a \cdot \cos^2(n' \cdot \phi')) \cdot a \cdot \cos^2(n' \cdot \phi') + \\ & \omega' \cdot b(Ro' - \tfrac{1}{2} a \cdot \sin^2(n' \cdot \phi')) \cdot a \cdot \sin^2(n' \cdot \phi') \end{aligned}$$

at constant rotor speeds ω and ω', or:

$$Q = b\cdot(\omega\cdot a\cdot R_o+\omega'\cdot a\cdot R_o'-\tfrac{1}{2}\cdot\omega\cdot a^2\cdot\cos^4(n\cdot\phi)$$
$$-\tfrac{1}{2}\cdot\omega\cdot a^2\cdot\sin^4(n\cdot\phi)-\tfrac{1}{2}\cdot\omega'\cdot a^2\cdot\cos^4(n'\cdot\phi')$$
$$-\tfrac{1}{2}\cdot\omega'\cdot a^2\cdot\sin^4(n'\cdot\phi')) \qquad (5.8)$$

From this equation it appears that the oil flow Q is not constant. However, the system with three rotors offers the possibility to correct the shape of the rotors in such a way that a constant oil flow is obtained. In the first place it is possible to choose an other value of α, but in order to avoid a restriction of the oil flow to the rotors it is preferable to choose a value of $\alpha=\pi$. This means that the axes of all three rotors lie in one plane. The second solution is to apply a correction x to the radius R and a correction x' to the radii R' and R'' as shown in the following equations:

$$R = R_o-a\cdot\sin^2(n\cdot\phi)-x$$
$$R' = R_o'-a\cdot\cos^2(n'\cdot\phi')+x'$$
$$R'' = R_o'-a\cdot\cos^2(n'\cdot\phi'')+x'$$

If the equation 5.8 is changed according to the relations above the demand for a constant oil flow Q leads to:

$$x = \frac{a}{2}\cdot(\surd(1+\sin^2(2\cdot n\cdot\phi))-1)$$

and:

$$x' = \frac{a}{2}\cdot(\surd(1+\sin^2(2\cdot n'\cdot\phi'))+1)$$

and the condition:

$$\omega\cdot R_o=\omega'\cdot(R_o'+a)$$

This last condition means that the difference of the circumferential speeds of the rotors is very small. The equations 5.5, 5.6 and 5.7 change into:

$$R = R_o-\frac{a}{2}\cdot(2\cdot\sin^2(n\cdot\phi)+\surd(1+\sin^2(2\cdot n\cdot\phi))-1) \qquad (5.9)$$
$$R' = R_o'-\frac{a}{2}\cdot(2\cdot\cos^2(n'\cdot\phi')-\surd(1+\sin^2(2\cdot n'\cdot\phi'))-1) \qquad (5.10)$$
$$R'' = R_o'-\frac{a}{2}\cdot(2\cdot\cos^2(n'\cdot\phi'')-\surd(1+\sin^2(2\cdot n'\cdot\phi''))-1) \qquad (5.11)$$

The oil flow through the motor can be expressed by the following equation:

$$Q = \omega\cdot b(R_o\cdot a-\frac{a^2}{2}) + \omega'\cdot b(R_o'\cdot a+\frac{a^2}{2}) \qquad (5.12)$$

The second demand for the motor concerns the fact that the rotor circumferences have to touch each other. This means that the tangent planes in the line of contact have to coïncide. In figure 10 the circumferences of two rotors are shown. In two corresponding points P and P' the angles γ and γ' between the tangents in these points and the radii OP and O'P' have to be identical.

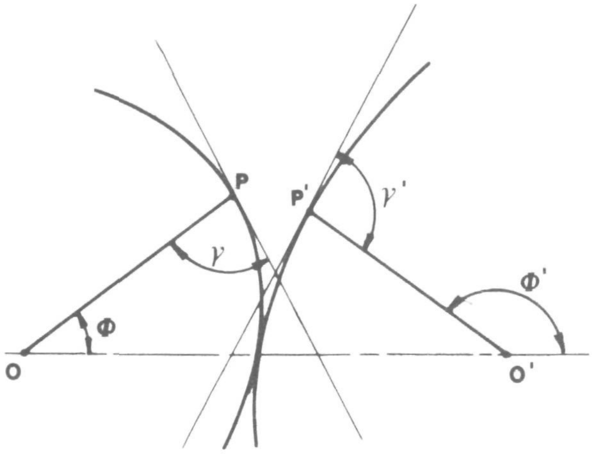

FIGURE 10.

Tangent lines in corresponding points of the rotor circumferences.

As:

$$tg\gamma = \frac{R}{dR/d\phi} = \frac{R_o - \frac{a}{2}\cdot(2\cdot\sin^2(n\cdot\phi) + \surd(1+\sin^2(2\cdot n\cdot\phi))-1)}{-\frac{a}{2}(4\cdot\sin(n\cdot\phi)\cdot n\cdot\cos(n\cdot\phi) + \frac{2\sin(n\cdot\phi)\cdot n\cdot\cos(n\cdot\phi)}{2(1+\sin2(2\cdot n\cdot\phi))})}$$

and:

$$tg\gamma' = -\frac{R'}{dR'/d\phi'} = \frac{R_o' - \frac{a}{2}\cdot(2\cdot\cos^2(n'\cdot\phi') - \surd(1+\sin^2(2\cdot n'\cdot\phi'))'-1}{-\frac{a}{2}(4\cdot\cos(n'\cdot\phi')\cdot n'\cdot\sin(n'\cdot\phi') + \frac{2\cdot\sin.(n'\cdot\phi')\cdot n\cdot\cos(n'\cdot\phi')}{2(1+\sin2(2\cdot n'\cdot\phi'))})}$$

it appears that this condition is not met. However, by choosing the ratio of R_o and n equal to the ratio of R_o'+a and n' the difference between γ and γ' becomes very small, especially at values of a that are small compared with the value of R_o and R_o'. In the calculations concerning the final design of the motor, in appendix C, is shown that an increase of the distance between the rotor axes of only 0.003 mm is sufficient to provide a clearance between the rotor circumferences. Manufacturing tolerances make it necessary to apply an increase of the distance between the rotor axes that is at least 0.01 mm. So practically the rotor circumferences touch each other continuously if the conditions mentioned above are met.

At last it is necessary that the rotor circumferences touch the cylindrical borings in which they are rotating. From figure 9 it appears that the central rotor has to touch the boring at least in two places, while the secondary rotors have to touch the boring at least in one place. In the lines of contact of the rotorcircumferences and the borings the value of $n\cdot\phi$ respectively $n'\cdot\phi'$, respectively $n'\cdot\phi''$ equals π or a multiple of π. In these lines the value of γ respectively γ' and γ'' equals $\frac{\pi}{2}$, so the tangent planes to the rotor circumferences and to the cylindrical borings coincide. From the above it appears that the minimum value of n is 1.5, resulting in three lines on the rotor circumference where the radius R shows a maximum value. In two of these lines the rotor circumference touches the boring of the housing. The minimum value of n' equals 1. It is decided to choose these values for the rotors of the motor and that because of the following. In order to keep the value of $n\cdot\phi$ equal to $n'\cdot\phi'$ and equal to $n'\cdot\phi''-n\cdot\alpha$ it is necessary to use an accurate gear transmission as the shape of the rotors, even at high values of n and n', is not suited for this purpose. As the influence of errors in the gears becomes smaller at small values of n, respectively n', it is advisable to choose these values as small as possible. Even in this case the gears have to be very accurate. The final design of the motor is schematically drawn in figure 11.

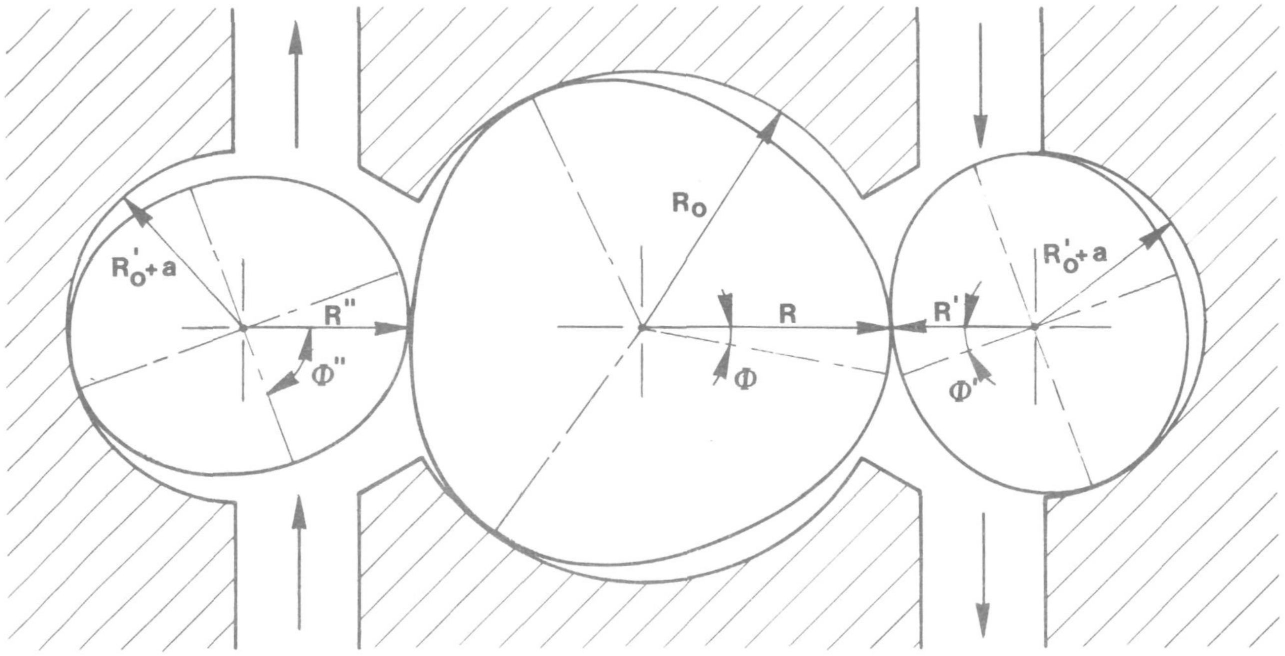

FIGURE 11.

Schematic representation of the hydraulic motor.

This figure shows that, as there is always a difference in the pressure in the inlet chambers and the outlet chambers, this pressure difference results in varying forces perpendicular to the rotor axes. In order to balance these forces on both sides of the main rotors a system of compensating rotors is arranged. These rotors have the same shape as the main rotors and are mounted in the same position as the main rotors. Only the value of a in the relations 5.9, 5.10 and 5.11 is smaller. Besides the width of these rotors is half the width of the main rotors. If the inlet and outlet chambers have positions opposite to that of the main rotors, the forces applied to these rotors make balance with the forces applied to the main rotors. Based on the design described above the calculations concerning the geometry of the motor will be carried out, according to the demands calculated before.

5.2. Geometrical design

The basic data for the design of the motor are the values of the torque and the speed at which this torque has to be realized. From the chapter 3 it follows that the maximum power at the grinding wheel P_{max} has to be 150 kW, at a speed range from 5730 to 9550 r.p.m. Consequently the maximum torque at the grinding wheel M_{max} has to be 250 Nm at a speed of 5730 r.p.m. Similar to the derivation of the equation 5.12 the torque at the hydraulic motor can be expressed by:

$$M = p\cdot b\cdot(R_o\cdot a-\frac{a^2}{2}) + \frac{\omega'}{\omega}\cdot p\cdot b(R_o'\cdot a+\frac{a^2}{2}) \qquad (5.13)$$

where p is the pressure of the oil. As $\phi' = \frac{n}{n'}\cdot\phi$ the same ratio applies to ω and ω', so $\frac{\omega'}{\omega} = \frac{n}{n'} = 1.5$.

In the first place it is necessary to determine the maximum value of the pressure p. It is obvious that at high values of p the dimensions of the motor, mainly determined by R_o, R_o' and b can be small. Although a high pressure results in a higher leakage, the leakage gaps are smaller at smaller dimensions of the motor. So it is decided to apply the maximum pressure at which standard hydraulic components, like pumps and valves, can be used. This pressure is at this moment 35.10^6 N/m^2.

It is clear that a certain part of the power that is needed for the drive gets lost by both leakage of oil in the motor and friction in the motor and the bearings of the spindle. As the real values of both the volumetric efficiency of the motor and the total mechanical efficiency of the spindle drive are not known at this stage it is assumed that the mechanical losses at a speed of 5730 r.p.m. are 10 per cent of the power supplied at maximum pressure and that the volumetric efficiency at these conditions comes to 95 per cent. So the maximum torque that is applied by the oil pressure on the rotors:

$$M_{r\ max} = \frac{10}{9}\cdot M_{max} = 278\ \text{Nm}$$

As $\omega\cdot R_o = \omega'\cdot(R_o'+a)$, the equation 5.13 changes into:

$$M_r = p\cdot b\cdot a(2\cdot R_o-1.25a) \qquad (5.14)$$

This equation shows that it is possible to choose different values of b, a and R_o that lead to the torque that is required for the motor. However, in the first place a value of a that is small compared with the value of R_o reduces the difference of the circumferential speeds of the rotors. Secondly a small value of R_o makes it impossible to create a supply opening of satisfactory dimensions. At last the value of a cannot be too small, as this may lead to undesired hydrodynamic effects in the oil gap between the rotor circumference and the housing. Based on these considerations the values of a, R_o and b will be chosen.

As described before a system of compensating rotors will be applied in order to balance the hydrostatic forces on the rotor axes. The value of a for these rotors will be a_c = 1 mm while the value of a for the main rotors will be a_m = 4 mm. As the center distance of the main rotors has to be the same as the center distance of the compensating rotors:

$$R_{om} + R'_{om} = R_{oc} + R'_{oc}$$

The values of R_o and R_o' are chosen as follows:

R_{om} = 39.0 mm	$R_{o'm}$ = 22 mm
R_{oc} = 37.2 mm	$R_{o'c}$ = 23.8 mm

The above results in the following equation:

$$M_r = p\cdot b\cdot\{2(R_{om}\cdot a_m - R_{oc}\cdot a_c)-1.25\cdot(a^2_m-a^2_c)\}$$

or:

$$M_r = 218.85\cdot p\cdot b$$

As $p_{max} = 35.10^6 N/m^2$ and $Mr_{max} = 278$ Nm:

$$\underline{b = 36 \text{ mm}}$$

Starting from the dimensions of the rotors the gear transmission between the three rotor shafts can be calculated. The data that are prescribed by the dimensions of the rotors are the center distance of the gears and the ratio of the transmission. If a hardened steel with a tensile strength of at least 750 N/mm^2 and a Brinell hardness greater than 5000 N/mm^2 is used a module of 1.25 and a width of 16 mm meet the demands both with regard to the bending stress in the teeth and the normal pressure on the face of the teeth. Finally it is necessary to apply bearings to support the rotor shafts. As the forces on the rotor shafts only consist of the forces caused by the gear transmission it is clear that the bearing forces are very low. This means that the dimensions of the bearings are mainly determined by the geometry of the other parts of the motor, like the rotor shafts and the gears. The choice of the bearing type is determined by the properties at high speeds and the accuracy that can be realized. For this reason ball-bearings will be applied. In order to reduce the play of the bearings two bearings are mounted and a small preload is applied. In the drawing 1 the final design of the motor is shown. From this drawing it can be seen that the motor-housing is composed of nine parallel plates that are held together by accurate bars that also locate the position of each plate very accurately. The plates 3, 5 and 7 contain the borings in which the rotors revolve, while the plates 4 and 6 separate the compensating rotor systems from the main rotor system. In order to prevent any unbalance in the rotating parts of the motor no fixing arrangements like splined shafts, keys or screw thread are applied. Both the rotors and the gears are mounted on the shafts by means of glueing. The type of glue that is used is an anaerobic product that hardens in very small gaps at the absence of air. This way of mounting parts together reduces the cost of manufacturing considerably.

5.3. The manufacture

It is clear that the rotors are the parts that are most complicated with regard to the manufacture. There are two possibilities to obtain the correct shape of the rotor circumference. In the first place the rotors may be machined on a numerically controlled milling machine, either with a so called x-y control or a R-ϕ control. However, there are very few machines available with sufficient accuracy. A second method is to make use of the typical shape of the rotors. As derived before the shape of the rotor is determined by

$$R = R_o - \frac{a}{2} (2\cdot\sin^2(n\cdot\phi) + \sqrt{(1+\sin^2(2\cdot n\cdot\phi))}-1)$$

This equation can be written as follows:

$$R = R_o + \frac{a}{2} \cdot \cos(2\cdot n\cdot\phi) - \frac{a}{2} \cdot \sqrt{(2-\cos^2(2\cdot n\cdot\phi)} \qquad (5.15)$$

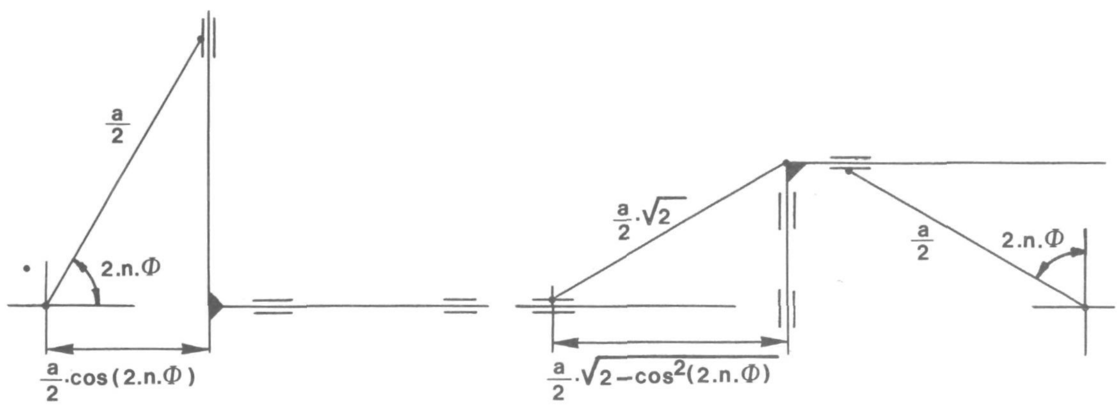

FIGURE 12.

Mechanisms that generate the shape of the rotors.

The parts of the equation 5.15 that depend on the value of ϕ can be generated by the mechanisms that are shown in figure 12. If these mechanisms are connected with the table drive of a milling machine it is possible to machine the rotors with a high accuracy. However, this system only effects the position of the center of the cutter relative to the workpiece according to the equation 5.15. So a correction has to be carried out in order to obtain the correct shape of the rotor. The way in which this correction is effected is shown in figure 13. In each point of the circumference of the rotor the tangent to the cutter has to coincide with the tangent to the rotor circumference. This demand can be met by a rotation of the rotor on the point in question that equals $\frac{\pi}{2} - \gamma$, where γ represents the angle between the radius vector and the tangent in that point. The value of this angle follows from:

$$tg(\frac{\pi}{2} - \gamma) = - \frac{dR/d\phi}{R} .$$

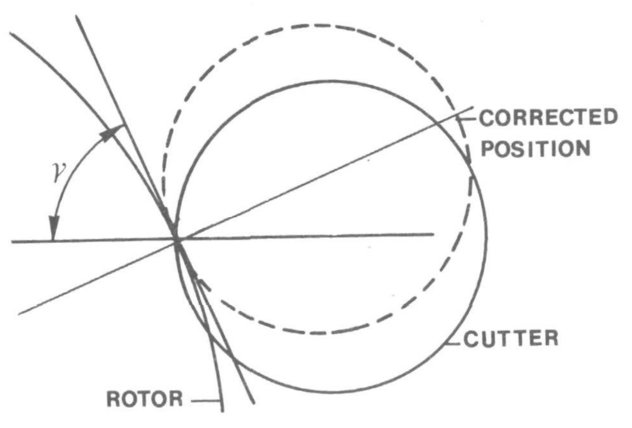

FIGURE 13.

Correction of the position of the cutter relative to the workpiece.

In order to simplify the system that has to realize this rotation the value of $\frac{\pi}{2} - \gamma$ is approximated by the value of the angle β that meets the equation:

$$tg\beta = \frac{1.2 \cdot n \cdot a \cdot \sin(2 \cdot n \cdot \phi)}{R_o} \qquad (5.16)$$

The total system for the manufacture is shown schematically in figure 14.

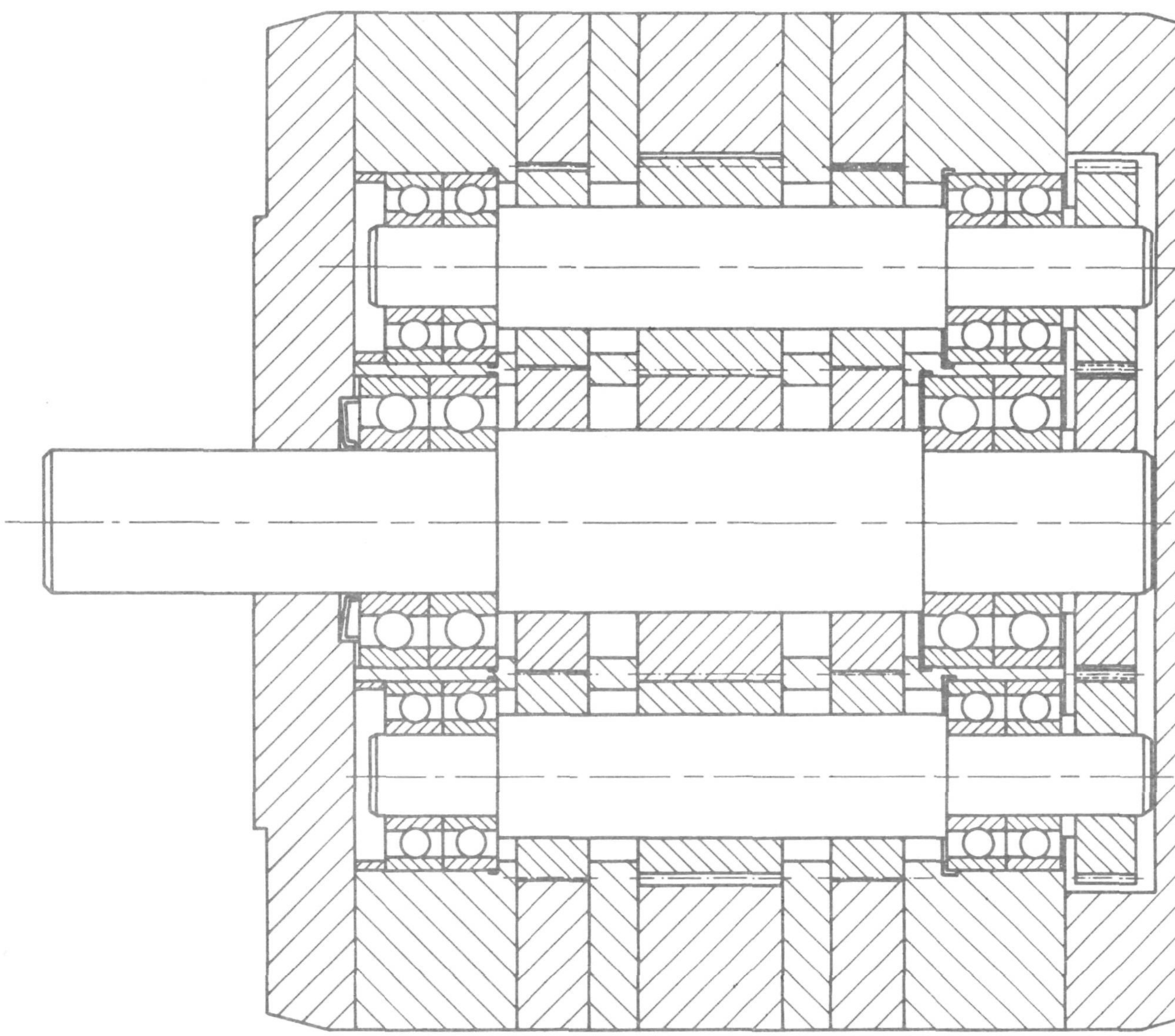

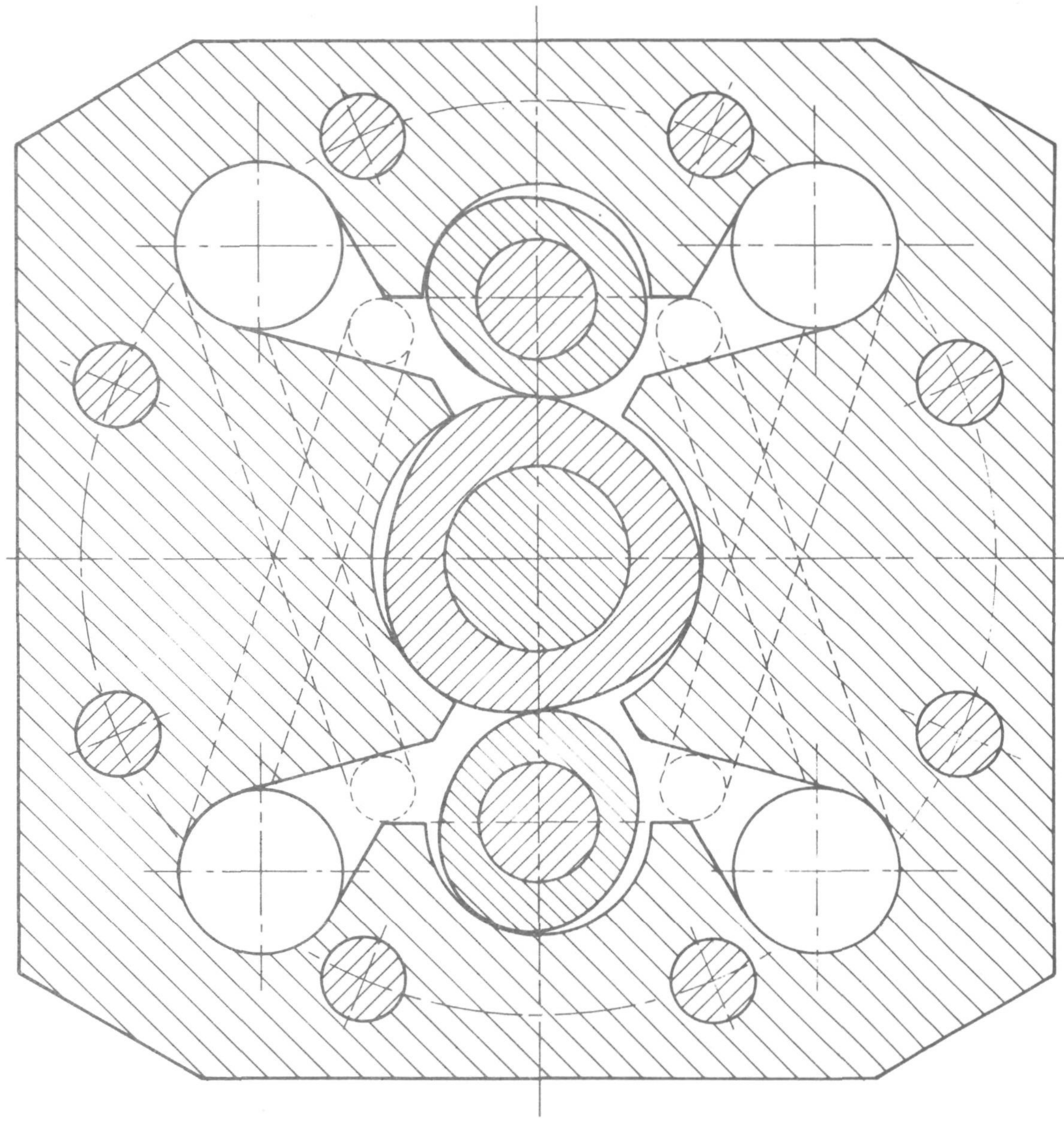

DRAWING 1: *Hydraulic motor.*

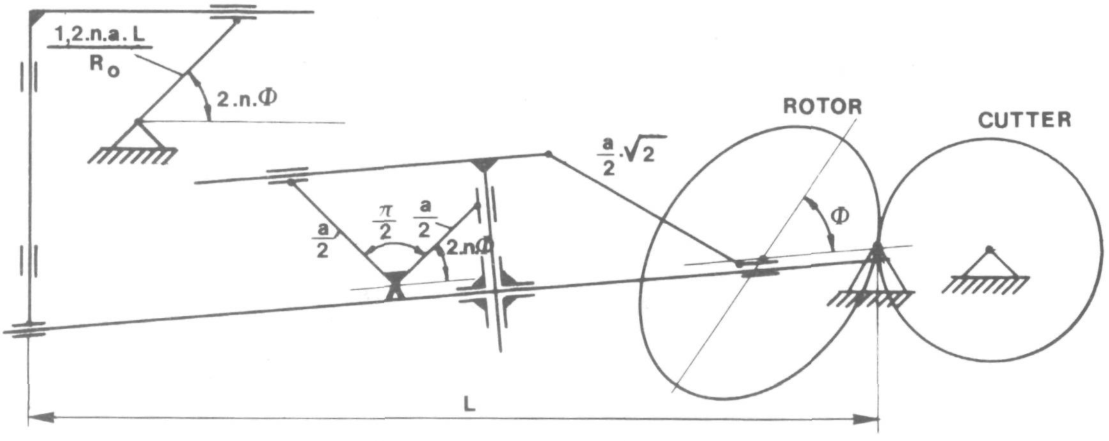

FIGURE 14.

Schematic representation of a system for the manufacture of the rotors.

This figure shows also the way in which the angle β is adjusted. From the foregoing it follows that, in order to machine the circumference of the rotor, three movements of the rotor relative to the cutter are necessary. At first a rotation of the rotor on its own axis with a speed ω_r, where the value of ω_r depends on the cutting conditions. Secondly there is a linear movement according to the equation 5.15, based on a rotation of the cranks of the mechanism with a speed $2 \cdot n \cdot \omega$. At last a rotation of the rotor on a line on the rotor circumference is applied, also based on a rotation of a crank mechanism with a speed $2 \cdot n \cdot \omega$. The ratio of the speeds of rotation has to be maintained exactly. In the laboratory of the University of Technology, where the hydraulic motor has been built, the system described above has been applied. In this case electric stepping motors were used for the drive of the crank mechanisms. With these motors the ratio of the drives is determined by the ratio of the frequencies of the pulses supplied to the stepping motors. The correct adjustment of the frequency ratio can be realized very simple. Figure 15 shows the manufacturing set-up as it has been used on a small milling machine in the laboratory.

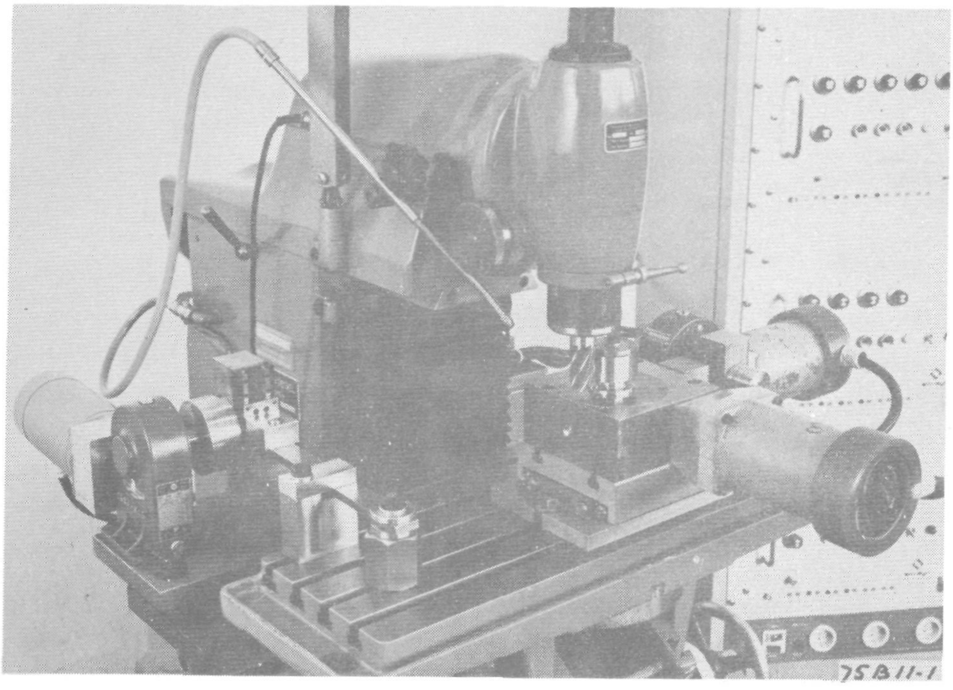

FIGURE 15.

Set-up for the manufacture of the rotors.

As mentioned before both the rotors and the gears are mounted by means of glueing. Figures 16a and b show two typical stages of the assembly of the motor. In figure 17 the motor is shown after assembling.

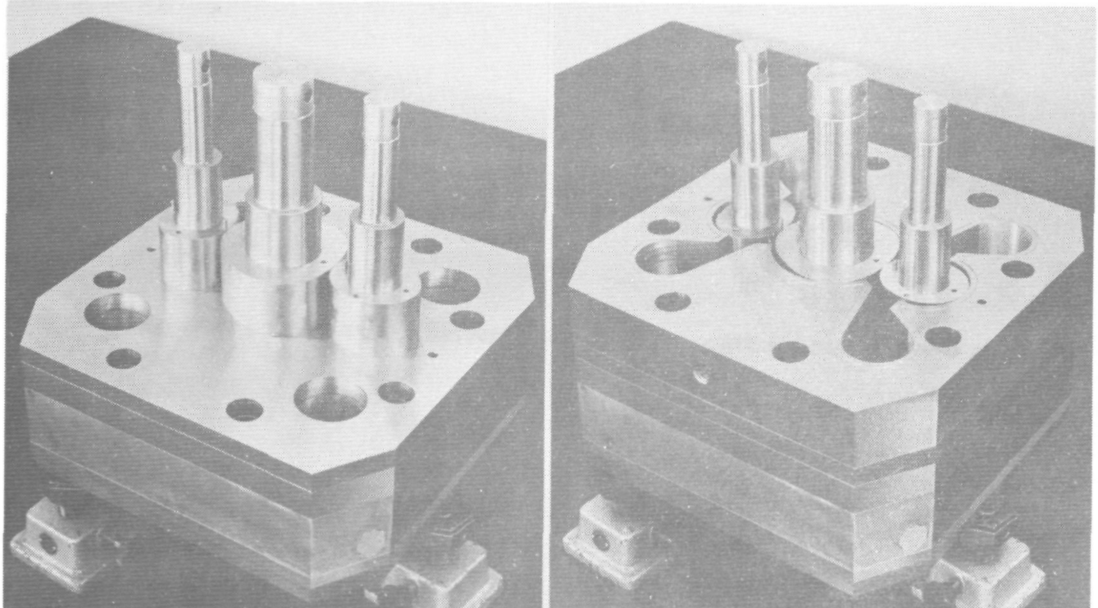

FIGURE 16.

Two stages of the assembly of the motor.

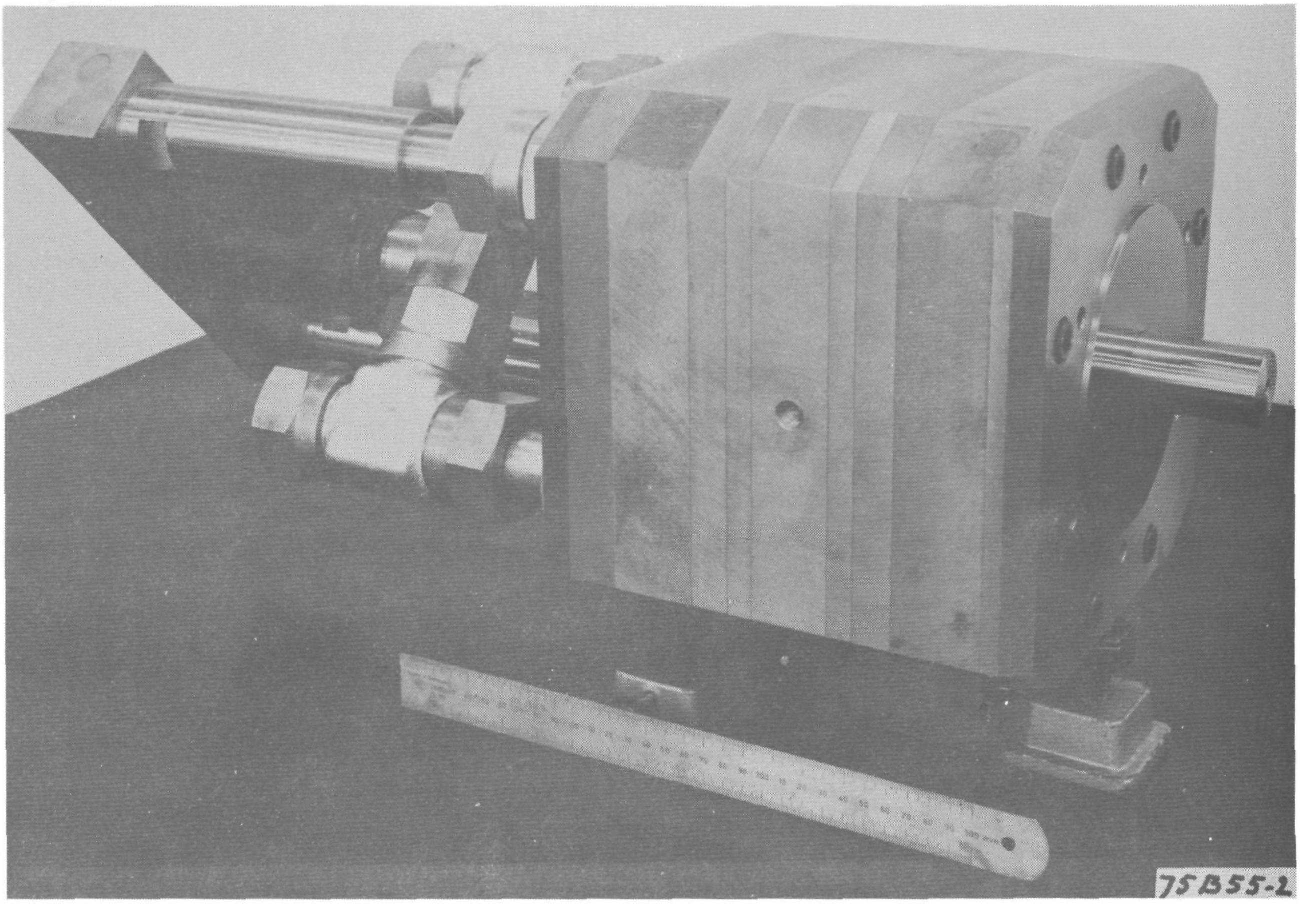

FIGURE 17.

Hydraulic motor according to the final design.

5.4. Conclusion

The hydraulic motor described before is in a stage of development. This means that there is a number of aspects to be regarded before an optimum design can be realized. In the scope of this thesis it is not possible to cover all these points. For this reason the foregoing describes the basic aspects of the design. The calculations concerning the leakage flows and the friction losses in the motor are carried out in the Appendix D. Summarizing the description of the motor the following data determine the design of this motor:

Maximum speed	$n_{max} = 9550$ r.p.m.
Maximum torque	$M_{max} = 250$ N.m
Displacement per revolution	$5 \cdot 10^{-5}$ m^3
Maximum pressure	$p_{max} = 35 \cdot 10^6$ N/m^2
Weight	$G = 120$ kg

In the chapter describing the total power supply for the grinding machine the oil supply system for the hydraulic motor will be discussed.

6. THE CONSTRUCTION OF THE MACHINE

6.1. General design

The basis for the design of the grinding machine is the movement of the grinding wheel relative to the workpiece. This movement can be devided in three parts: a rotation of the workpiece, a movement parallel to the axis of the workpiece and a movement perpendicular to the axis of the workpiece. Both linear movements can be carried out either by the grinding wheel or by the workpiece. It is decided to effect these movements by the wheel head and that based on the following considerations. The deformations of the bed and the slide of the machine depend strongly on the dimensions of these parts. Specially the parts that carry out movements along guideways have a considerable influence on the deformation of the machine. The length of a slide, carrying the workpiece and the work heads that support the workpiece, has to be much greater than the length of a slide that carries the wheel head. Besides a smaller slide reduces also the dimensions of the complete machine structure. The above concerns both movements of the grinding wheel relative to the workpiece. So, in order to reduce the deformation of the structure, both movements will be carried out by the wheel head. In figure 18 the workpiece and the grinding wheel with the grinding spindle are drawn schematically. In this figure x and y represent the directions according to which the wheel head is moving. From this figure it appears that it is possible to achieve a movement in y-direction by composing a translation in y'-direction, parallel to the center line of the grinding spindle, and a movement in x-direction. This way of moving the wheel head has the following advantages. In the first place the drive of the wheel head in this direction will not meet with any force caused by the grinding process, as the forces perpendicular to the grinding wheel are eliminated as described in chapter 3.

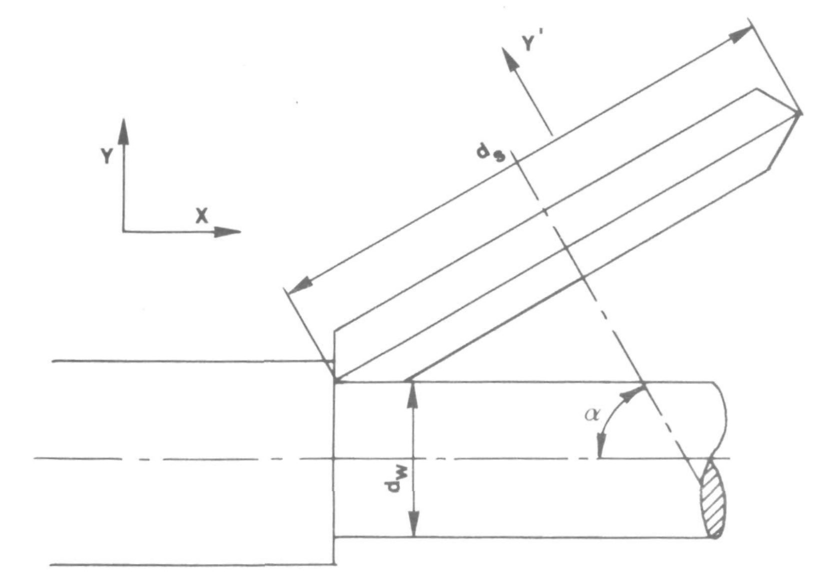

FIGURE 18.

Grinding wheel and workpiece drawn schematically.

This means that the influence of the drive with regard to deformations caused by the grinding forces is also eliminated. Secondly the construction of the wheel head can be more simple as the center lines of the grinding spindle and the guideways are parallel to each other. Besides the directions of the movements of the wheel head it is necessary to know the length of the travel of the wheel head in each direction. The length of the travel in y-direction is determined by the dimensions of the grinding wheel and the diameter of the workpiece. From figure 18 it can be derived that the length of the travel in y-direction

$$l_y = \frac{d_{w\,max}}{2} + \sin 30^o \cdot \frac{(d_{s\,max} - d_{s\,min})}{2} + l \qquad (6.1)$$

where l is a displacement of the wheel head that is necessary to handle the workpiece during loading and unloading with sufficient safety. From the above equation it follows that the travel in y'-direction

$$l_{y'} = (175 + l) \cdot \cos 30^o \qquad (6.2)$$

The travel in x-direction is determined by the length of the workpiece and the value of $l_{y'}$. In this case also an extra length l' is added. So

$$l_x = 750 + l_{y'} \cdot \sin 30^o + l' \qquad (6.3)$$

Based on the equations 6.2 and 6.3 the following values are chosen:

$\underline{l_{y'} = 225 \text{ mm}}$ and $\underline{l_x = 1075 \text{ mm}}$

These dimensions, together with the dimensions of the workpiece, the grinding wheel, the grinding spindle and the spindle drive determine the design of the machine structure and the slides. However, before working out this design it is necessary to consider a number of aspects that have an important influence on the design.
In the first place it has to be decided whether the material for the machine will be cast iron or steel plates. It is difficult to make a decision based on both technical and economical aspects as this decision requires an extended knowledge about the production of these machines, specially with regard to the total number of machines to be manufactured per year, the number of types and so on. So only technical aspects are taken into account. The advantages of cast iron concern in the first place the freedom in the design of the machine parts. Secondly the damping of cast iron is better than the damping of steel plates; however, a construction of welded steel plates offers good possibilities to apply sufficient damping to the complete structure. The disadvantages of cast iron concern in the first place the relatively low modulus of elasticity. This results in an increase of the weight of the machine parts in order to obtain the same stiffness as when applying welded steel plates. Secondly the flexibility of the design is very small. Even a little change of a part of the machine entails great expense. Based on the above considerations it is decided to apply welded steel plates for the machine structure, the slide, the wheel head and the work heads.
Another aspect concerns the guideways for the slide and the wheel head. As it will be necessary in some cases to move the wheel head and the slide with low velocities a stick-slip effect may appear. In order to avoid this effect guideways with rolling elements or hydrostatic guideways can be applied. As the damping in roller or ball guideways is very poor and as there is already a hydraulic system for the spindle bearings and the spindle drive, in which a third system can be incorporated, hydrostatic guideways will be used.
A third point is the fact that there will not be any possibility to inspect the grinding process visually. In the first place it has no sense to look at a phenomenon that does not give any information about relevant data concerning the process. Secondly the safety of the machine can be increased by avoiding openings or windows for inspection.
Although there are some other points that are of interest for the final design, the above data give sufficient information to set up a preliminary design. The drawings 2, 3 and 4 show the front view, the top view and a cross section of the machine. The first point to notice is the triangular cross

section of both the bed and the slide. This shape has the following advantages. First a triangular cross section of both the bed and the slide makes it possible to obtain a high stiffness of the structure at relatively small dimensions, not only with regard to the area of the cross section of the machine, but also regarding the plate thickness. Secondly, as can be seen from the drawings, it is possible to realize small dimensions of that part of the machine that is most influenced by the forces between the grinding wheel and the workpiece. Particularly the distance between the guideways and the place where the grinding forces apply is chosen as small as possible. Another point of interest is the box-shaped construction of bed, slide, wheel head and work heads. From litterature [12] it is known that the application of closed box-shaped structures offer a high stiffness. In order to increase the torsional stiffness of the bed and the slide diagonally placed plates are applied as shown in the drawings. The drawings show also that the two work heads of the machine are identical, with the exception of the motor that drives the workpiece. Although in many applications the work head that carries the drive is much heavier and more rigid than the other work head in this case the forces that determine the accuracy of the machine are the same for both heads. So the requirements concerning the stiffness of the heads are also identical.
It is clear that the above considerations do not produce the evidence that the design as shown in the drawings is the only possibility to meet the demands that are made. The judgment about the shape of the complete machine or the shape of parts of the machine depends highly on the view of the designer. However, each design has to meet the requirements that are determined by the process and by other factors like the demands made by the manufacturing methods for the machine parts. Some of these requirements have already been the starting point for the preliminary design, like the dimensions of grinding wheel and workpiece, the length of the travel of the wheel head both in y- and x-direction and so on. Other requirements concern points like the supply of coolant, the dressing of the grinding wheel, the control of the machine and provisions with regard to the safety. These requirements will be discussed in separate chapters. At last there are requirements of which the question whether they are met or not can only be answered after calculations concerning a finished design. Should these calculations show that the requirements are not met the design has to be changed and the calculations in question have to be carried out again. In this case these requirements concern the deformation of the complete structure caused by the grinding forces. The calculation procedure concerning this point will be described in the following section of this chapter. In the last section of this chapter the design of the work heads will be considered.

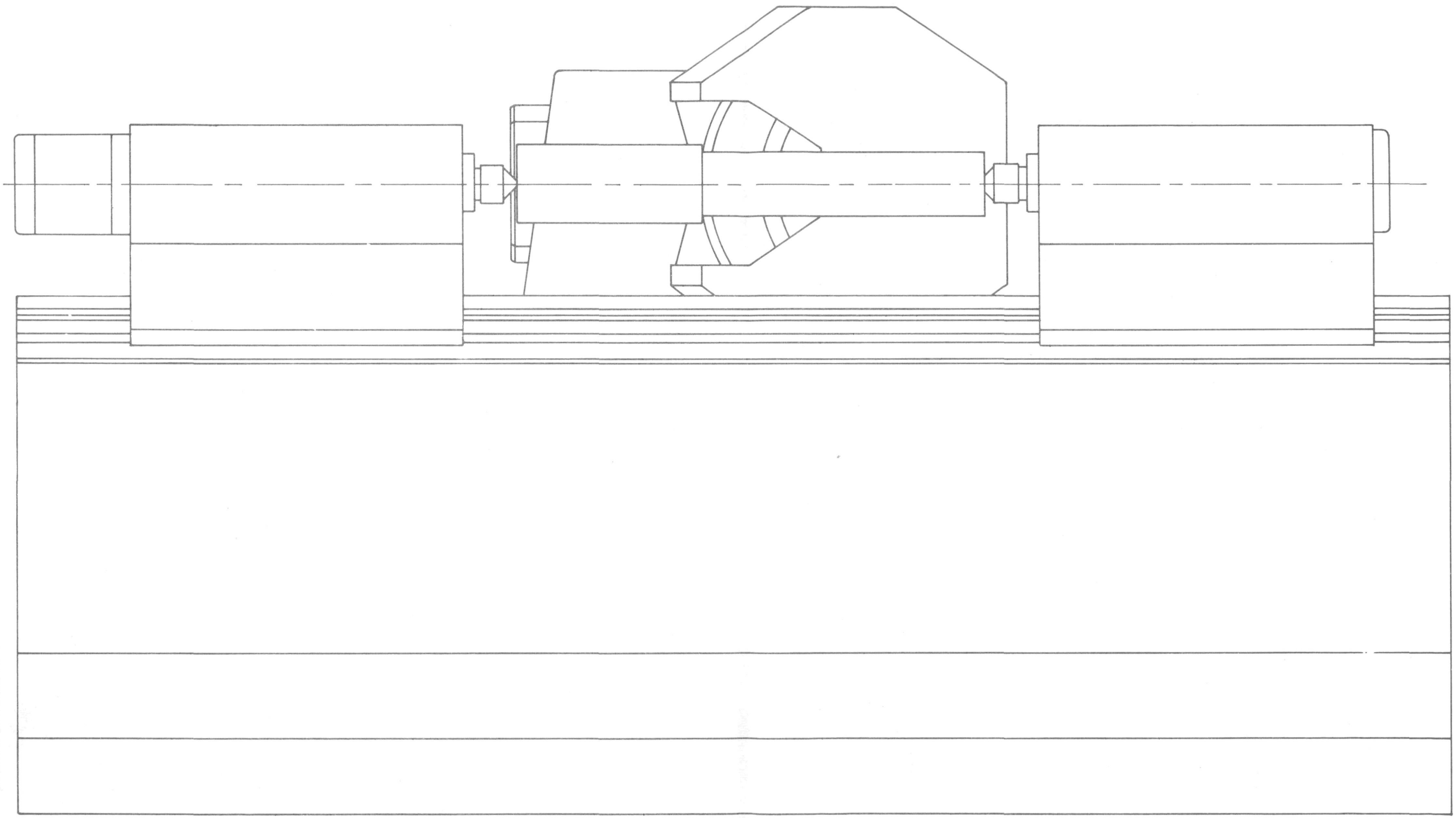

DRAWING 2: Front view of the grinding machine.

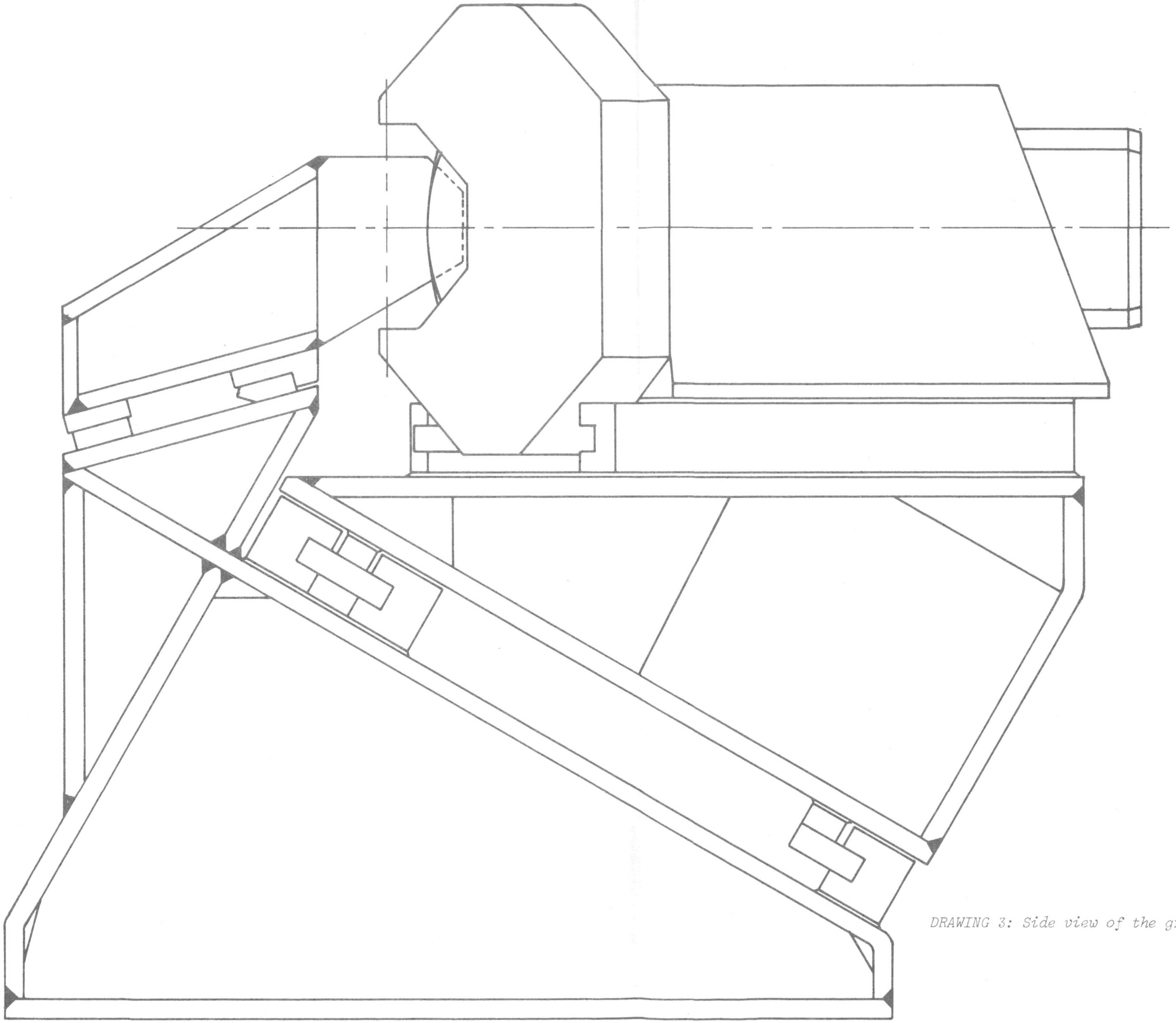

DRAWING 3: Side view of the grinding machine.

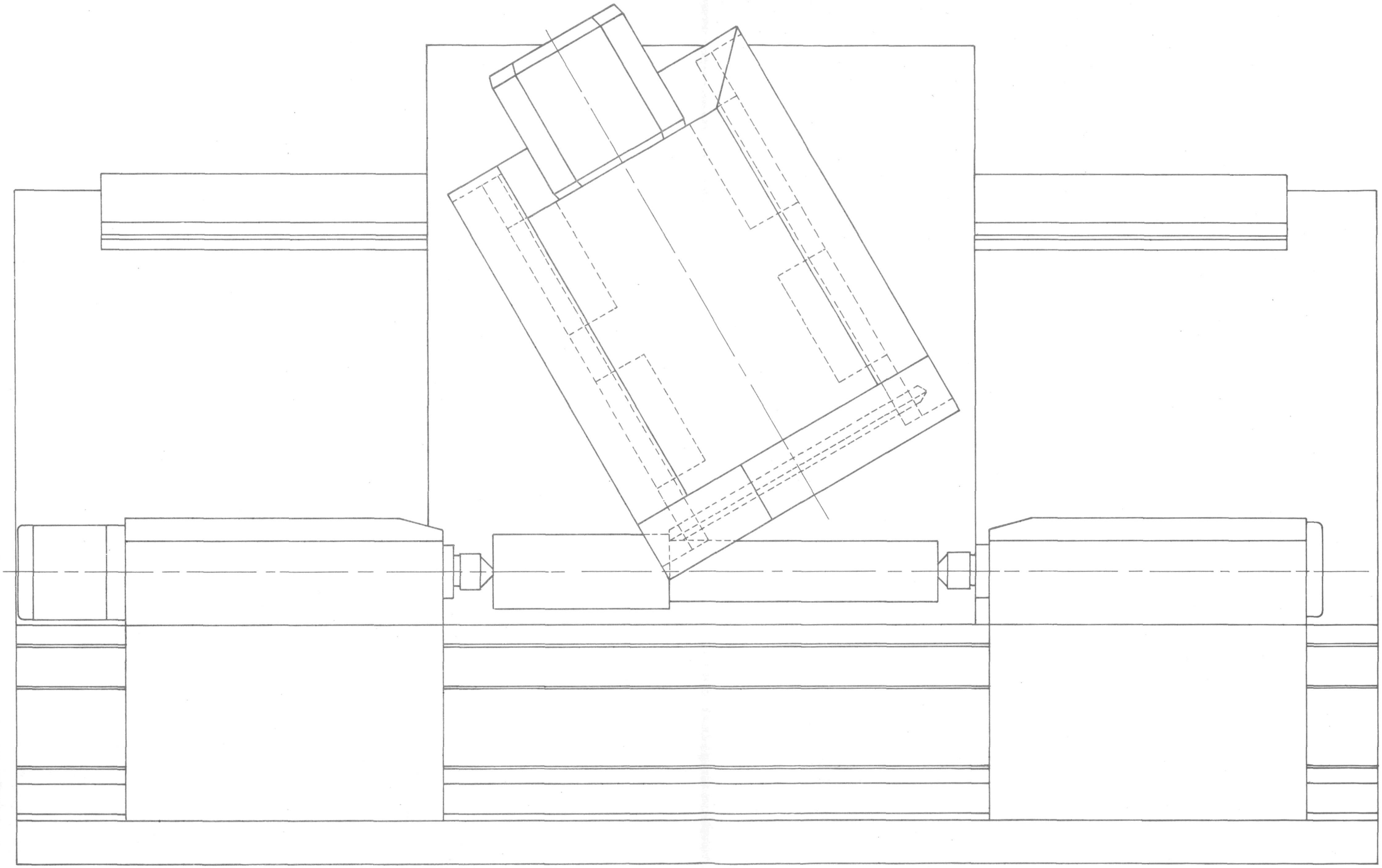

DRAWING 4: Top view of the grinding machine.

6.2. Deformation of the machine structure

6.2.1. Method of calculation

The deformation of the grinding machine as a result of the grinding forces will be regarded as far as this deformation causes a change of the relative position of the grinding wheel and the workpiece. According to the considerations in chapter 4.1 it is assumed that the deformation of the machine structure shall not cause an error in the diameter of the workpiece greater than 0.01 mm. The error in the axial direction, caused by this deformation, is equally not allowed to exceed 0.01 mm. The deformations of the grinding spindle and the work head spindles are not included in these values. First the method according to which the calculations will be carried out has to be determined. These calculations have to take into account both deformations in the plane of the plates of the structure and deformations perpendicular to this plane. As besides diagonally placed plates are applied it is obvious to choose the so called "finite element" method to calculate the relevant deformations. This method can be described as follows [13]. A machine part can be devided into a number of elements of a relative simple shape c.q. bars, squares, triangles and so on. The elements are connected one to another at their corners, called nodal points. The basis for the calculations is given by the relations between the forces in the nodal points of an element and the displacements of the nodal points caused by these forces. From these relations for each element the relations between external loads and deformations of relevant points of a machine part can be calculated. It is obvious that the solution of a large number of equations with a large number of unknowns leads to matrix solutions that can only be solved by using computers. As a consequence computer programs have been developed in order to allow for the solutions of these calculations. One of these programs, called ASKA *) is available at the Computing Centre of the University of Technology in Delft [14] and this program has been used to calculate the relevant deformations of the structure of the grinding machine. In this thesis only the input and the output of this program will be considered, the program itself will be regarded as a calculation tool of which only the directions for use are of importance. The parts of the program input that are important for the user are the "ASKA Processor Control step", the "Topological Description" and the "Data Input". The "ASKA Processor Control step" comprises the instructions that take care of the way and the order in which the data have to be processed in order to obtain the desired results. The "Topological Description" describes the elements in which the structure is divided and numbers the nodal points. Besides in this part the degrees of freedom that are restricted are mentioned. Finally the "Data" input comprises the co-ordinates of the nodal points, the material properties, the loads and the prescribed displacements.
The output of the program depends on the instructions in the "Processor Control step" and contains in the first place the numerical results of the calculations. Besides information concerning errors in the program

*) *"Automatic System for Kinematic Analysis", developed by the "Institut für Statik und Dynamik der Luft- und Raumfahrtkonstruktionen" in Stuttgart, W.-Germany.*

or the data, the degrees of freedom in each nodal point, data concerning the structure of the matrices and so on may be printed out. The following section describes the calculation of the deformation of the structure of the grinding machine.

6.2.2. Execution of the calculations

First of all the type of element that will be used has to be chosen. As different types of elements in one structure lead to more complicated calculations one type of element will be applied for the complete structure. As the plates of the structure are loaded both in a direction in the plane of the plates and perpendicular to this plane the element has to accommodate this load. Besides the shape of the element has to allow for a division that approximates the real structure as accurate as possible. On account of this the so called TRIB 3 element is chosen. This element is a triangular plate element that takes six degrees of freedom into account in each nodal point. The only disadvantage of this element is the fact that there is no stiffness against a rotation on an axis perpendicular to the plane of the element. However, a stiffness in this direction can be taken from adjacent elements or, in case this is not possible, a rotation in this direction can be suppressed in the program without affecting the accuracy too much. In order to keep the calculations surveyable the main structure of the machine is devided into substructures. These substructures are the bed, the slide, the wheel head and both work heads. Each of these substructures is connected to one or more of the other substructures by means of a fixed connection like bolts or by means of movable connections like guideways. The fixed connection shall be approximated by connecting the nodal points of both substructures in that area where the connection of the real structure is arranged. The two parts of each guideway are regarded as being a part of the substructure on which they are mounted. On the two parts of each guideway nodal points are chosen and connected in such a way that a movement in the desired direction is allowed. This means that in each nodal point of this connection only one or two degrees of freedom are connected. The deformation of the oil film of the hydrostatic guideways is neglected as this deformation is relatively small compared with the deformation of other parts of the structure. Finally the drive elements for the slide and the wheel head have to be regarded. These drive elements may be cylinders and pistons or screw drives. In this stage of the design it is assumed that screw drives will be used both for the drive of the wheel head and the slide. In the first section of this chapter it has already been mentioned that the drive of the wheel head is not affected by the grinding forces. As a consequence this drive has not to be taken into account in the calculations concerning the deformations of the structure. However, the drive of the slide has to be considered in the calculations. For this reason the drive of the slide is represented by a substructure with the same elastic behaviour as a real drive screw. The ends of this substructure are connected to the bed and the slide in a number of nodal points that represent the real mountings. Although the wheel head drive is not affected by the grinding forces it will be necessary to connect the wheel head to the slide in at least two corresponding nodal points of the guideways. In figure 19 the main structure of the grinding machine is shown, while figure 20 shows the composing structures. Starting from the above the relations between the loads and the displacements in relevant points of each substructure are calculated. These

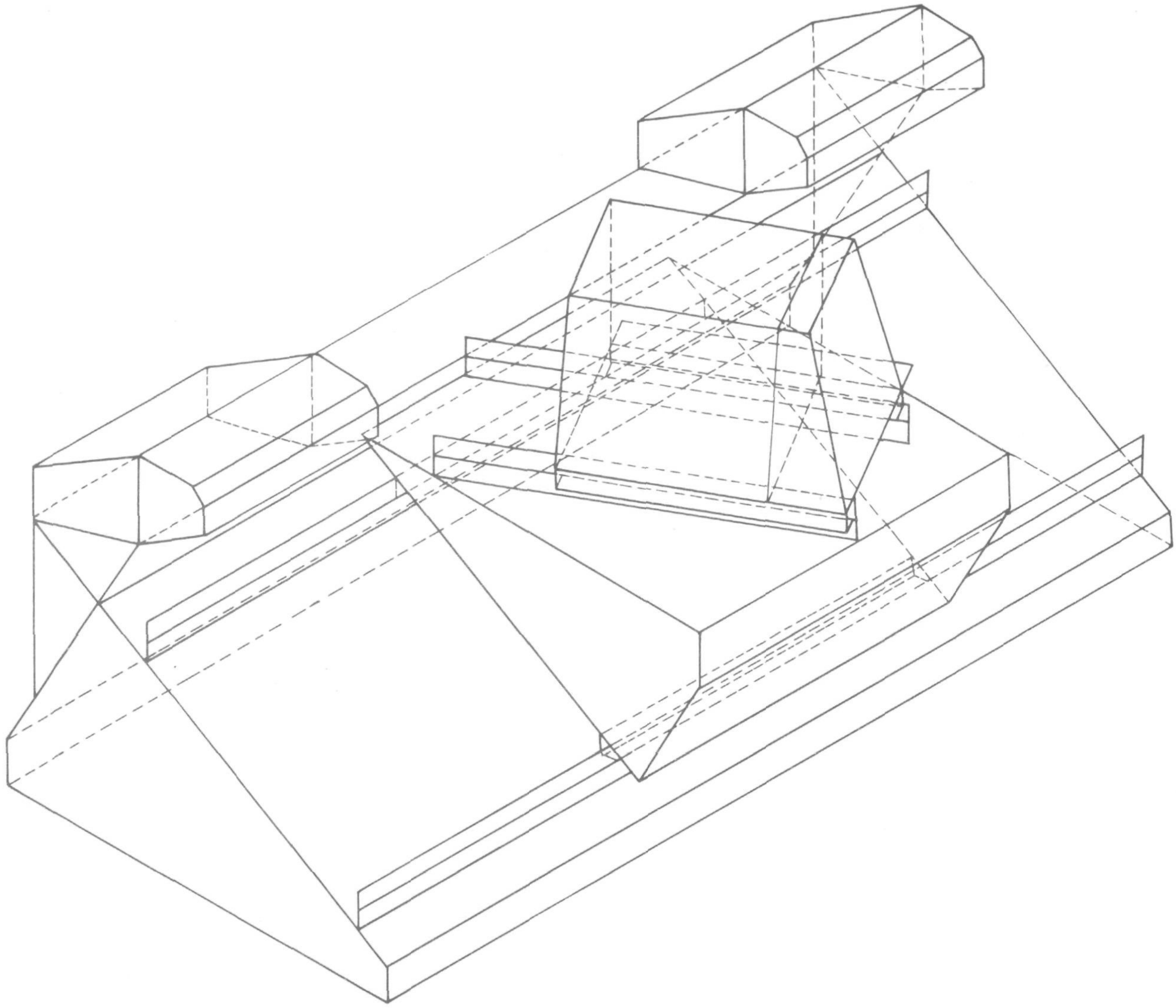

FIGURE 19.
Main structure of the grinding machine.

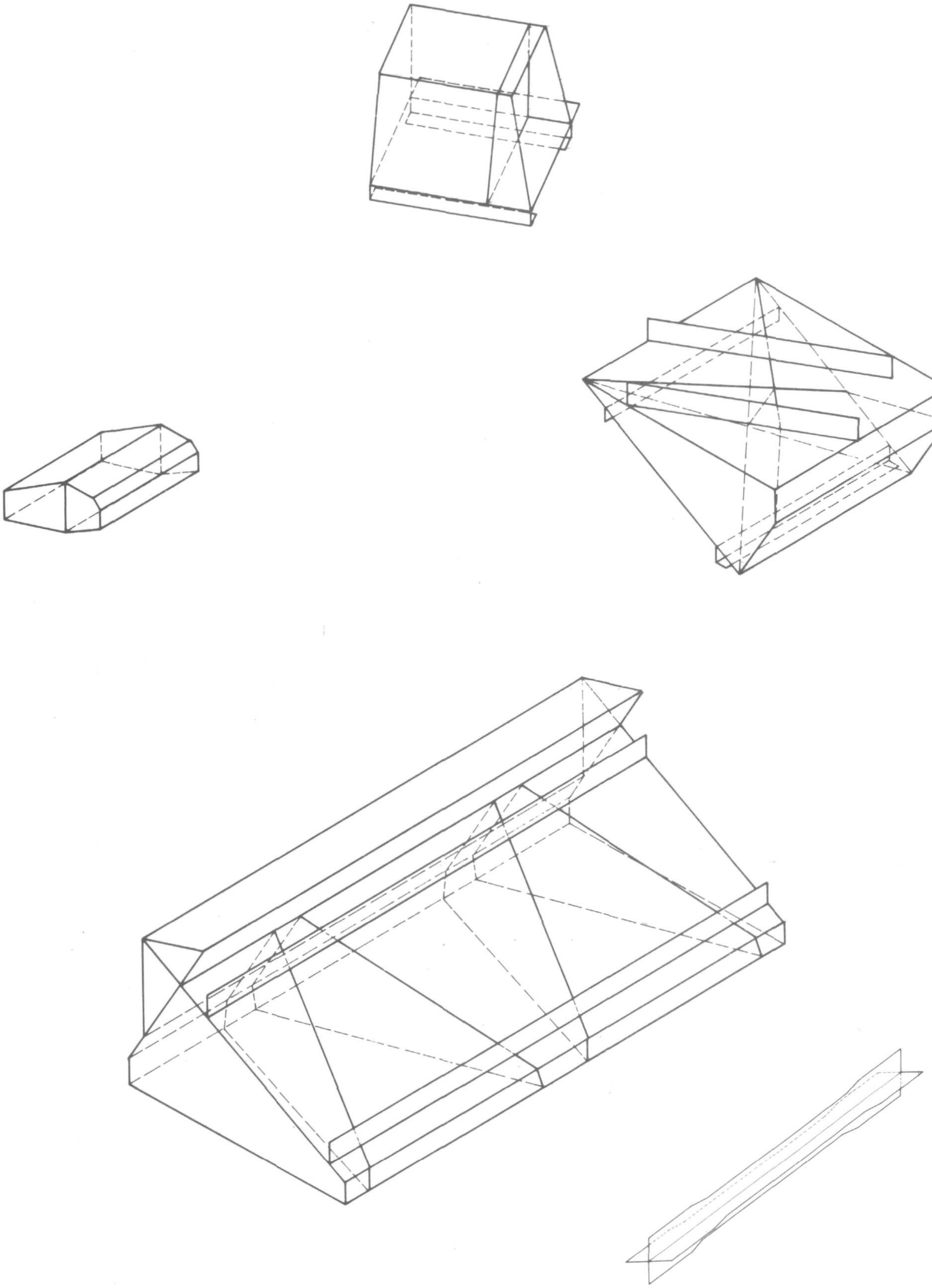

FIGURE 20.

Substructures, representing the wheel head, the work head, the slide, the bed and the drive screw.

relations are laid down in so called stiffness matrices. After these stiffness matrices have been drawn up the substructures are connected into the main structure and from the values of the external loads the displacements of the points of the structure in question can be determined.
First of all the topological description and the data input of each substructure have to be considered. The first substructure, representing the wheel head, is shown in figure 21. In the figure the division of the plates of the structure into the TRIB 3 elements is indicated. In this substructure two parts are of major interest. First the nodal points in which the grinding spindle is connected to the wheel head, the points 1 to 8 and 52 to 59. In these points the load, caused by the grinding forces, is applied to the structure. Secondly the nodal points in which the wheel head is connected to the slide by means of guideways, the points 9, 24, 39, 62, 11, 26, 41 and 64. It is obvious that, with regard to the deformations of relevant points of the main structure, only the forces and the displacements in these points of the substructure are of importance. The data input concerns in the first place the co-ordinates of the nodal points of the structure. The co-ordinate system for this substructure is chosen as follows: the x-direction is parallel to the line from point 14 to point 16, the y-direction is parallel to the line from point 14 to point 67 and the z-direction is parallel to the line from point 14 to point 20. It will appear from the description of the other substructures that only the substructure of the wheel head is related to a co-ordinate system that differs from the co-ordinate system in which the other substructures are described. The reason for this is the fact that the calculation of the co-ordinates of the nodal points is more simple if the plates of the substructures are parallel either to the x-y-plane, or to the x-z-plane, or to the y-z-plane. In this respect the position of the wheel head differs from the position of the other substructures. However, an important consequence is that in the data output the values of the displacements are also related to this co-ordinate system. The second part of the data concerns the thickness of the plates of the substructure. In first instance a thickness of 25 mm is chosen for all the substructures, with the exception of the guideways as the dimensions of these parts are known and fixed. From the results of the calculations it will appear for which substructures or parts of substructures other values have to be chosen in order to meet the requirements mentioned before. Finally the data concerning the material of the substructure have to be given, namely the Young's modulus and the Poisson's ratio, in this case for steel.
The second substructure represents one of the two work heads and is shown in figure 22. In this substructure also two parts are of interest. First the nodal points where the work head spindle is connected to the work head, the points 1, 5, 2, 3, 9, 4 and 16 and the points 52, 53, 41, 54, 55, 45 and 56. Secondly the points where the work head is connected to the bed of the grinding machine, the points 13, 25, 37, 39, 15, 27, 39 and 51. The co-ordinate system for this substructure is chosen as follows: the x-axis is parallel to the line from point 46 to point 10, the y-axis is parallel to the line from point 46 to point 44 and the z-axis is parallel to the line from point 51 to point 46. Both the values of the plate thickness and the data of the material are the same as those for the first substructure.
The third substructure represents the bed of the machine and is shown in figure 23. In this substructure a large number of nodal points are of interest, not only with regard to the calculations, but also with regard to a general view concerning the deformation of this substructure. In the first place the nodal points in which the slide is connected to the bed, the points 14, 31, 48, 65, 82, 99, 116, 133, 150, 167 and 16, 33, 50, 67, 84, 101, 118, 135, 152 and 169 are taken into account. Although the slide is

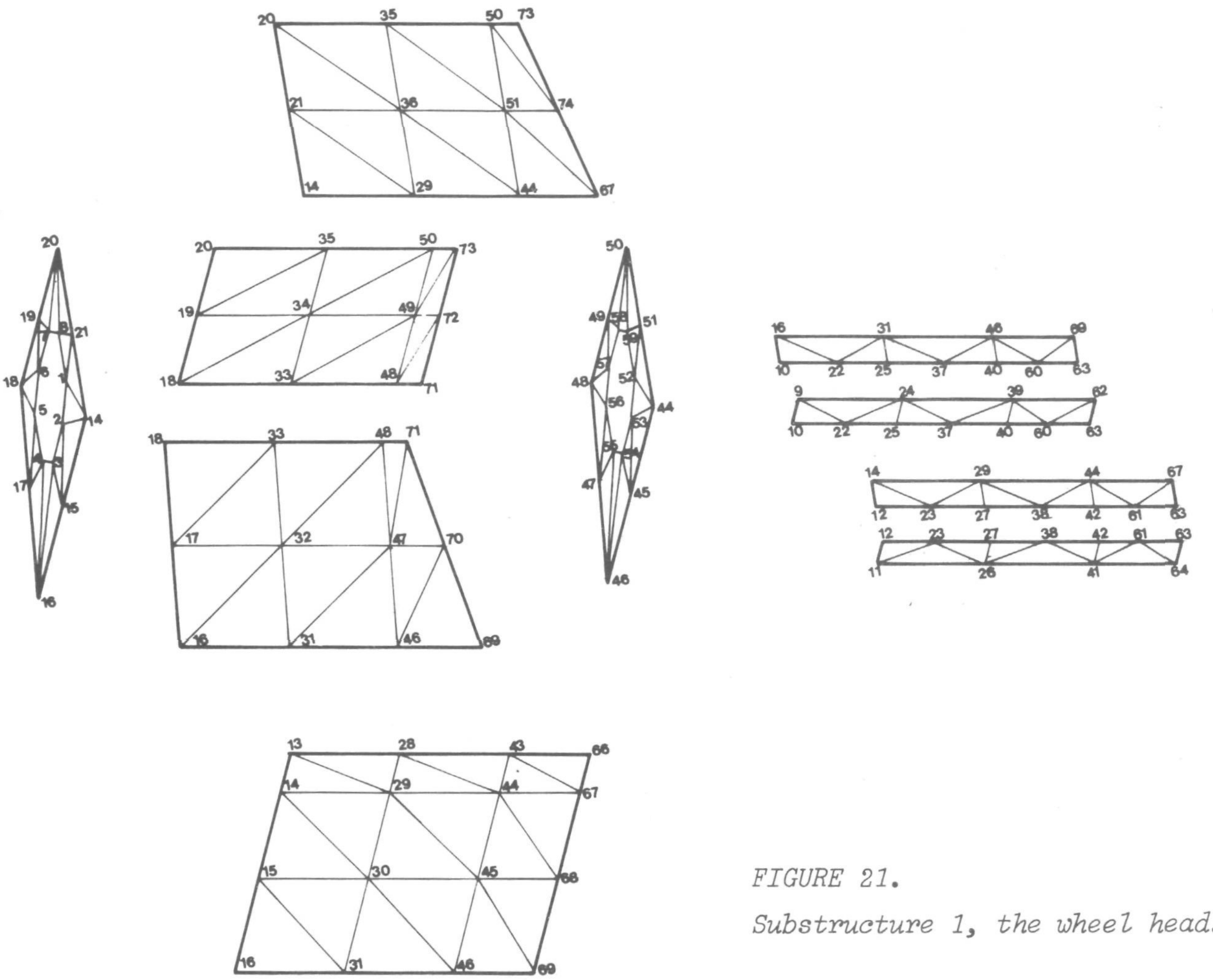

FIGURE 21.
Substructure 1, the wheel head.

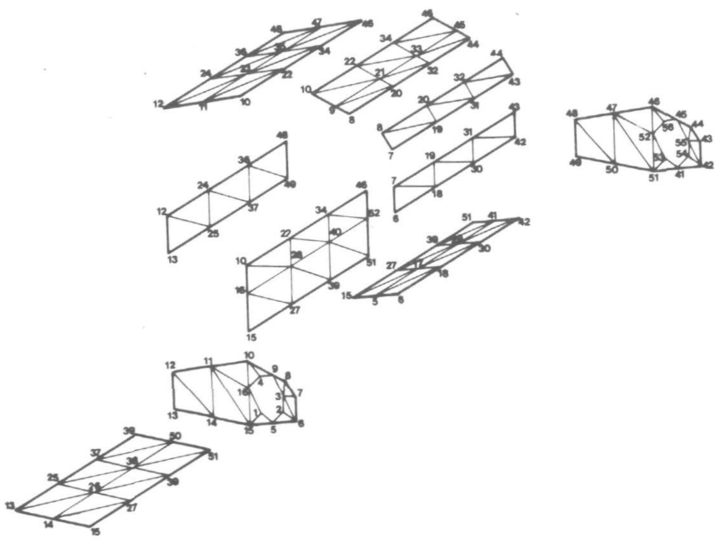

FIGURE 22.
Substructure 2, respectively 6, the work head.

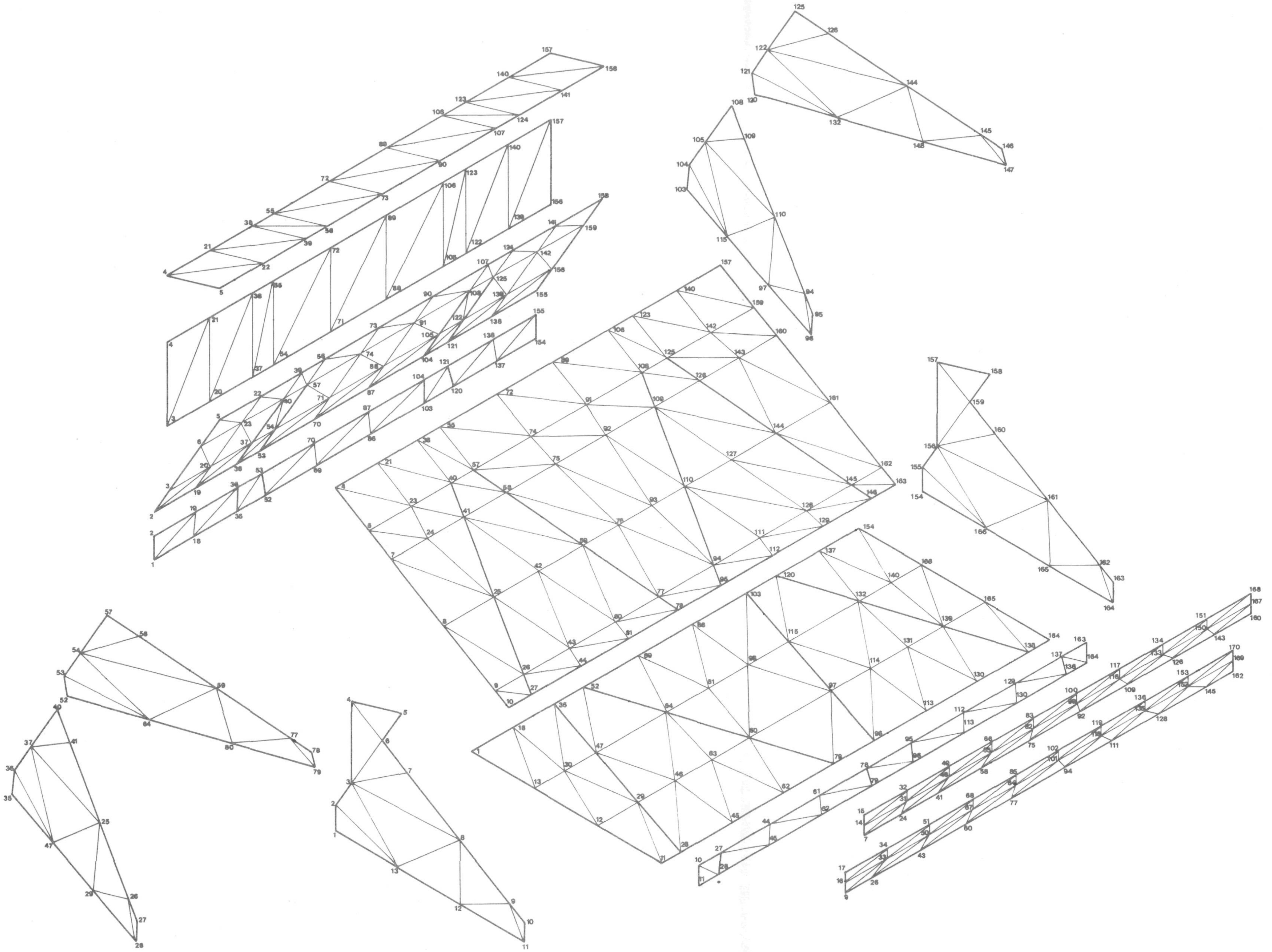

FIGURE 23.

Substructure 3, the bed.

connected to the bed in only ten nodal points it is possible to consider different positions of the slide by drawing more points of the guideways into the calculations. Besides the deformation of the complete guideways shows clearly the deformation of the bed as a whole. The same considerations concern the nodal points where the work heads are connected to the bed. In this case the points 4, 21, 38, 55, 72, 89, 106, 123, 140, 157, 5, 22, 39, 56, 73, 90, 107, 124, 141 and 158 are drawn into the calculations. In the points 7, 24, 8 and 25 the end of the screw that drives the slide is connected. Finally the complete structure will be supported in three points, represented by the nodal points 35 and 52, 79 and 96 and 103 and 120. The co-ordinate system for this substructure shows the same directions of the axes as the co-ordinate system of the second substructure, besides the material and the plate thickness are the same.

In figure 24 the fourth substructure, representing the slide of the machine is shown. In this substructure also the nodal points in which the slide is connected to the other structures have to be taken into account. The nodal points of the guideway between the slide and the bed are the points 15, 34, 53, 72, 91, 3, 22, 41, 60 and 79, those of the guideway between the bed and the wheel head are the points 16, 18, 35, 37, 39, 55, 57, 74, 76 and 93. In the points 89, 70, 58 and 78 the screw that drives the slide is connected. Both the orientation of the co-ordinate system and the material are the same as in the previous substructure, just as the thickness of the plates.

The fifth substructure, representing the drive screw, is shown in figure 25. This drive screw is connected to the bed in the points 67, 68, 72 and 73 and to the slide in the points 4, 5, 9 and 10. From the assumption that this substructure has to represent a screw with a diameter of 40 mm follow the dimensions of the plates. The material is steel with the same properties as the material for the other substructures.

The sixth substructure represents the second work head and is identical with the first work head. The only difference concerns the load applied to this substructure, as this work head is provided with the work head drive.

Based on the calculations of the stiffness matrices of the substructures the deformations of the main structure are calculated. The program for these calculations also comprises a topological description of the structure. In this case this description generates nodal points in such a way that all the significant points of the composing substructures are indicated as nodal points of the main structure and are renumbered. As the co-ordinates of the nodal points of the main structure are determined by the relative position of the substructures it is necessary to determine what position will be decisive for the calculations. As it is not significant to choose the most unfavourable conditions the calculations shall concern a workpiece diameter of 150 mm, a length of the workpiece of 750 mm and a grinding wheel diameter of 400 mm, while the position of the grinding wheel is in the middle of the workpiece. In the topological description the points in which one or more degrees of freedom are suppressed are mentioned. This is necessary in order to obtain a correct support of the structure. In this case, where a support in three points is applied, in one point three degrees of freedom have to be suppressed, in the second point two degrees of freedom and in the third point one degree of freedom. In figure 26 the main structure with the significant nodal points is shown.

The data input of this program concerns the loads applied to the nodal points of the structure. These loads are based on the grinding forces at maximum grinding power. As the workpiece, the grinding spindle and the work head spindles are not included in the calculations, these forces have to be replaced by the loads applied to the structure.

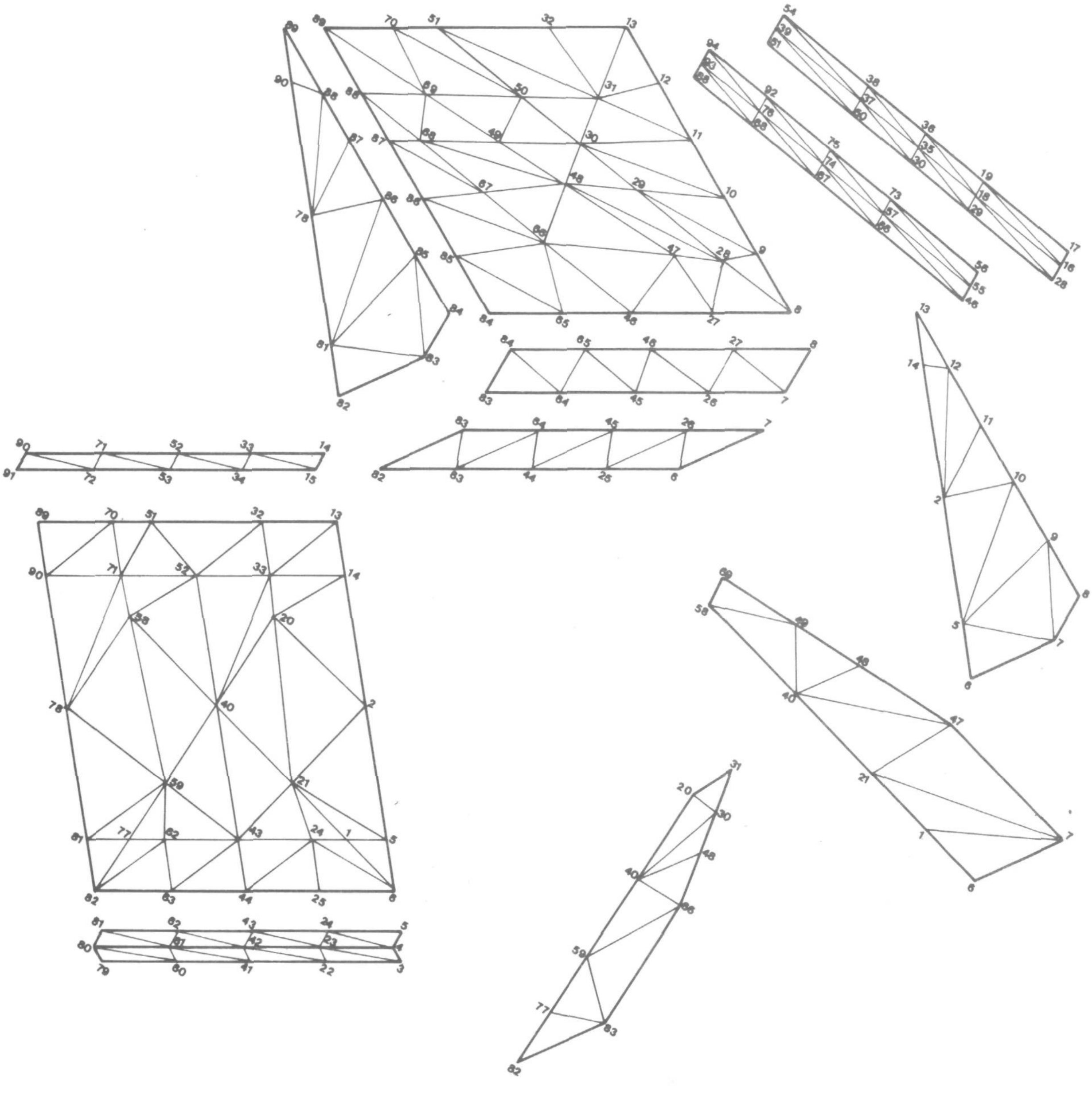

FIGURE 24.

Substructure 4, the slide.

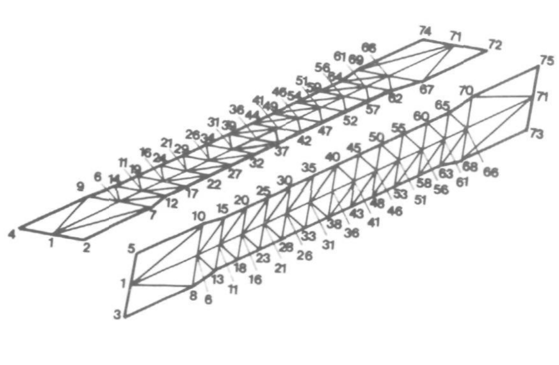

FIGURE 25.

Substructure 5, the drive screw.

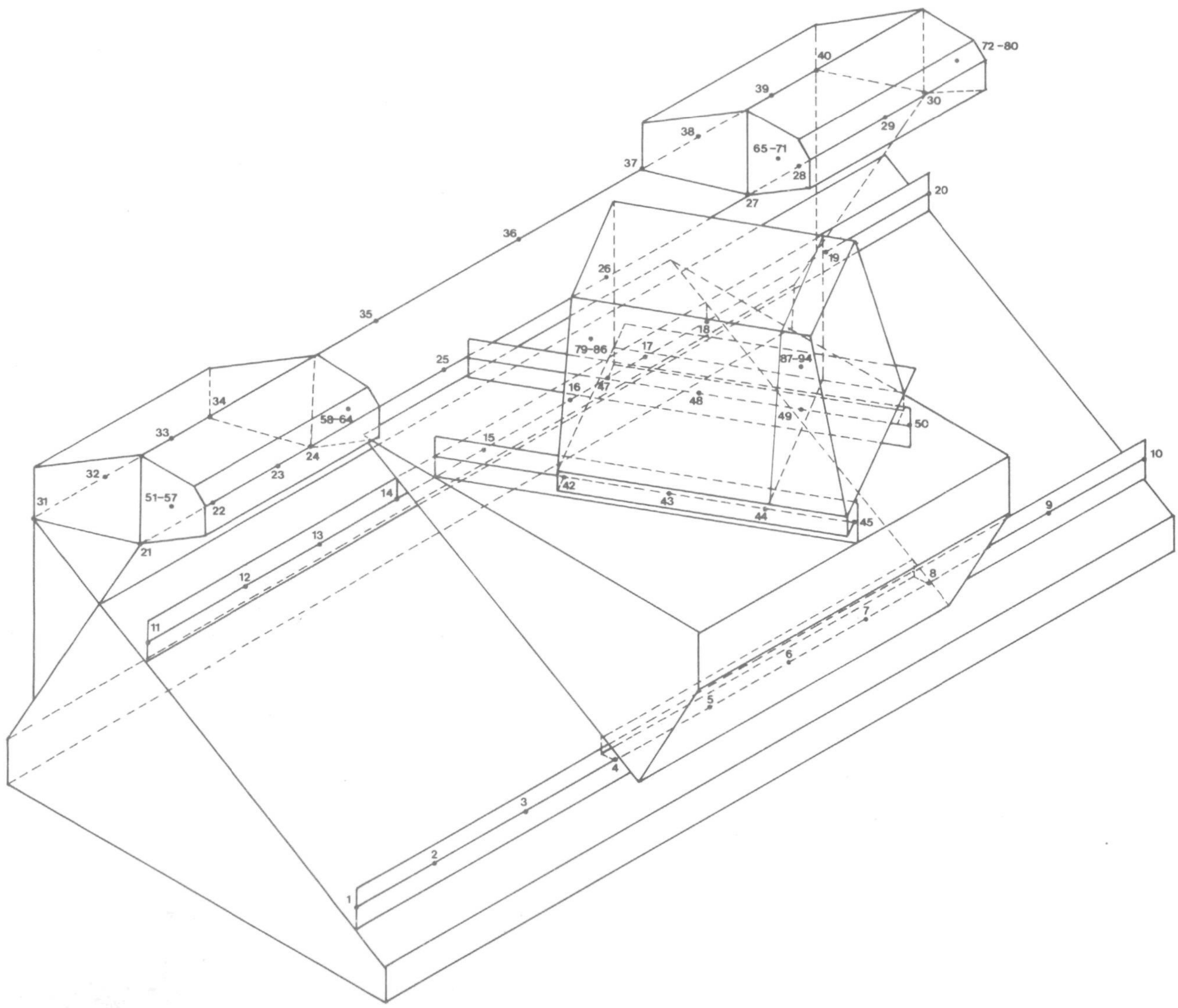

FIGURE 26.

Main structure with significant nodal points.

In figure 27 a top view of the grinding machine is shown schematically. In this figure the loads are indicated, while the places where the grinding spindle and the work head spindles are connected to the structure are shown as points. Actually these points represent a number of nodal points. In figure 28 the division of the load in each of these connections is shown. From these data the deformations according to the six degrees of freedom are calculated. The results of these calculations are obtained as a list of numerical values of the deformations in each nodal point of the structure. In order to get a better insight in the deformation of the structure as a whole and in the contribution of each substructure to this deformation the deformations are plotted in the figures 29 and 30. The displacements of the center lines of the grinding spindle and the work head spindles are shown in figure 31. In these figures the deformation of the drive screw is eliminated, as this deformation exceeds the deformations of other substructures to such an extent that the figures do not show the deformation in the substructures clearly. The deformation of the screw is 0.007 mm in x-direction. The total deformation of the structure results in an error in the diameter of the workpiece of 0.0045 mm and an error in axial direction of the workpiece of 0.0105 mm. From these values it can be concluded that a reduction of the thickness of the plates of the various substructures is possible. At the same time the diameter of the drive screw has to increase. Based on the deformations of the substructures as shown in figure 29 and figure 30 the following values of the plate thicknesses are chosen:

wheel head	-	18	mm	
work heads	-	12.5	mm	
bed	-	16	mm	
slide	-	18	mm	
drive screw	-	16	mm	(corresponding with a diameter of 50 mm)

According to these values the calculations are carried out again. The result of these calculations is shown in the figures 32, 33 and 34. In these figures the deformation of the drive screw is eliminated for the same reason as in the previous figures. The value of this deformation is reduced to 0.0054 mm. The total deformation of the structure is now increased in that way that an error in the diameter of the workpiece of 0.0075 mm appears, while the error in axial direction of the workpiece becomes 0.0107 mm at the grinding conditions mentioned before. If compared with the demands it may be possible to reduce the stiffness of the structure further specially with regard to the deformation in radial direction of the workpiece. However, the deformation in axial direction is not allowed to increase. Although it may be possible, by extended calculations, to obtain a more optimum distribution of the deformations the cost of these calculations do not balance the savings that can be obtained. So it is decided to apply the plate thicknesses mentioned above. If compared with the original thickness of 25 mm the weight of the structure is reduced with 35 per cent. Not only the reduction of the cost of the machine but also the saving in the material itself justifies the calculations carried out. The complete programs and the data output of the computer calculations are not incorporated in this thesis but they are available at the University of Technology in Delft.

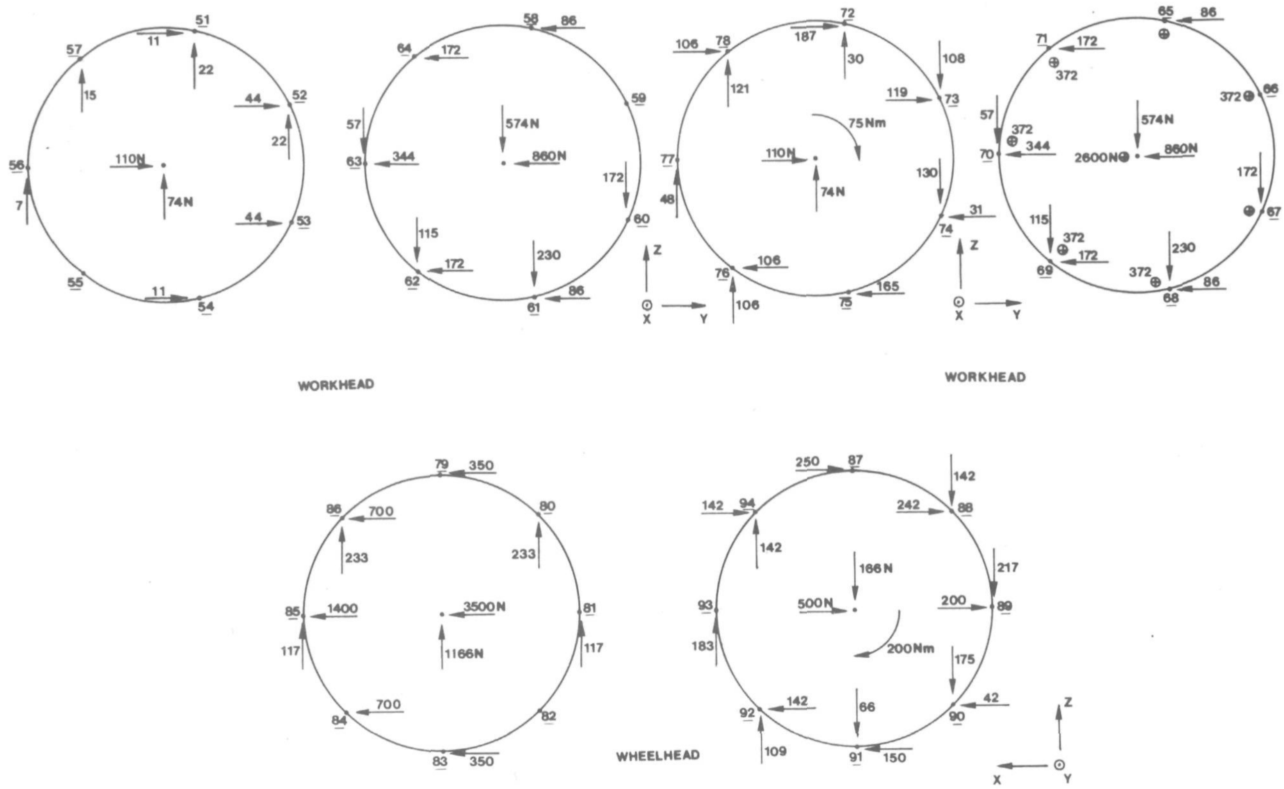

FIGURE 27.

External loads, applied to the structure.

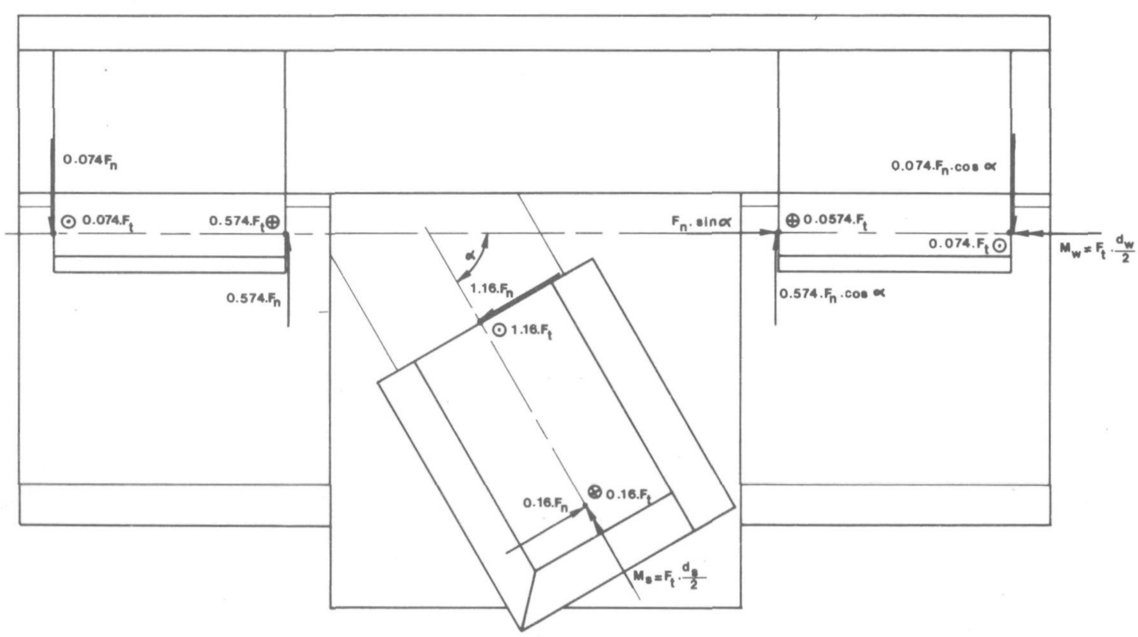

FIGURE 28.

Division of the loads in the connections of the spindles to the structure.

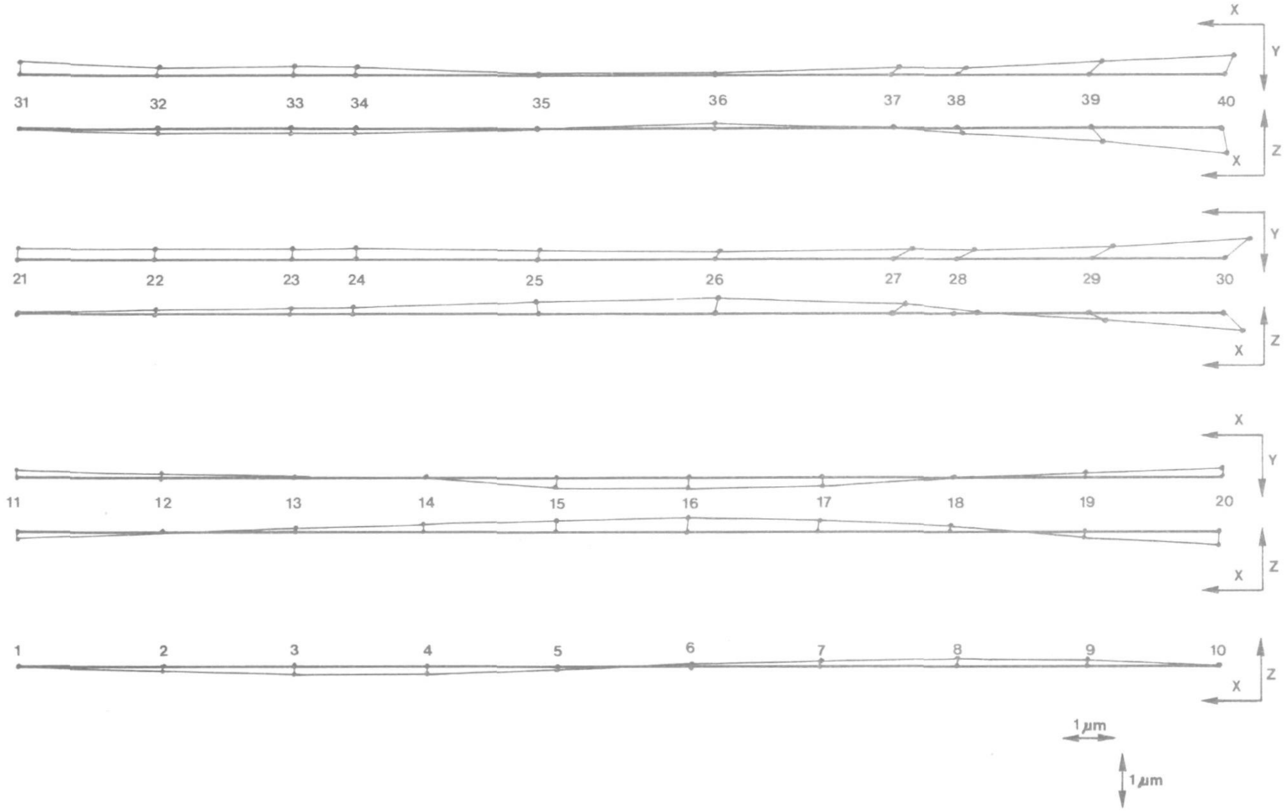

FIGURE 29.

Deformation of the bed in four significant lines.

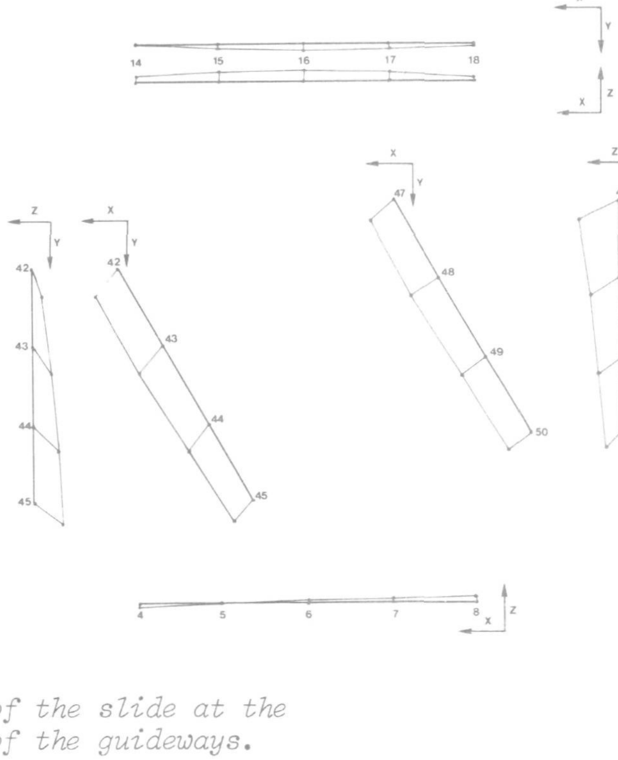

FIGURE 30.

Deformation of the slide at the connections of the guideways.

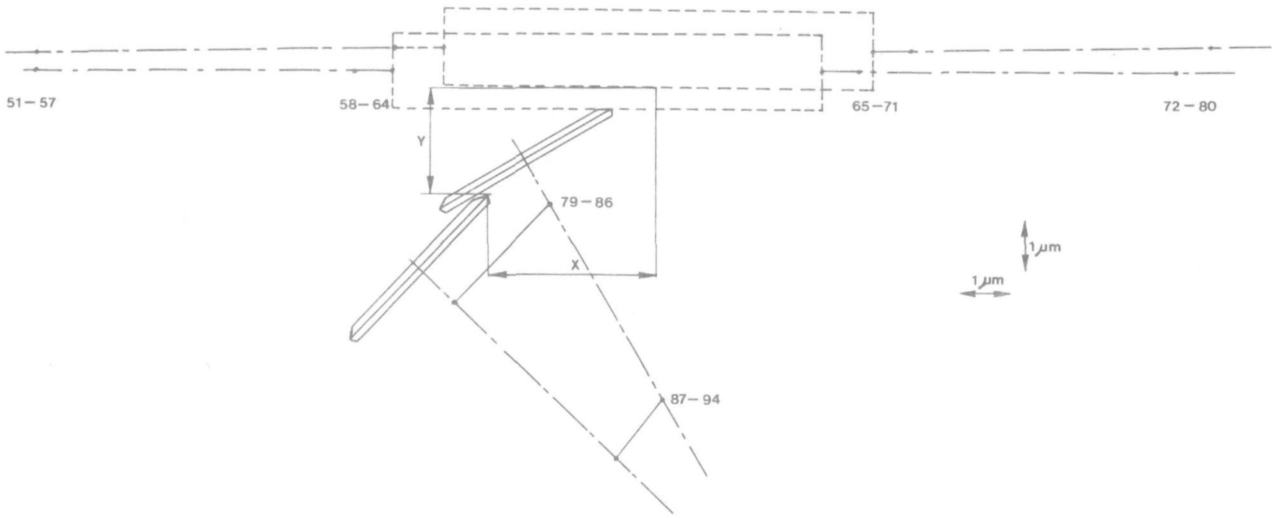

FIGURE 31.

Relative displacement of the grinding wheel and the workpiece.

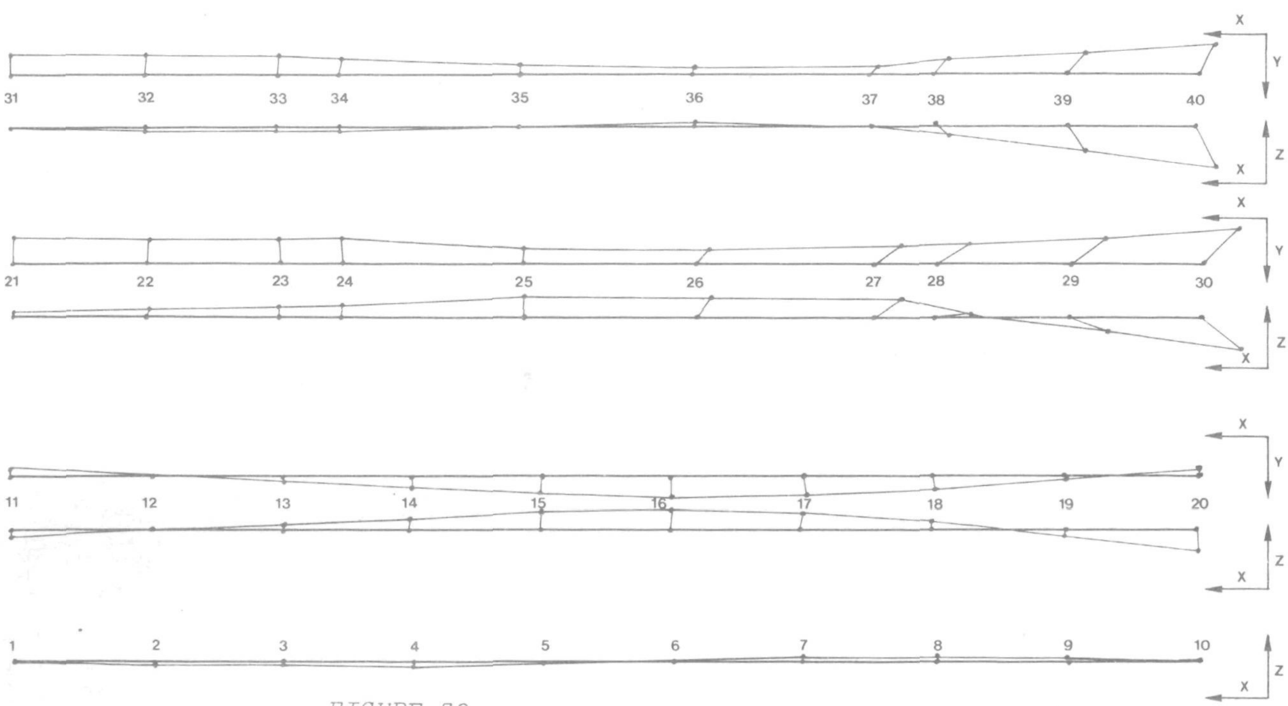

FIGURE 32.

Deformation of the bed after changing the plate thickness.

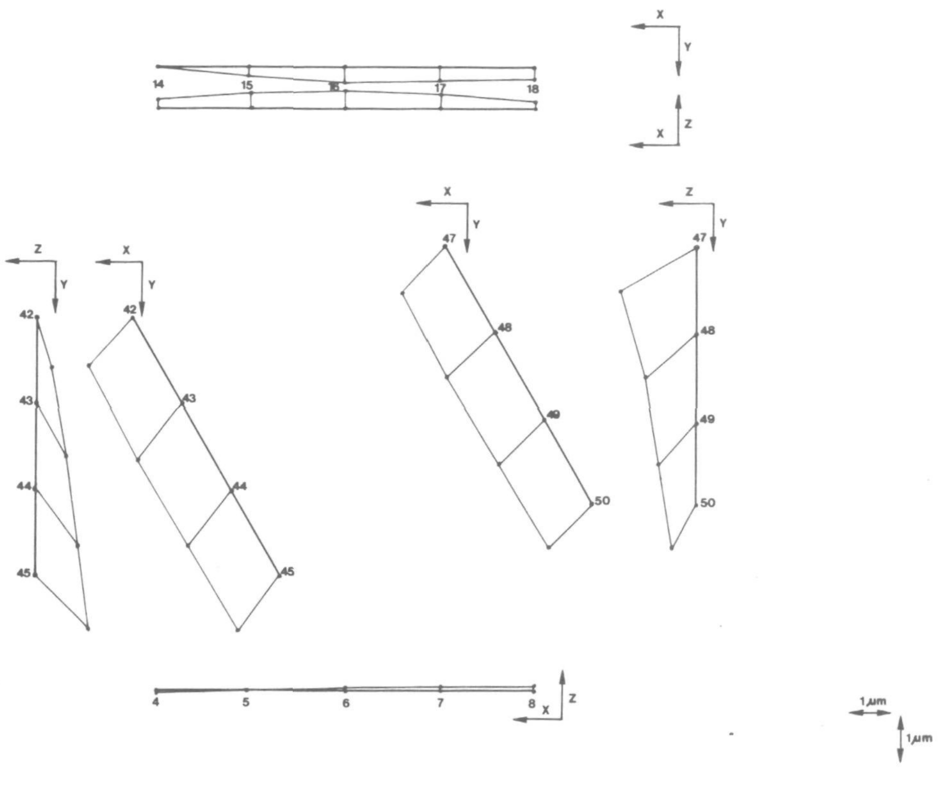

FIGURE 33.

Deformation of the slide after changing the plate thickness.

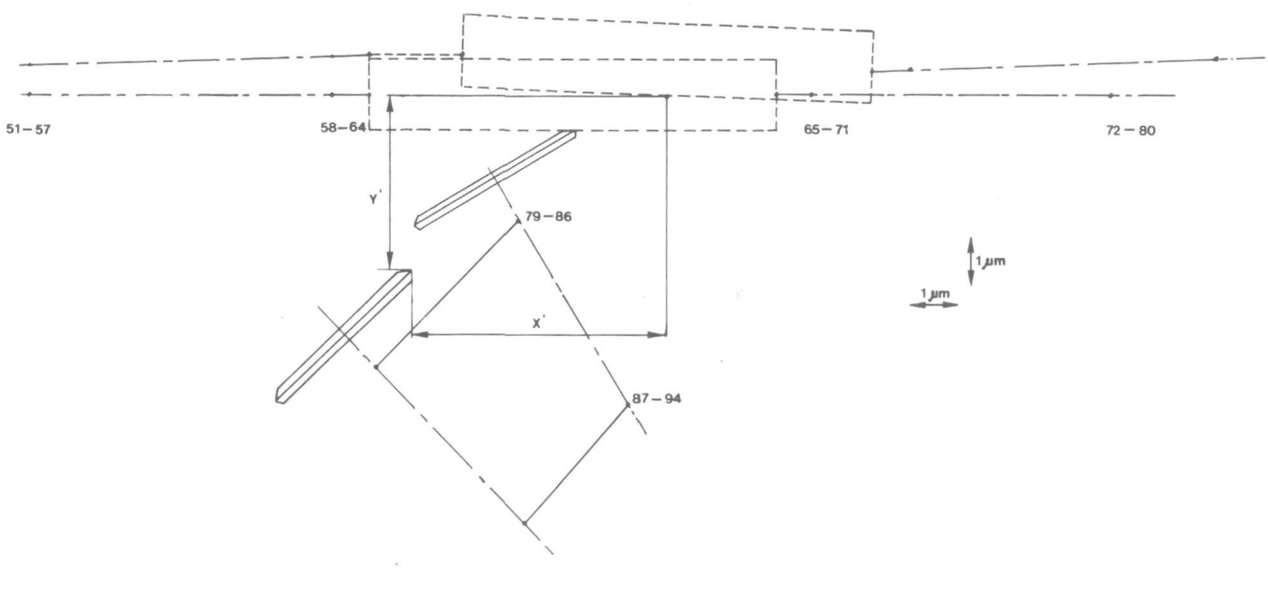

FIGURE 34.

Relative displacement of the grinding wheel and the workpiece after changing the plate thicknesses of the structure.

6.3. Design of the work heads

In addition to the machine structure and the wheel head the work heads and particularly the work head spindles determine the accuracy of the position of the grinding wheel relative to the workpiece. According to the considerations in chapter 4.1 the errors in the workpiece dimensions both in axial and radial direction, caused by the deformations of the work head spindles and the bearings, are not allowed to exceed a value of 0.005 mm at maximum grinding forces. It has already been mentioned that both work heads are almost identical. The difference concerns the drive of the workpiece and the axial bearing of one of the spindles. Based on the same reasons as mentioned with regard to the guideways of the slide and the wheel head hydrostatic bearings will be applied for both work head spindles. An important advantage of these bearings is the possibility to move the spindle in axial direction without special arrangements. As one of the spindles has to move in axial direction in order to fix the workpiece there is no need for any special design of the work head in question. Besides the oil supply for the bearings can be used to apply the clamping force for the workpiece. As the load and the speed at the work head spindles are not such as to make it necessary to design special bearings standard hydrostatic bearings will be applied. The dimensions of the spindles and the bearings follow from calculations similar to those carried out at the design of the grinding spindle. The results of these calculations lead to the following data:

spindle diameter	$d_{w \cdot s}$	$= 105$ mm
bearing distance	b	$= 250 - 350$ mm
radial stiffness front bearing	C_V	$= 150 \cdot 10^4$ N/mm
radial stiffness rear bearing	C_A	$= 50 \cdot 10^4$ N/mm
stiffness axial bearing	C_{AX}	$= 60 \cdot 10^4$ N/mm

7. DRIVE OF WHEEL HEAD, SLIDE AND WORKPIECE

The design of the drive system for the wheel head, the slide and the workpiece is determined by the following requirements. First the grinding wheel has to move according to the geometry of the workpiece in a direction parallel to the center line of the workpiece and in a direction perpendicular to this center line. Secondly this movement and the rotation of the workpiece have to be realized at a speed that is determined by the required metal removal rate. Besides the ratio of the linear speed of the grinding wheel and the circumferential speed of the workpiece has to meet the requirements concerning the grinding forces as described in chapter 3. The way in which the drive system will be designed depends on the types of products that have to be machined and on the number of products of each type.
As the products that will be machined, according to the considerations in chapter 2.1, are generally manufactured in medium to small batches, the system that generates the path of the grinding wheel relative to the workpiece has to be flexible. This means that the information concerning the geometry of the workpiece and the speeds of the wheel head, the slide and the workpiece has to be provided in such a way that a change of this information related to a new workpiece can be achieved as simple as possible.
As besides during the grinding process corrections have to be carried out in order to compensate the wear of the grinding wheel and as movements in a direction perpendicular to the center line of the workpiece are realized by movements of both the wheel head and the slide it is obvious to apply a numerical control for the grinding machine. This means that the information concerning the geometry of the workpiece, the speeds of the wheel head, the slide and the workpiece are supplied to the control of the machine in numerical form. During the process the speed of the workpiece is adapted in such a way that the resulting force at the grinding wheel is perpendicular to the center line of the grinding spindle while the position errors of the grinding wheel caused by the wheel wear are corrected continuously. These two control systems will be discussed in the next chapters.
Starting from the above considerations it has to be decided what type of drive will be applied. First the drive of the workpiece will be discussed. This drive has to achieve a rotation of the workpiece at a speed that varies from 21 to 130 r.p.m. and a maximum torque of 125 Nm. The maximum power for the workpiece drive is 3.4 kW. These data follow from the calculations in chapter 3.2. The requirements for the drive can be met by both electrical and hydraulic motors. The possibility to incorporate a hydraulic drive in the existing hydraulic system leads to the application of a hydraulic motor controlled by an electro-hydraulic servo valve. The main requirement for the motor concerns the stability at low speed while the stiffness of the drive, mainly determined by the volume of oil under pressure of the motor is a second important factor. On account of these demands a so called roll-vane motor is chosen. An advantage is the fact that these motors are available as a complete drive system, including the servo valve and the tacho-generator that are built together with the motor.
Secondly the drivesfor the wheel head and the slide have to be designed. These drives have to move the grinding wheel according to a well defined path at a well defined speed. The drives for the wheel head and the slide can be arranged in different ways. First it is possible to apply linear actuators like hydraulic or pneumatic cylinders. Although these drives are simple the control systems for the position and the speed are complicated, specially as linear position measuring units are necessary as feedback elements, which increases the cost considerably. A second possibility is the application of a screw drive with an electrical or a hydraulic motor. In this case rotating position measuring units can be used which re-

sults in a reduction of the cost. However, the accuracy of the position measurement depends on the accuracy of the drive screw. Third it is possible to apply stepping-motors and screw drives. In this case both the position and the speed of the slides are controlled by controlling the number and the frequency of the pulses supplied to the stepping motors. The accuracy depends also on the accuracy of the drive screws. As the cost of the drive and the control with electrical stepping motors is less than the cost of the other drives mentioned above and as the risk of damage, caused by dirt from the grinding process is relatively small because of the absence of precise measuring units, it is decided to apply electrical stepping motors both for the drive of the slide and the wheel head. Besides the application of electrical stepping motors has another advantage, namely the fact that the complete data handling from the input to the drive motors is in digital form. Because of this parts of the control system can be simplified, c.q. the part that controls the movement of the grinding wheel in a direction perpendicular to the center line of the workpiece. This movement has to be realized by moving both the slide and the wheel head at a speed ratio that equals 2. This ratio can be achieved by a fixed frequency ratio for the stepping motors that drive the wheel head and the slide.
The choice of the power of the stepping motors and the design of the drives depend on the load applied to the drive both as a result of the grinding forces and as a result of the inertia forces caused by acceleration and deceleration of the slides. As the grinding forces in the direction of the movement of the wheel head are eliminated the drive of the wheel head is only determined by the inertia forces. The stepping motors that are considered for the drives generally show a step angle of 1.8° and a maximum step frequency of 5000 steps per second. By means of a so called half step drive it is possible to drive the motors at a step angle of 0.9°.
First the drive of the slide will be considered. The grinding process requires a maximum speed of the slide of 6.7 mm/s, while a rapid travel speed of 50 mm/s has to be realized. As this speed has to correspond with a maximum step frequency of 5000 steps per second each step represents a displacement of 0.01 mm. The accuracy that has to be obtained allows a smallest increment of the positioning system of this value. In order to reduce the speed of the rotating parts of the drive system, and in consequence the inertia forces, a step of 0.9° is chosen. This means that one revolution of the stepping motor corresponds with a displacement of the slide of 4 mm. The screws that will be applied are so called "roller screws". These screws consist of a threaded screw shaft, an internally threaded nut and a number of threaded rollers. The rollers are positioned in the space between the screw shaft and the nut and mesh with the threads of both. The stiffness of these screws is very high because of the large number of contact points between screw, rollers and nut. The diameter of the screw has already been determined, based on requirements concerning the stiffness of the machine and will be 50 mm. Although it is possible to choose a pitch of 4 mm for this screw it is decided to apply a transmission with a ratio 1 : 3 and a pitch of 12 mm in order to reduce the effect of the inertia of the screw. The transmission between the motor shaft and the screw is realized by means of a toothed belt. These belts provide an accurate and stiff transmission together with a good damping, specially with regard to the stepping effect of the motors at low speeds. It is assumed that the diameters of the gears are 36 mm respectively 108 mm at a width of 25 mm. After calculation of the power for the drives the dimensions of the transmission will be determined and a correction will be carried out if necessary. The torque M required at the motor shaft can be devided in two parts, one part M_g, necessary to meet the grinding forces, and another part M_a required to accelerate the slide. In practice the value of M_g reaches its maximum value when accelerations of the slide are negligible and also the maximum acceleration is required at a moment when the grinding

process has not started. So the maximum value of M is determined by either the maximum value of M_g or the maximum value of M_a. The value of M_g can be calculated from the following equation:

$$M_g = \frac{F_n \cdot \cos 30^o \cdot s}{2 \cdot \pi \cdot i} \tag{7.1}$$

in which $F_n \cdot \cos 30^o$ is that component of the grinding force that affects the drive of the slide, s is the pitch of the screw and i the ratio of the transmission between the motor and the screw. As the maximum value of F_n equals 3000 N, the maximum value of M_g becomes:

$$\underline{M_{g\ max} = 1.65 \text{ Nm}}$$

The value of M_a follows from the equation:

$$M_a = I \cdot \dot{\omega} \tag{7.2}$$

in which I represents the total moment of inertia of the slide, the screw, the gears and the motor, determined at the motor shaft, while $\dot{\omega}$ represents the angular acceleration of the motor shaft. The moment of inertia I can be calculated from:

$$I = I_m + I_o + \frac{I_1 + I_s}{i^2} + m \cdot \left(\frac{s}{2 \cdot \pi \cdot i}\right)^2 \tag{7.3}$$

where I_m is the moment of inertia of the motor, I_o and I_1 the moments of inertia of the gears, I_s the moment of inertia of the screw and m the mass of the slide including the wheel head. As the data of the motor are not known a value of $I_m = 1 \cdot 10^{-3}$ kgm^2 is chosen. If necessary a correction is carried out when the exact data of the motor are determined. The moment of inertia of a cylindrical part is calculated from:

$$I_c = 0.125 \cdot m \cdot d^2 \tag{7.4}$$

in which m is the mass of the part and d the diameter. The values of I_o, I_1 and I_s are:

$$I_o = 0.125 \cdot 0.0712 \cdot 0.036^2 = 1.15 \cdot 10^{-5} \text{ kgm}^2$$

$$I_1 = 0.125 \cdot 0.64 \cdot 0.108^2 = 9.4 \cdot 10^{-4} \text{ kgm}^2$$

$$I_s = 0.125 \cdot 15.3 \cdot 0.05^2 = 4.8 \cdot 10^{-3} \text{ kgm}^2$$

So:

$$I = 1 \cdot 10^{-3} + 1.15 \cdot 10^{-5} + \frac{5 \cdot 74 \cdot 10^{-3}}{3^2} +$$

$$+ 1200 \cdot \left(\frac{12 \cdot 10^{-3}}{2 \cdot \pi \cdot 3}\right)^2 \text{ kgm}^2$$

or:

$$I = 2.13 \cdot 10^{-3} \text{ kgm}^2$$

The value of $\dot{\omega}$ is determined by the time or the distance in which the maximum speed has to be reached. In this case the distance is assumed to be 4 mm at a constant acceleration. This distance corresponds with a rotation of the motor shaft of $2 \cdot \pi$ radians. As this value has to be reached after t seconds:

$$2 \cdot \pi = 0.5 \cdot \dot{\omega} \cdot t^2$$

As the value of ω after t seconds has to be $25 \cdot \pi$ rad/s the value of t equals 0.16 s. This leads to an angular acceleration $\dot{\omega} = 500$ rad/s^2 and from this value to:

$$M_a = 2.13 \cdot 10^{-3} \cdot 500 = \underline{1.06 \text{ Nm.}}$$

If the efficiency of the drive is assumed to be 75 per cent the above calculations lead to the choice of a stepping motor with a maximum torque of 2.2 Nm at a speed range from 0 to 700 steps per second and a maximum torque of 1.4 Nm over the whole speed range. A stepping motor that meets these requirements is e.g. a "Slo-Syn" motor type M 112 - FD25, of which the relation of torque and speed is shown in figure 35. The moment of inertia of this

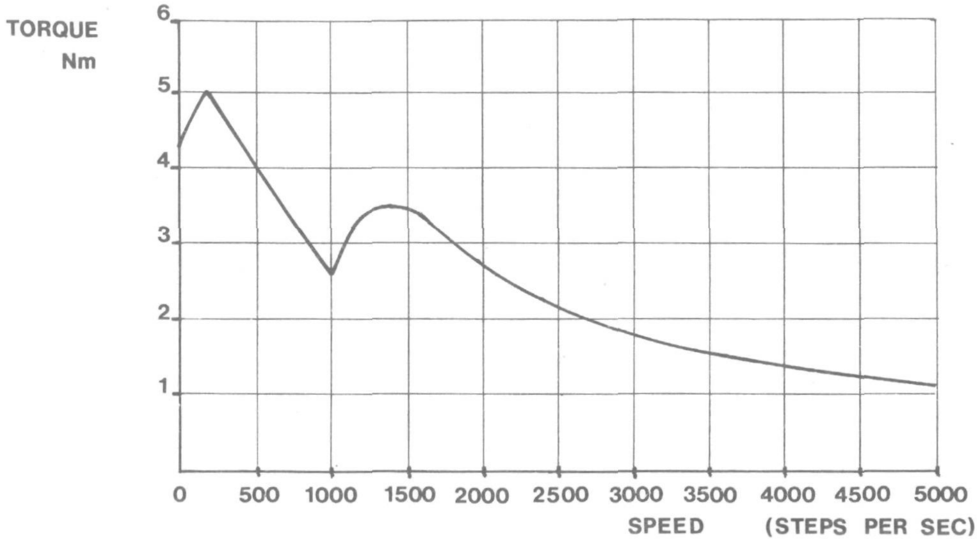

FIGURE 35.

Relation of torque and speed of a "Slo-Syn" stepping motor type M 112-FD 25.

motor equals $8 \cdot 10^{-4}$ kgm^2. A correction of the calculations according to this value does not lead to a smaller motor.
According to the manufacturer's instructions the type of belt and the dimensions of the gears are determined. It appears that a toothed belt with a pitch of 5 mm and a width of 25 mm and gears with 16 teeth respectively 48 teeth meet the requirements based on the calculations above. Although the dimensions of the gears are smaller than assumed before the decrease of the total moment of inertia does not lead to the application of a smaller motor.
The design of the drive of the wheel head is based on the following considerations. The grinding process requires a speed of the wheel head in a direction perpendicular to the center line of the workpiece of 5 mm/s, while a rapid travel speed of 25 mm/s will be applied. As this speed has to correspond with

the maximum step frequency of 5000 steps per second the smallest increment of the displacement is 0.005 mm. However, it appears that a smallest increment of at most 0.001 mm has to be achieved and that because of the following. During grinding the grinding wheel wears and this wear causes an error in the dimensions of the workpiece. In order to correct this wear the position of the wheel head has to be adapted to the new dimensions of the grinding wheel. If the correction steps are too large marks or even measurable steps on the workpiece surface will appear. A smallest step of 0.001 mm seems to be acceptable. As it is not possible to meet these requirements with one stepping motor a second stepping motor is applied. While the first motor drives the screw the second motor drives the nut. This means that the absolute displacement of the wheel head depends on the relative angular displacement of the screw and the nut. It has already been mentioned that a movement of the wheel head perpendicular to the center line of the workpiece is achieved by moving both the wheel head and the slide according to a fixed ratio that is determined by the angle between the center lines of the grinding spindle and the workpiece. As this angle equals 60^{o} a displacement of the slide of x mm and a displacement of the wheel head of $2 \cdot x$ mm, relative to the slide, result in an absolute displacement of the wheel head of $x \cdot \sqrt{3}$ mm. As the input data for the drive system are related to the absolute displacement of the wheel head a conversion of these data to the numbers of pulses supplied to the stepping motors is necessary. In order to realize an absolute speed of the wheel head of 25 mm/s the speed of the wheel head relative to the slide has to be 28.87 mm/s. As it is not very important to determine the rapid travel speed accurately the drive system is designed as follows. One motor is driving the screw in such a way that one step corresponds with a relative displacement of the wheel head of 0.005 mm. The second motor drives the nut in such a way that one step of this motor corresponds with a displacement of the wheelhead relative to the slide of 0.001 mm. If both stepping motors act together the rapid travel speed becomes 30 mm/s. It is decided to drive both stepping motors at the same frequency, while a correction of the position of the wheel head is realized by supplying pulses to the stepping motor that drives the nut. The power of the stepping motors is calculated as follows. During acceleration of the wheel head in a direction perpendicular to the center line of the workpiece the ratio of the accelerations of both the slide and the wheel head relative to the slide is 1 : 2. In order to reduce the acceleration and deceleration time as much as possible the acceleration of the wheel head will be twice the maximum acceleration of the slide. The acceleration of the wheel head is composed of the two parts, one part achieved by the motor that drives the screw, the other part by the motor that drives the nut. As the acceleration of the slide $a_s = 0.3125$ m/s^2 the acceleration of the wheel head will be $a_w = 0.625$ m/s^2. The motor that drives the screw has to accelerate the wheel head at $\frac{5}{6} \cdot 0.625 = 0.52$ m/s^2. In order to avoid a large transmission ratio between the second stepping motor and the nut a pitch of 3 mm is chosen for the screw. At a step angle of 0.9^{o} the ratio of the transmission between the first motor and the screw equals 1.5. Based on the same considerations as mentioned at the design of the drive of the slide a transmission by means of a toothed belt is applied. The calculations of the moment of inertia of the drive are based on the following assumptions. The diameter of the screw will be 25 mm. Although the load allows a smaller diameter this value has been chosen on account of secondary demands like mounting facilities for gears and bearings. The moment of inertia of the stepping motor is assumed to be $2 \cdot 10^{-4}$ kgm^2. As the mass of the wheel head, including the grinding wheel and the motor is 500 kg, the value of the total moment of inertia I' at the shaft of the motor comes to $3 \cdot 10^{-4}$ kgm^2. The angular acceleration follows from the value of the linear acceleration of the

wheel head and equals 1633 rad/s^2. The torque required to realize this acceleration $M_a' = 1633 \cdot 3 \cdot 10^{-4} = 0.49$ Nm. A "Slo-Syn" stepping motor, type M 093-FC 14 meets this requirement. The inertia moments of both the motor and the transmission gears do not exceed the assumed values.
The motor that drives the nut has to achieve an acceleration of the wheel head of $\frac{1}{6} \cdot a_w = 0.1$ m/s^2. As one step of the motor corresponds with a displacement of the wheel head of 0.001 mm and as the pitch of the screw equals 3 mm the transmission ratio between the motor and the nut has to be 7.5 at a step angle of 0.9^o. The moment of inertia of the motor is assumed to be $7 \cdot 10^{-5}$ kgm^2 while the nut is regarded as a cylinder with a diameter of 60 mm and a length of 100 mm. A calculation according to the equation 7.3 shows that the total moment of inertia at the motor shaft $I'' = 1.2 \cdot 10^{-4}$ kgm^2. As the value of the angular acceleration is also 1633 rad/s^2 for this motor, the required torque $M_a'' = 0.2$ Nm. A "Slo-Syn" stepping motor type M 063-FC 06 meets the requirements for this drive.
In the survey the relevant data of the drives of the work head spindle, the slide and the wheel head are given. The arrangement of these drives is shown in figure 36.

Work head spindle

Motor:	Hydraulic "roll-vane" motor controlled by electro-hydraulic servo valve
Speed:	20 - 130 r.p.m.
Maximum torque:	125 Nm

Slide

Motor:	Electric stepping motor with step angle 0.9^o
Speed:	0 - 5000 steps per second
Maximum torque:	2.2 Nm at 0 - 700 steps per second 1.4 Nm at 0 - 5000 steps per second
Screw:	roller screw, 50 mm diameter and pitch 12 mm
Speed ratio motor screw:	3 : 1
Smallest increment:	0.01 mm
Speed of slide:	0 - 50 mm/s

Wheel head

a. Drive of the screw

Motor:	Electric stepping motor with step angle 0.9^o
Speed:	0 - 5000 steps per second
Maximum torque:	0.7 Nm at 0 - 5000 steps per second
Screw:	roller screw, 25 mm diameter and pitch 3 mm
Speed ratio motor screw:	15 - 1
Smallest increment:	0.005 mm
Speed of wheel head:	0 - 25 mm/s

b. Drive of the nut

Motor:	Electric stepping motor with step angle 0.9^o
Speed:	0 - 5000 steps per second
Maximum torque:	0.2 Nm at 0 - 5000 steps per second
Speed ratio motor nut:	7.5 : 1
Smallest increment:	0.001 mm
Speed of wheel head:	0.5 mm/s

The control of the drives and the way in which the position corrections are carried out are described in chapter 9.

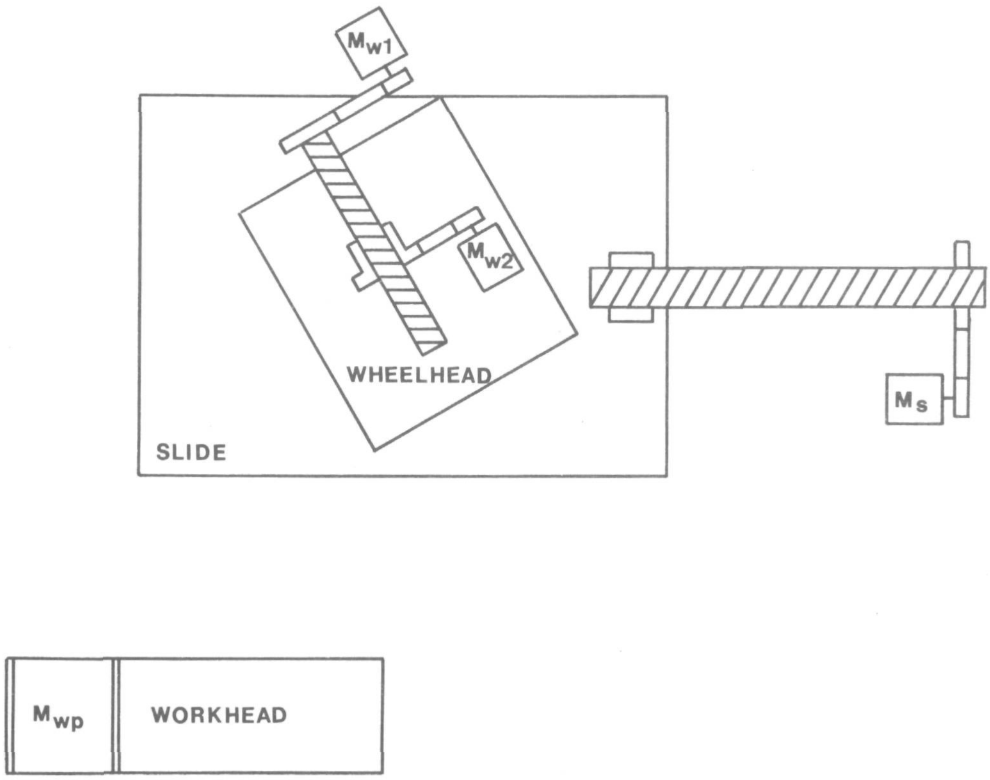

FIGURE 36.

Drives of the slide, the wheel head and the workpiece.

8. APPARATUS FOR DRESSING THE GRINDING WHEEL

8.1. Wheel wear and dressing conditions

The grinding process as described in the chapters 2 and 3 involves a considerable wear of the grinding wheel. At high metal removal rates the grinding ratio G may even reach a value of 4 [10]. This means that during the grinding process the position of the grinding wheel has to be corrected in order to eliminate the errors in the dimensions of the workpiece caused by the wheel wear. Besides it will be necessary to correct the shape of the grinding wheel as the wear is not equally distributed over the wheel surface. This correction will be carried out by dressing the grinding wheel with a diamond dressing wheel. The reason why a diamond wheel is applied is the fact that stationary dressing tools need an interruption of the grinding process. This interruption, together with the time needed for the dressing operation itself, results in a considerable increase of the machining time. Although it is not known how the dressing process at circumferential speeds of the grinding wheel up to 150 m/s will proceed, the research carried out on this subject [15, 16, 17] gives an indication how to choose the dressing conditions. This research did concern in the first place the influence of the speed of the diamond wheel with regard to the speed of the grinding wheel. It appeared that at high values of the relative speed between the diamond wheel and the grinding wheel the influence of the directions of the circumferential speeds of the diamond wheel and the grinding wheel is not significant. However, at high relative speeds the roughness of the dressed wheel surface decreases, which results in a smaller value of the metal removal rate than can be realized. In order to reduce this effect it is possible to choose a wheel with a smaller number of active cutting edges, which means a smaller diamond concentration. Based on these facts a speed at the circumference of the diamond wheel adjustable from 10 to 50 m/s is chosen. In the area of contact the directions of the speeds at the circumference of both wheels are the same, resulting in a relative speed of 100 - 140 m/s. In order to determine the depth of cut of the diamond wheel a_d in mm per revolution of the grinding wheel it is necessary to consider the wear of the wheel. In figure 37 the

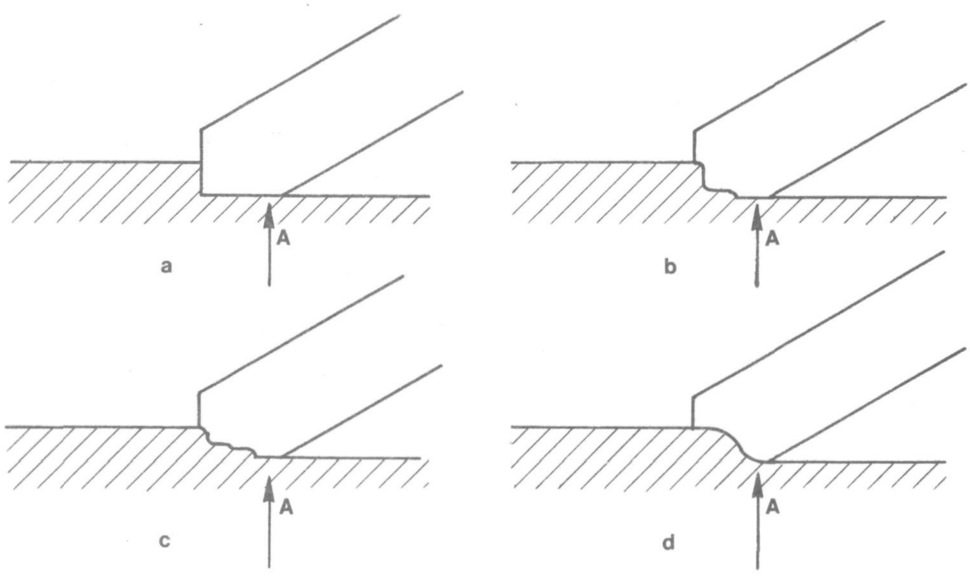

FIGURE 37.

Progress of the wear of the grinding wheel.

progress of the wear at the surface of the grinding wheel is shown. This wear starts during the first revolution of the workpiece at the edge of the wheel and finally generates a shape of the wheel as shown in stage d. If only a cylindrical surface has to be machined the wear at the part A of the grinding wheel is important. In this case the correction can be little as the total wear is distributed over a wider part of the grinding wheel. However, the dressing conditions will be based on the requirement that the original shape of the grinding wheel has to be maintained continuously. In chapter 3 it has been determined that at the wheel surface A_r the maximum value of the specific metal removal rate $z'_{max} = 2000\ mm^3/mm.s$. This means that at this part of the grinding wheel the maximum wear per mm width of the wheel $w'_{max} = z'_{max}/G$. As the minimum value of G comes to 4 the maximum value of the specific wear $w'_{max} = 500\ mm^3/mm.s$. As the circumferential speed of the grinding wheel $v_s = 150$ m/s the depth of cut of the diamond wheel a_d has to be at least w'_{max}/v_s. So the infeed of the diamond wheel has to be such as to realize a value of $a_{d\ max} = 0.0033$ mm. In order to know the power that is required for the drive of the diamond wheel it is necessary to determine the tangential force at the circumference of the diamond wheel. From research concerning dressing with diamond wheels [18] only data concerning radial forces are known with sufficient reliability. However, the relation between radial and tangential forces has been determined at single point diamond dressing tools [19]. As the shape of these diamonds does not differ very much from the shape of the diamonds applied in diamond wheels this relation will be used for the calculation of the tangential forces at the circumference of the diamond wheel. Also in this case an extrapolation has to be carried out as data concerning the process described in this thesis are not known. Based on the results of the research mentioned above it is assumed that the minimum value of the specific tangential force $F'_{dt} = 2$ N/mm at a specific radial force $F'_{dr} = 10$ N/mm. In figure 38 the position of the diamond wheel relative to the grinding wheel is shown. From this figure it appears that at the maximum depth of cut of the diamond wheel $a_{d\ max}$ at the surface A_r, the depth of cut at the surface A_a $a'_{d\ max} = a_{d\ max}/tg30^o = 0.0057$ mm. As both the radial and tangential dressing forces are proportional to the depth of cut the values of these forces come to $F'_{dta} = 3.4$ N/mm and $F'_{dra} = 17$ N/mm. As, according to chapter 3, the width of the wheel surface A_r equals 12 mm and the width of the surface A_a equals 16 mm the value of the resulting tangential force $\underline{F_{dt} = 78\ N}$ and the value of the resulting radial force $\underline{F_{dr} = 295\ N}$.

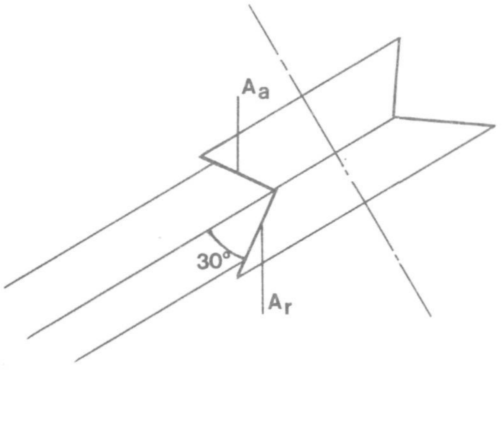

FIGURE 38.

Grinding wheel and diamond wheel during dressing.

It is obvious that the above calculations are related to the most unfavourable situation. In cases where the amount of grinding wheel material that has to be removed reaches the values mentioned above it is advisable to apply a smaller wheel width. Besides at high metal removal rates a substantial part of the grinding wheel material is removed by the grinding process itself. Nevertheless the design of the dressing apparatus will be based on the forces and speeds calculated above, in order to be sure that extreme conditions can be realized if necessary. A disadvantage of the method of continuous dressing is the fact that the drive of the grinding wheel has to provide also the power for the dressing process. This power P_d can be expressed by the relation $P_d = F_{dt} \cdot v_s$. However, the tangential dressing force F_{dt} seldom reaches a value that exceeds 25 per cent of its maximum because of the fact that in extreme situations a smaller wheel width will be applied and the fact that in most cases the dressing process has to correct only a part of the surface of the grinding wheel. The maximum power for the drive of the diamond wheel $P_{dw} = F_{dt\ max} \cdot v_{d\ max}$, in which v_d represents the circumferential speed of the diamond wheel. So $\underline{P_{dw} = 4\ kW}$. In order to keep the speed of rotation at a low value and on the other hand to obtain a longer life of the diamond wheel the diameter of this wheel will be 200 mm. This means that the drive of the diamond wheel has to provide a maximum speed of <u>4800 r.p.m.</u> at a maximum torque $\underline{M_{dw} = 7.8\ Nm}$.

8.2. Design of the dressing apparatus

From the first section of this chapter it appeared that the diamond wheel has to be driven at a speed of 4800 r.p.m. A direct drive without a transmission is preferred in order to avoid vibrations of the transmission at the high speeds that are applied and to reduce the mechanical losses of the total drive. As the dressing apparatus has to be mounted on the wheel head at the circumference of the grinding wheel it is important that both the weight and the dimensions of this unit are as small as possible. For this reason and because of the existence of a hydraulic system in which this drive can be incorporated a hydraulic motor is chosen. One of the very few motors that can meet the requirements is the "Vickers" axial piston motor, type MF 3911-25. This motor provides a torque of 12 Nm at a maximum speed of 5400 r.p.m. and an oil flow of 54 l/mm. Although the control of the speed of the diamond wheel does not make high demands upon the components of the control system, an electro-hydraulic servo valve will be applied and that by the following reason. Each diamond wheel will show errors in roundness. These errors may be transferred to the grinding wheel. If the ratio of the speeds of rotation of the grinding wheel and the diamond wheel is a whole number the surface of the grinding wheel will show wavings that lead to vibrations during grinding. In order to avoid this fenomenon a control of the speed of the diamond wheel is necessary as the speed of rotation of the grinding wheel varies between 5700 and 10.000 r.p.m. It is obvious that the accuracy of the bearings that support the spindle to which the diamond wheel is mounted has to meet requirements of the same kind of those related to the bearings of the grinding spindle and the work head spindles. Based on this fact and on the existence of a hydraulic system suited to supply the oil for the bearings hydrostatic bearings will be applied. In this case standard bearings meet the requirements both concerning accuracy and stiffness.
The dressing head has to move in a radial direction relative to the grinding wheel. In this case also hydrostatic guideways are applied in order to obtain an accurate movement of the diamond wheel and particularly to provide maximum damping with regard to vibrations caused by the grinding process itself or by unbalance of the rotating parts, specially the grinding wheel. As the dressing process is carried out at that speed of the grinding wheel at which the grinding process takes place and as the dressing apparatus is mounted to the wheel head the position of the dressing head relative to the grinding wheel does not influence the roundness errors caused by unbalance forces. For this reason the dressing apparatus is mounted opposite to the workpiece in order to reduce the deformation of

the grinding spindle caused by the normal grinding force F_n. The movement of the dressing head is realized by means of a screw driven by an electric stepping motor. It is obvious to apply this type of motor as this drive has to be incorporated in the system that determines the position of the grinding wheel relative to the workpiece. As the maximum depth of cut of the diamond wheel $a_{d\ max}$ = 0.0033 mm the maximum speed of the dressing head $v_{dr\ max} = a_{d\ max} \cdot n_{s\ max}/60$ = 0.525 mm/s. According to the smallest increment of the displacement of the wheel head the smallest increment of the displacement of the dressing head is also fixed at 0.001 mm. This means that at 400 steps per revolution of the stepping motor and a screw pitch of 1 mm a transmission between stepping motor and screw with a ratio 2·5 has to be applied. As in this case accelerations and decelerations are not of interest the power of the stepping motor is determined by the radial dressing force F_{dr}. The torque of the motor M_d follows from the following relation:

$$M_d = \frac{F_{dr} \cdot s}{2 \cdot \pi \cdot i} \tag{8.1}$$

in which s represents the pitch of the screw and i the ratio of the transmission between motor and screw. So M_d = 0.02 Nm. In this drive a "Slo-Syn" motor type M061 - FC02 will be applied.
The complete control of the grinding machine, including the control of the dressing apparatus, will be described in the following chapter.

9. THE CONTROL OF THE GRINDING MACHINE

The control of the grinding machine can be divided in two parts, one part related to the grinding process itself, the second part related to the generation of the geometry of the workpiece.

9.1. Control of the grinding process

The control of the grinding process concerns in the first place the control of the circumferential speed of the grinding wheel. This speed is determined by the oil flow to the hydraulic motor that drives the grinding spindle and by the diameter of the grinding wheel. In figure 39 the simplified block diagram of this control is shown. The value of the diameter

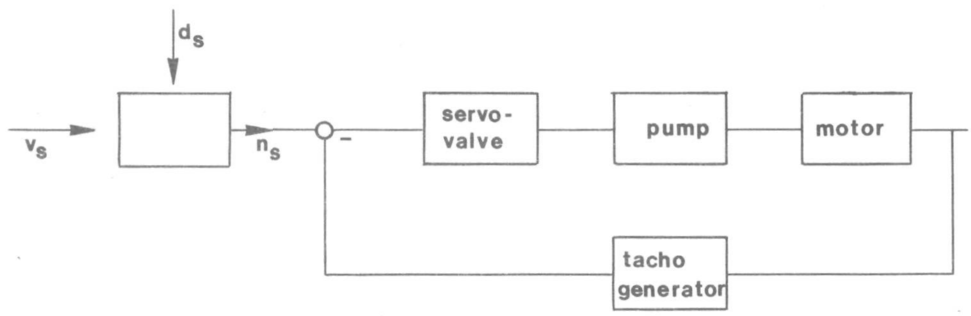

FIGURE 39.

Simplified block diagram of the speed control of the grinding wheel.

of the grinding wheel d_s is derived from the control of the dressing apparatus as will be shown in the discussion of this part of the control. Secondly the control of the grinding process concerns the elimination of grinding forces perpendicular to the plane of the grinding wheel. In figure 5 in chapter 3 the relation between the depth of cut a and the feed s at different values of the diameters of the grinding wheel and the workpiece is shown. At the values of a and s that meet this relation the grinding forces perpendicular to the plane of the grinding wheel are eliminated. As the value of a is determined by the dimensions of the unmachined workpiece and the final geometry that has to be realized the only controlable parameter is the feed s. The value of s depends on the speed of rotation of the workpiece n_w and the speed of the wheelhead in axial direction of the workpiece v_a. As a change of the value of n_w does not affect the value of the metal removal rate it is decided to apply a control of the speed of rotation of the workpiece in order to keep the direction of the resulting grinding force perpendicular to the center line of the workpiece. It is obvious that it is necessary to apply a device that determines whether the requirement concerning the direction of the grinding force is met. As this requirement means that the load in axial direction of the grinding spindle equals zero this device can be a transducer that measures the load applied to the axial bearing of the grinding spindle. Because of the application of hydrostatic bearings this load can be determined from the difference in pressure in the opposite chambers of the hydrostatic bearing. As the only function of this axial bearing concerns the location of the grinding spindle in axial direction the pressure in the oil chambers can be very little. For this reason the oil that flows out of the radial front bearing is led to the chambers of the axial bearing and from there through oil gaps combined with two adjustable restrictors as shown schematically in figure 40. The restrictors are applied to adjust

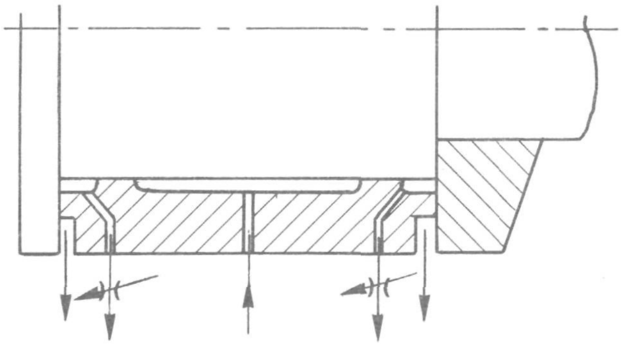

FIGURE 40.

Combined radial and axial spindle bearing.

the pressure in the chambers of the axial bearings more accurately by choosing the correct dimensions of the bearing gap. As the oil supply to the radial bearings is realized by means of one pump for each chamber the properties of these bearings are hardly affected by these axial bearings. In figure 41 a simplified block diagram of the control of the direction of

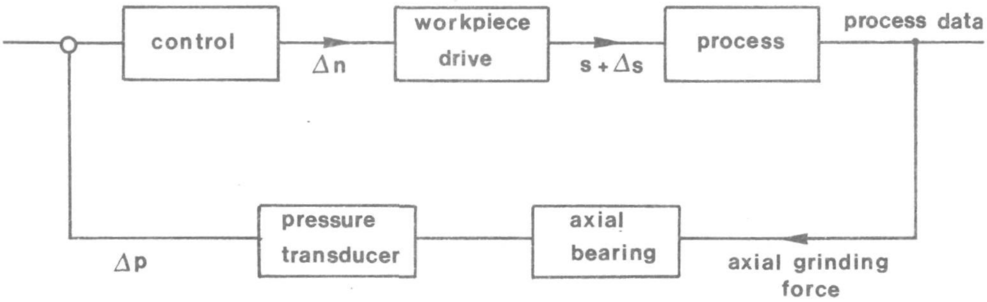

FIGURE 41.

Simplified block diagram of the control of the grinding forces.

the grinding forces is shown.

9.2. Control of the grinding wheel position

The geometry of the workpiece is determined by the path of the grinding wheel relative to the workpiece and by the shape of the grinding wheel. In chapter 2 this shape of the grinding wheel has already been determined. The relative positions of the workpiece, the grinding wheel and the dressing wheel are shown schematically in figure 42.

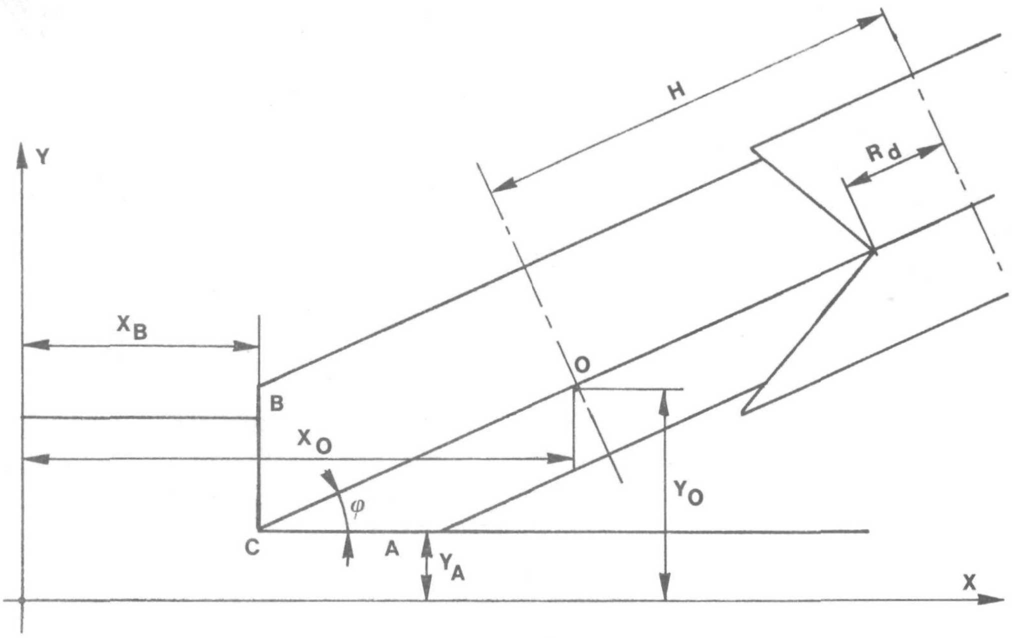

FIGURE 42.

Relative positions of grinding wheel, dressing wheel and workpiece.

From this figure it appears that three parts of the surface of the grinding wheel are of major interest with regard to the geometry of the workpiece. In the first place the position of part A determines the diameter of the workpiece. Secondly the part B determines the dimensions of the workpiece in axial direction and finally the part C determines the shape of the change of a cylindrical part of the workpiece into a plane perpendicular to the center line of this workpiece. According to this it is possible to consider three cases:
First the grinding wheel is machining a cylindrical part of the workpiece. In this case only the position of part A of the grinding wheel is of interest. According to figure 42 this position is determined by the value of y_A. This value can be expressed by:

$$y_A = y_0 - (H - R_d) \cdot \sin\phi \qquad (9.1)$$

in which y_0 represents the y-co-ordinate of the center of the grinding wheel O, H the center distance of the grinding wheel and the dressing wheel and R_d the radius of the dressing wheel as indicated in figure 42.
Secondly the grinding wheel is machining a plane perpendicular to the center line of the workpiece. This means that only the position of part B of the grinding wheel surface is of interest. This position is determined by the value of x_B, which follows from:

$$x_B = x_0 - (H - R_d) \cdot \cos\phi \qquad (9.2)$$

Thirdly the grinding wheel is machining the change of a cylindrical part into a plane perpendicular to the center line of the workpiece. In this case the position of part C as determined by the co-ordinates x_B and y_A is important. The reason to consider these three cases separately is the following. If a cylindrical part is machined the value of y_A has to be kept constant and independant of the wear of the wheel or the dressing. At the end of this chapter it will be shown that the part A will always keep its correct shape by means of the dressing operation. This means that a change of the center distance of the grinding wheel and the dressing wheel ΔH has to be followed immediately by a displacement of the center 0 of the grinding wheel $\Delta y_0 = \Delta H \cdot \sin\phi$. In order to keep this correction procedure as simple as possible the displacement Δy_0 is realized by a displacement $\Delta y_0/\cos\phi$ of the wheel head relative to the slide. Although this leads to a displacement of the point 0 in the x-direction it is sufficient to correct only the data concerning the dimensions in axial direction by a displacement of the origin of the co-ordinate system, a so called "zero shift". In the case of machining a plane perpendicular to the center line of the workpiece the same method of correction is applied. This means that the displacement of the point 0 in x-direction $\Delta x_0 = \Delta H \cdot \cos\phi$ is realized by a displacement $\Delta x_0/\sin\phi$ of the wheel head together with a zero shift in y-direction. Finally the machining of the change of a cylindrical part of a workpiece into a plane perpendicular to this cylinder needs a dressing operation that provides a correct shape of the part C and a simultaneous correction of the position of the point 0 in x- and y-direction. The control of the movement of the grinding wheel can be regarded as a control of the movement of the center 0 of the grinding wheel if the correction procedure is carried out properly. This means that it is possible to start from a standard two-axes numerical control as it is widely used at numerically controlled turning machines. As mentioned before the shape of the grinding wheel is corrected continuously by means of a dressing operation. However, it is necessary to determine the value of the displacement of the dressing wheel ΔH that is necessary to achieve the correct shape of the parts A, B or C of the grinding wheel. This means that this shape has to be determined by measuring. At the University of Aachen in Germany a method for measuring wheel wear during grinding has been developed [20]. This method uses a pneumatic device as shown in figure 43. By measuring

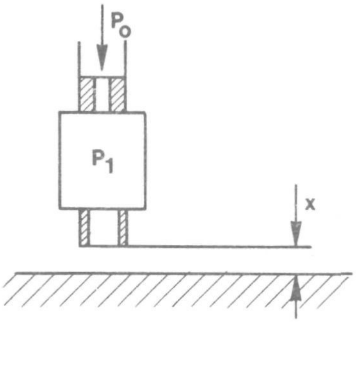

FIGURE 43.

Pneumatic device for the measurement of the wear of the grinding wheel.

the value of the air pressure p_1 the value of the height of the gap between the nozzle and the wheel surface x can be determined with a maximum error of about 0.001 mm. In figure 44 the positions of the measuring de-

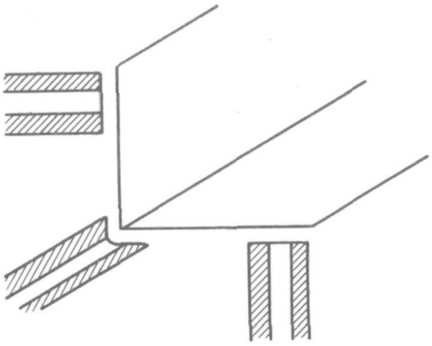

FIGURE 44.

Positions of the measuring devices.

vice with regard to the grinding wheel are shown. It is obvious that according to the parts of the grinding wheel that determine the shape of the workpiece three measuring devices are applied. These devices are placed quite near the place where the dressing wheel touches the grinding wheel. The value of ΔH will be determined as follows. Depending on the shape of the workpiece that is machined one of the measuring devices is considered. First the dressing head is moved towards the grinding wheel until the gap between the wheel surface and the nozzle reaches a certain value and this value is kept constant during grinding. This means that the dressing head has to be moved if the wear of the grinding wheel does affect the value of the gap. In this way an accurate control of the geometry of the workpiece can be achieved.

10. THE POWER SUPPLY OF THE GRINDING MACHINE

The power supply for the grinding machine concerns in the first place the hydraulic system for the drives of the grinding spindle, the workpiece and the dressing wheel and the oil supply for the hydrostatic bearings. Secondly an electric system is applied with regard to the electric motors that drive the pumps and the power supply for the drive of the stepping motors. This second part of the power supply is left out of consideration as only simple a.c.-motor drives are involved. Besides the power supply for the stepping motors is designed by the manufacturer and is included in the control system for these motors. However, the complete hydraulic system has to be designed based on the specific requirements of the machine. In figure 45 this hydraulic system is shown schematically.
The first part of this system concerns the drive of the hydraulic motor for the grinding spindle. The oil for this motor is supplied by a variable displacement axial piston pump PV1 controlled by a servo mechanism and an electrohydraulic servo valve SV1. As this system is a so-called closed system it is necessary to compensate the leakage flow of both the motor and the pump by means of a boost pump P. This pump provides also a cooling of the oil in this system by means of a flow of oil through the pump housing and a cooler. The oil supply for the servo mechanism is achieved by a pump PV3 that forms part of a second system. This part of the hydraulic system supplies also the oil for the drive of the work head, controlled by the servo valve SV2, and the drive of the dressing wheel, controlled by the servo valve SV3. Besides the oil for the hydrostatic bearings of the work head spindles and the hydrostatic guideways of the wheel head, the slide and the dressing head is supplied by this pump PV2. This means that this pump has to maintain a constant pressure in this part of the hydraulic system. The third part of the hydraulic system concerns the oil supply for the hydrostatic bearings of the grinding spindle and the dressing spindle. This part of the system has to be arranged separately as for this application a very low viscosity of the oil is required with regard to the heat generation at high spindle speeds. Two so-called multiple-pump units PV4 and PV5 are applied in order to supply the oil to the eight chambers of the bearings of the grinding spindle and to the bearings of the dressing spindle. It is obvious that in all the systems a very effective filtering of the oil is necessary. Besides cooling systems will be applied in order to remove the heat generated in the bearings, the pumps and the motors. Based on the calculations of the grinding power, the dressing power and the power for the hydrostatic bearings the total power for the grinding machine will be about 225 kW, taking into account the efficiency of the pumps and the electric motors.

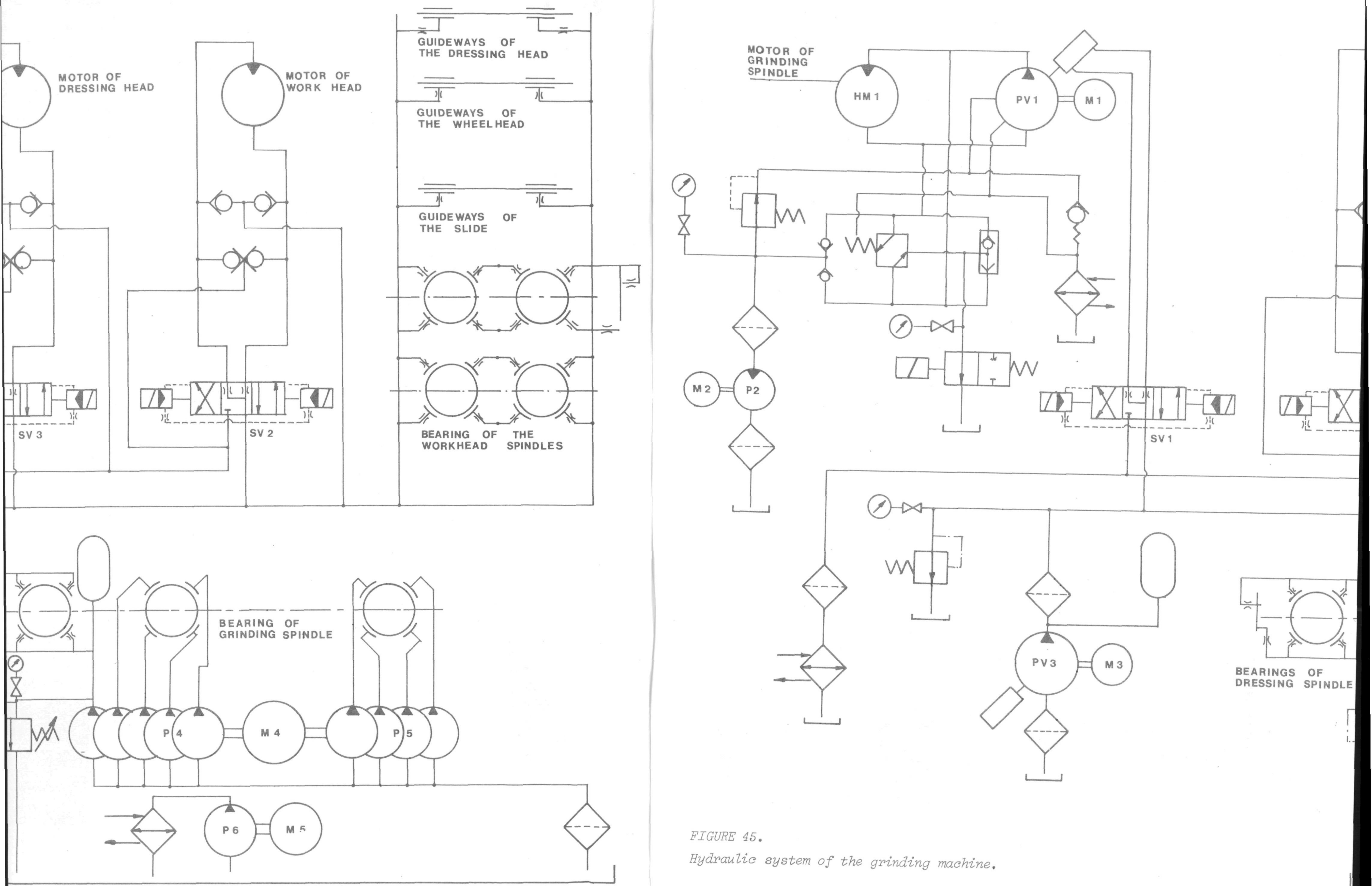

FIGURE 45.

Hydraulic system of the grinding machine.

11. SECONDARY ASPECTS OF THE DESIGN

11.1. Safety

One of the most important aspects of the application of high speed grinding concerns the safety of the machine in the event of a wheel bursting. In many institutes extended research has been carried out to develop wheel guards that offer satisfactory protection against operator injury and machine damage caused by fragments of a burst grinding wheel [21, 22, 23, 24].
The design of the grinding machine does already include a number of advantages with regard to the safety. First the machine will be closed completely when operating. Even inspection windows are avoided as these windows do not provide any facility for inspection of the grinding process. Secondly the plane of the grinding wheel is almost parallel to the front of the machine which enables an effective protection against fragments of a wheel leaving the wheel guard. Thirdly the width of the grinding wheel is only 20 mm which means that the kinetic energy of the rotating grinding wheel is relatively small.
Starting from these facts the following measures are taken. At first a heavy wheel guard is applied as shown in figure 46. In order to absorb the

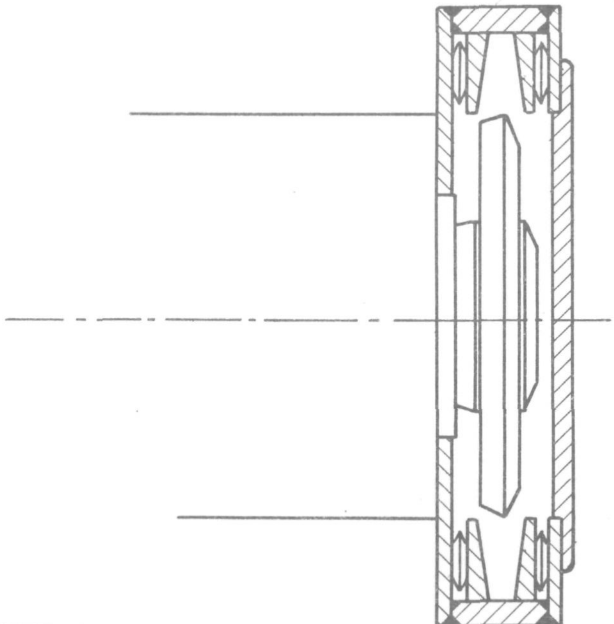

FIGURE 46.

Wheel guard with energy absorbing wedge.

energy of burst grinding wheels two plates forming a wedge-shaped opening, between which fragments of a burst grinding wheel can be caught, are applied. The plates are preloaded by means of diaphragm springs as shown in the figure. At the front of the wheel guard there has to be an opening in order to allow the grinding wheel to meet the workpiece. This opening is determined by the dimensions of the largest workpiece. This means that an additional protection from fragments which would escape from this opening is required. As a consequence special movable guard plates are arranged direct behind the workpiece. The guards have to be movable as from the frontside of the machine the workpiece has to be loaded. A second measure that is related to the prevention against the bursting of a grinding wheel concerns the shape of the grinding wheel. It has been calculated [25] and measured [22] that a small inner diameter of the grinding wheel reduces the stresses in the grinding wheel caused by centrifugal forces. These stresses reach a minimum value if no central hole is applied. So it is decided to use grinding wheels as shown in figure 47 provided with a number of small holes arranged at a circle. The wheels are mounted by means

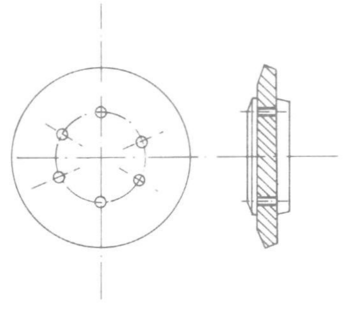

FIGURE 47.

Grinding wheel without central hole.

of a number of bolts that keep the flanges together as shown in the figure. It is obvious that a testprogram has to be carried out in order to investigate the measures that are taken with regard to the safety of the operator and the risk of damage of the machine.

11.2. Coolant-supply

A considerable part of the power supplied to the grinding process is transformed into heat. As the heat generation increases at high grinding speeds the problems related to an effective cooling are also increasing. One of the main problems at high circumferential speeds is the presence of an air film around the wheel which has to be penetrated before the coolant can be introduced into the grinding zone. Research on this subject [25, 26, 27] leads to the application of high pressure fluid delivery systems and scrapers that could remove the air layer. However, in consequence of the wheel wear these scrapers need to be adjusted frequently. For this reason an air nozzle is applied providing an air jet tangentially along the wheel circumference in a direction opposite to the wheel rotation as shown in figure 48. This system has proved to be satisfactory at high grinding

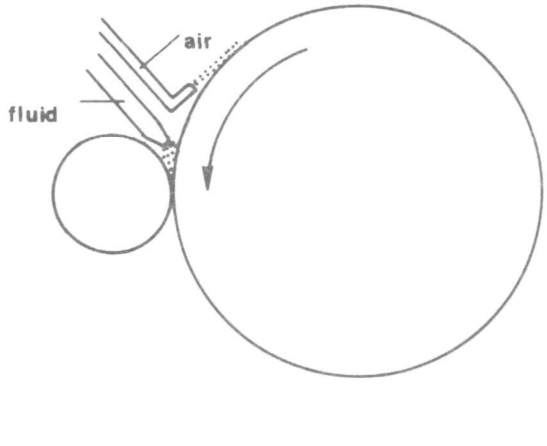

FIGURE 48.

Coolant supply to grinding zone.

speeds [27]. A second coolant supply is necessary at the dressing zone. In this case a scraper plate will be applied as this plate can be mounted to the dressing head and in this way follows the wheel circumference. A favourable aspect with regard to the cooling is the fact that at high metal removal rates a substantial part of the heat is removed by the chips as it has been investigated at the research concerning cut-off grinding at the University of Delft. It is obvious that an effective filtering of the grinding fluid is necessary in order to prevent strange particles entering the grinding zone.

12. THE DRAWINGS OF THE GRINDING MACHINE

The design of the grinding machine based on the considerations and the calculations in the preceding chapters is shown in a number of drawings.

Drawing A shows a section of the grinding spindle, including the bearings, the motor and the grinding wheel. The flow of oil and coolant to the bearings is shown schematically. The coupling between the motor and the spindle is a standard type, although a modification is applied.

Drawing B shows three views of the dressing apparatus with the stepping motor drive.

Drawing C shows a horizontal section of the wheel head. The wheel guard covers both the grinding wheel and the dressing wheel. The dressing unit is enclosed within a cover that is indicated by a -.-.- line.

Drawing D shows a front view of the wheel head. In order to show the design of the wheel head more clearly the wheel guard is left out partially. At the circumference of the wheel guard a part of this guard can be removed in order to mount the grinding wheel.

Drawing E shows a vertical section of both work heads. The driven work head is provided with a drive motor and an axial spindle bearing. The second work head is constructed in such a way that the oil that leaves the rear bearing is used to apply the axial clamping force to the workpiece.

Drawing F shows a cross section of the work heads and also the device that clamps the work head to the bed.

Drawing G shows the drives of the wheel head and the slide.

Drawing H shows the front view of the grinding machine. In this case the cover of the machine is indicated by a -.-.- line.

Drawing I shows the side view of the machine.

Drawing J shows the top view of the machine.

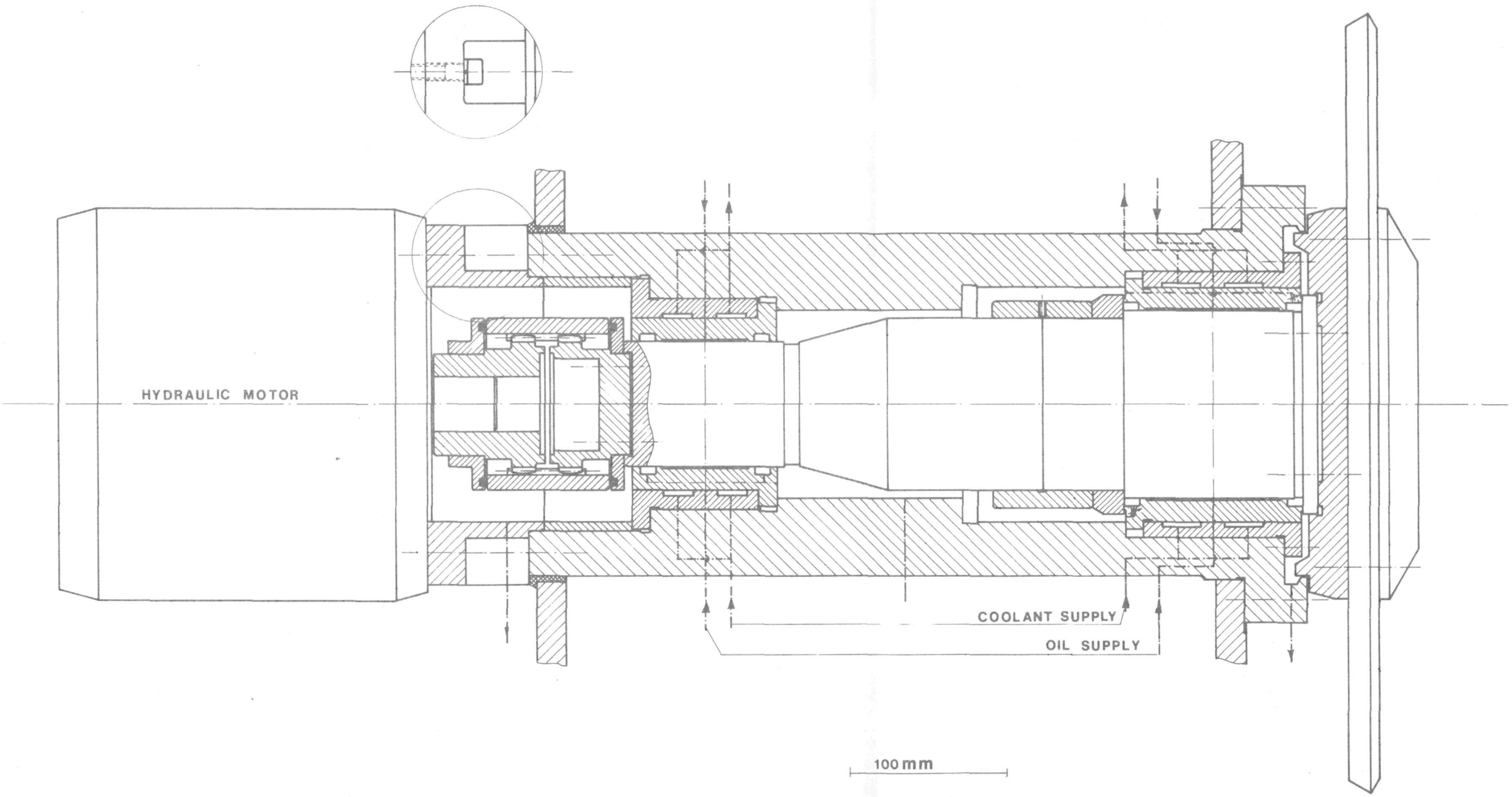

DRAWING A: Section of the grinding spindle.

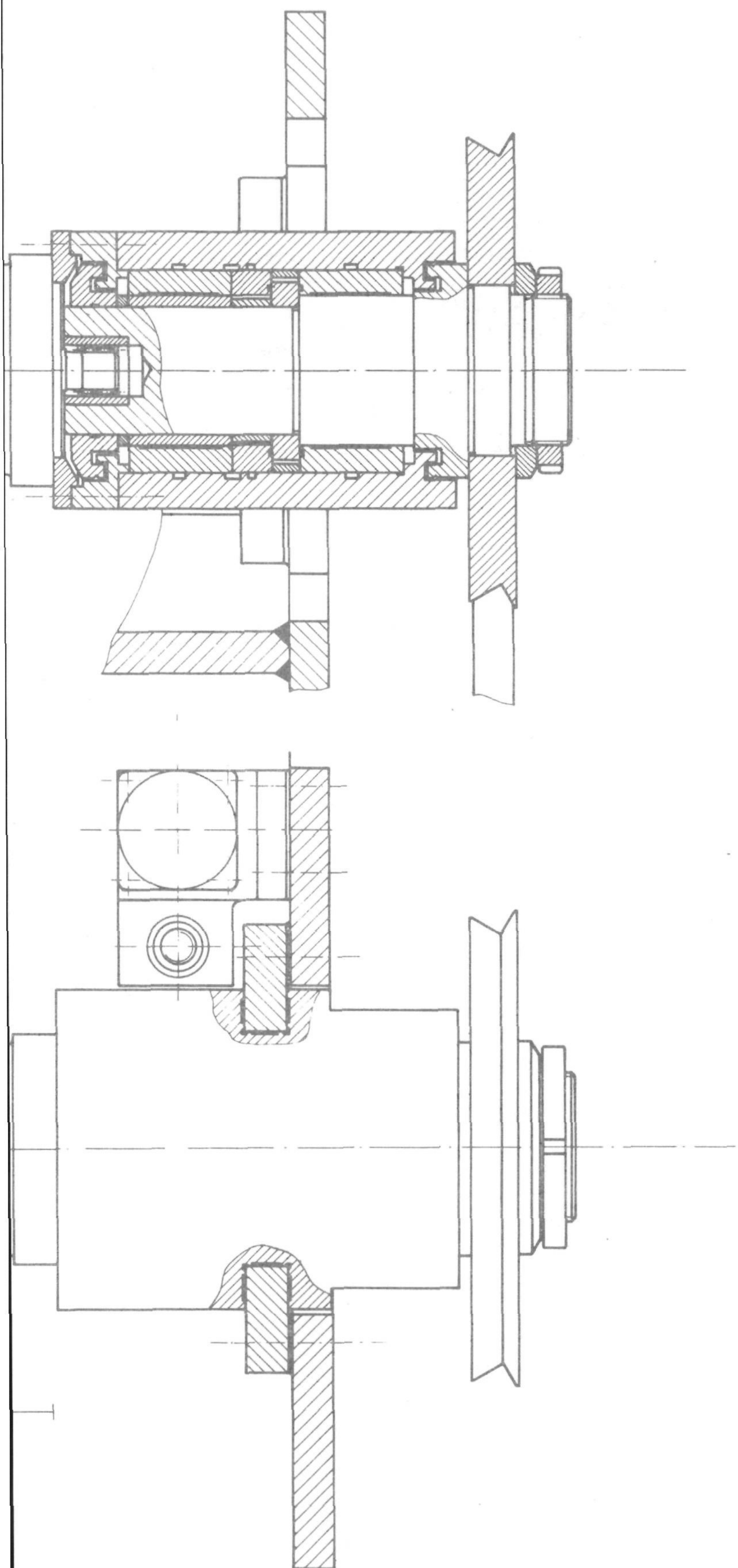

DRAWING B: The dressing apparatus.

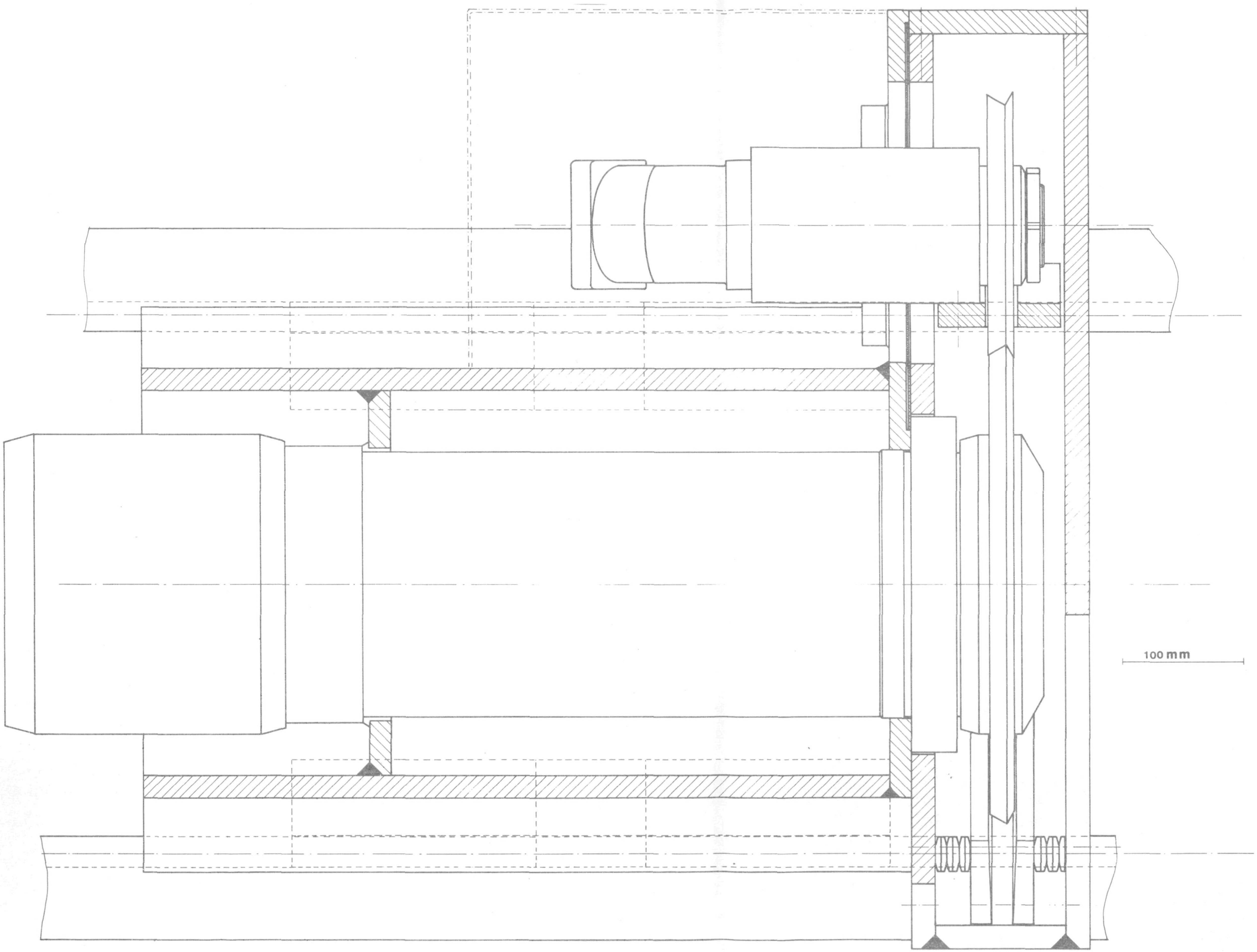

DRAWING C: Horizontal section of the wheel head.

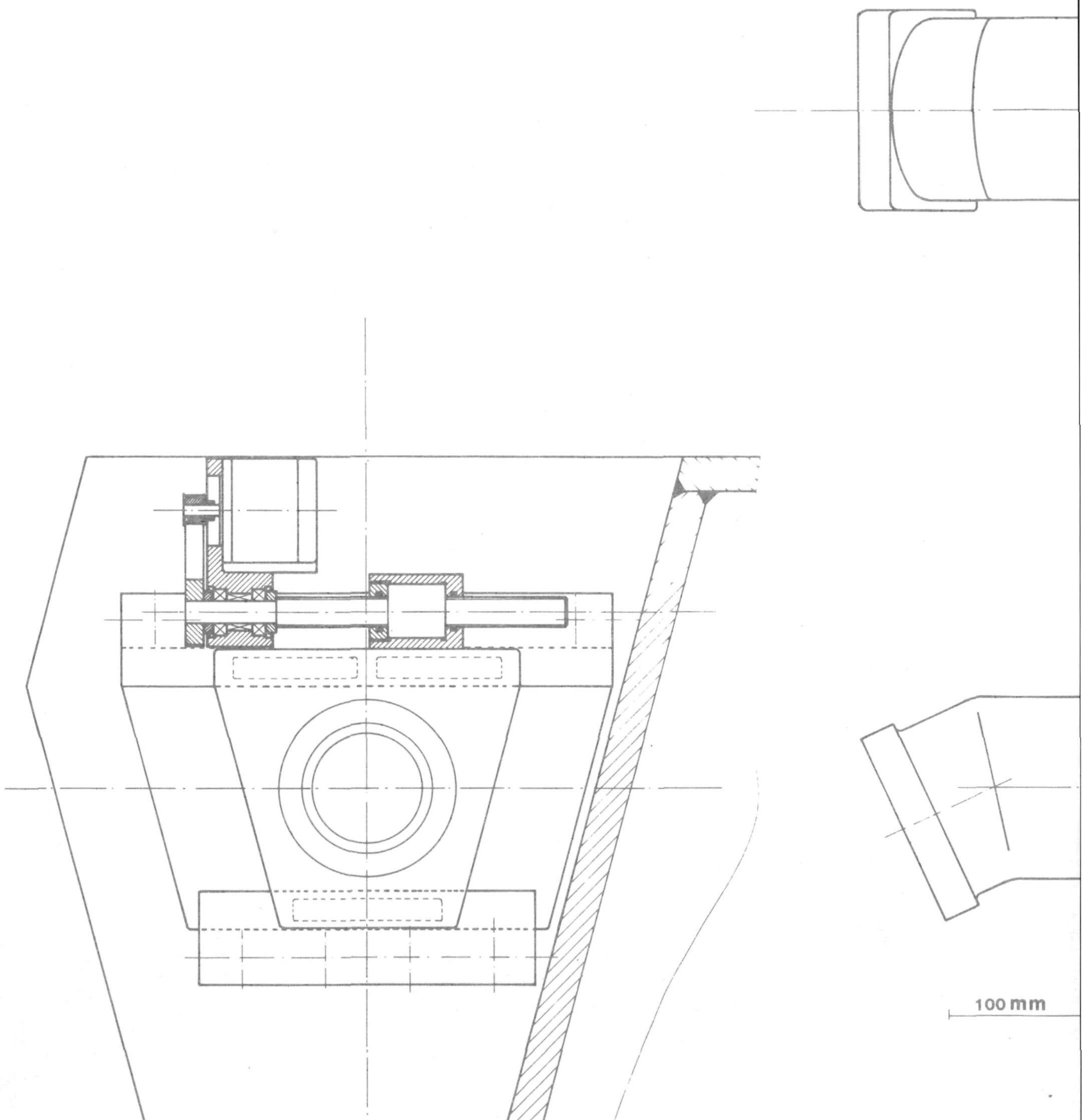
100 mm

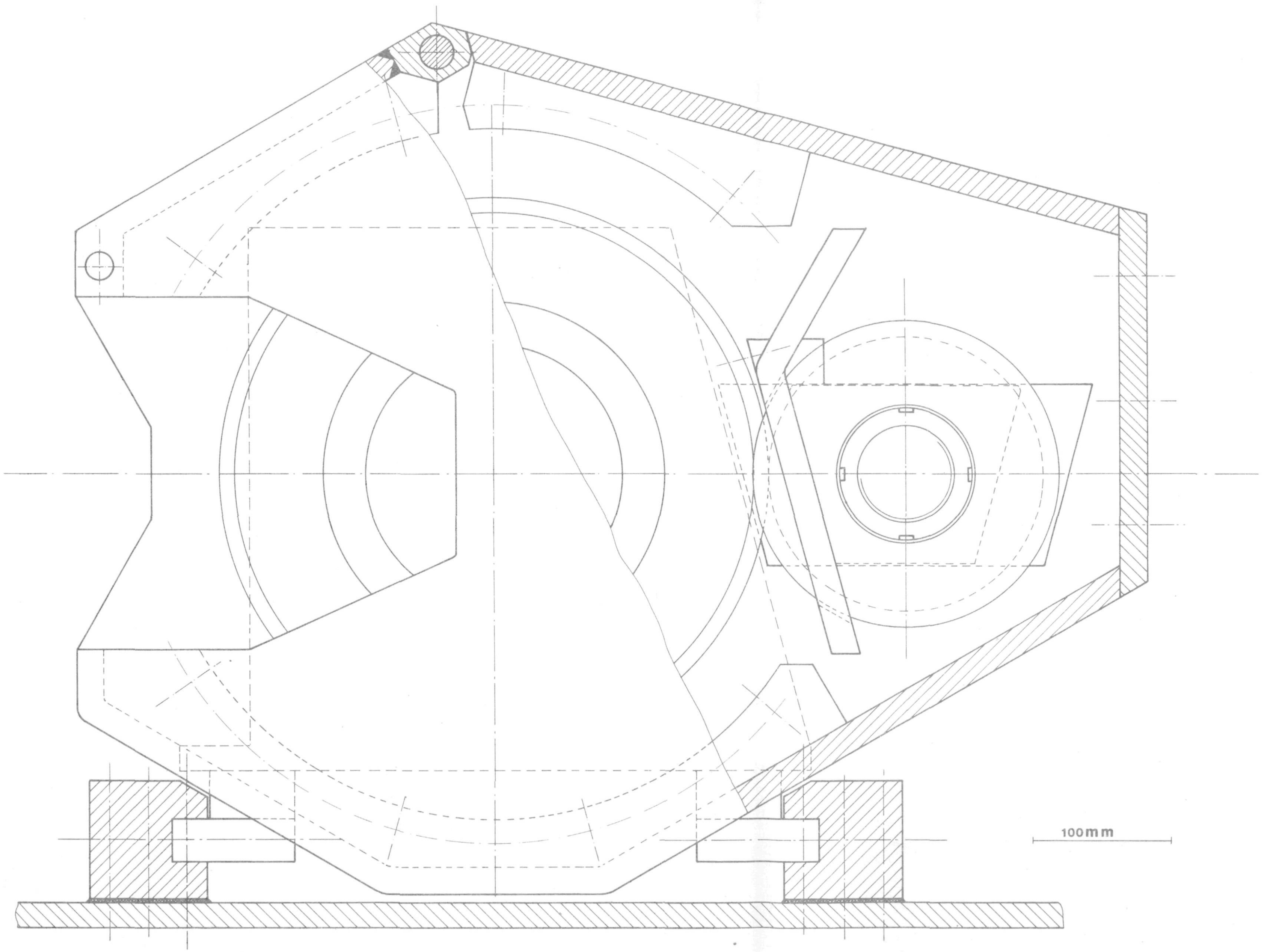

DRAWING D: *Front view of the wheel head.*

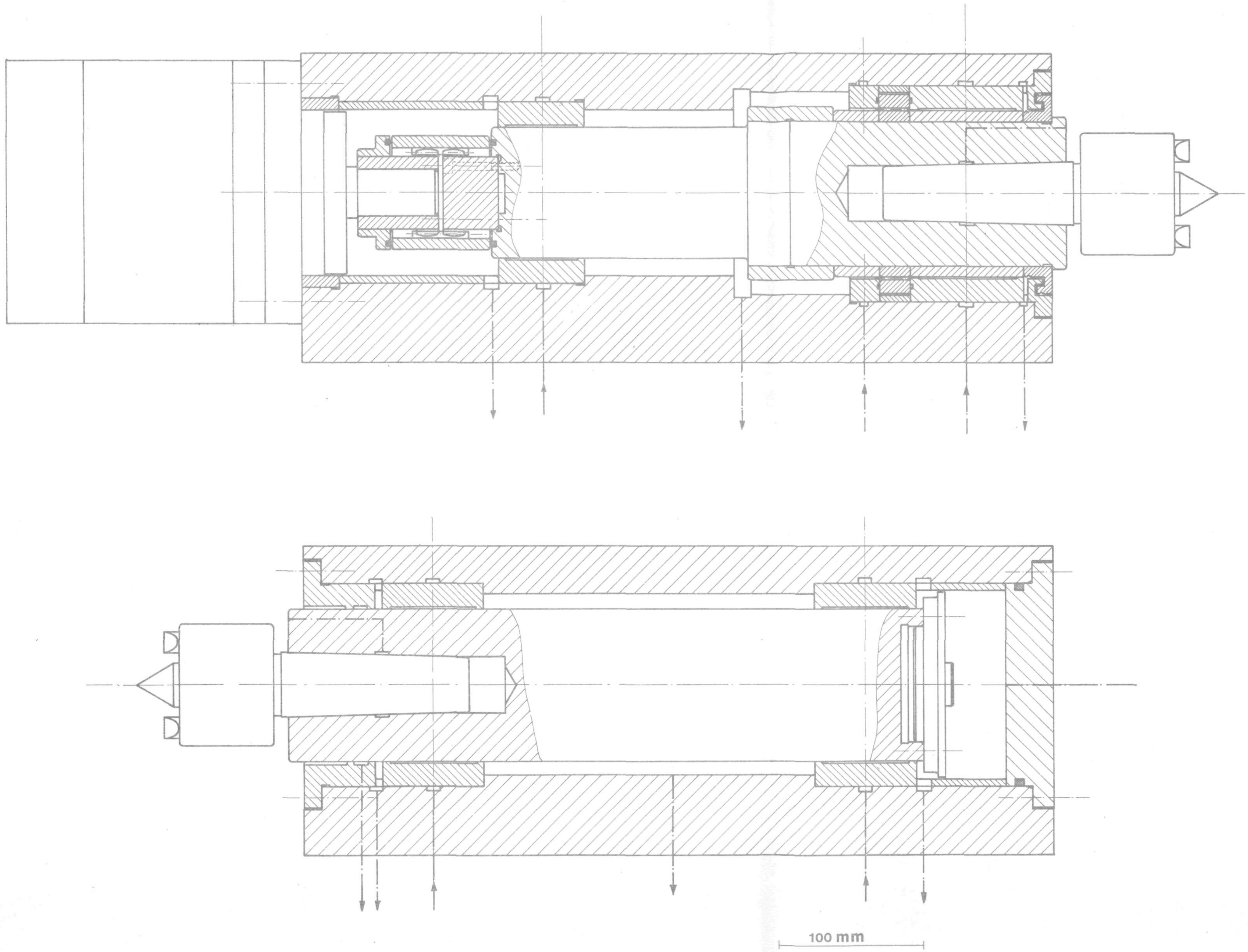

DRAWING E: Vertical section of the work heads.

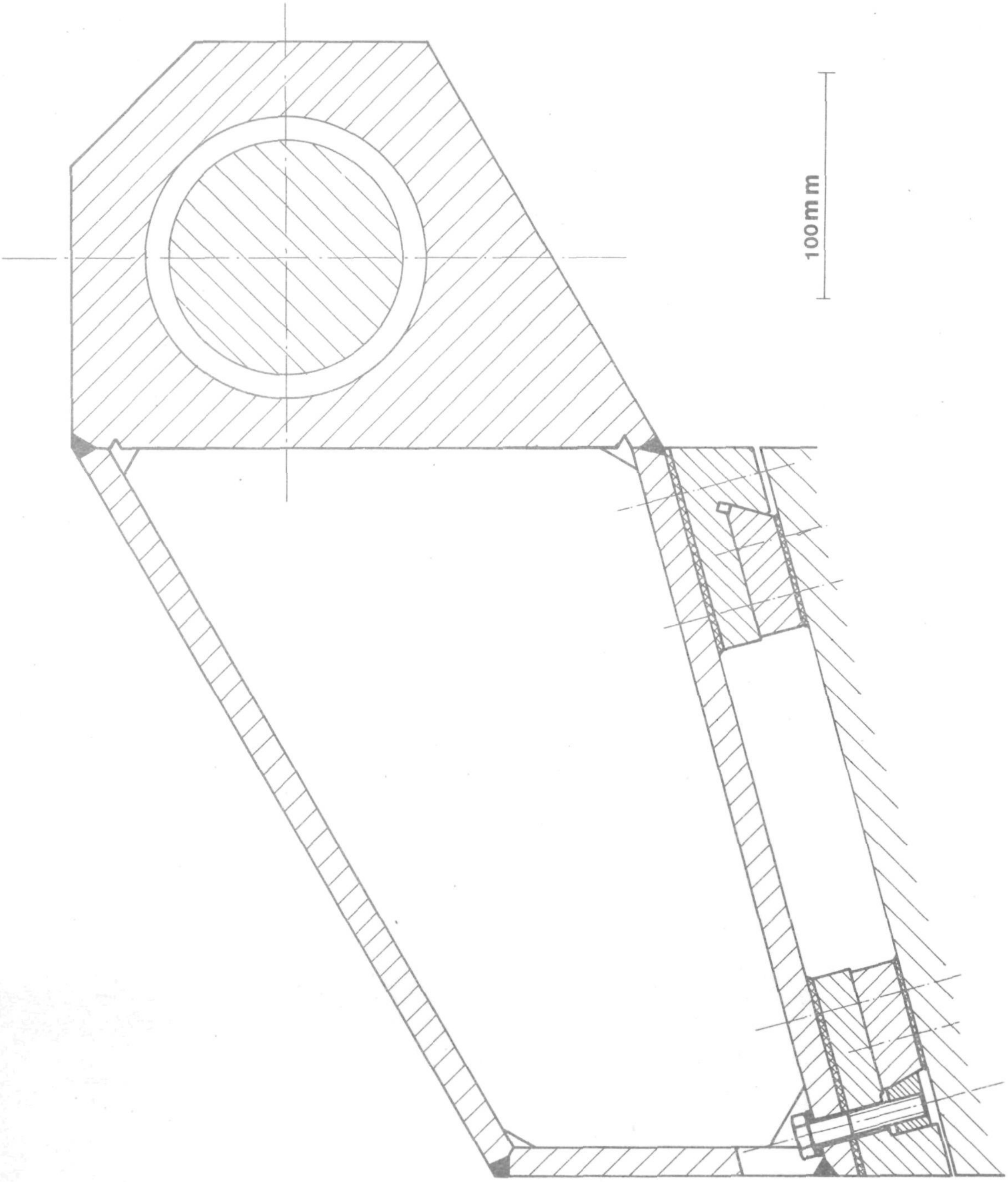

DRAWING F: Cross section of the work head.

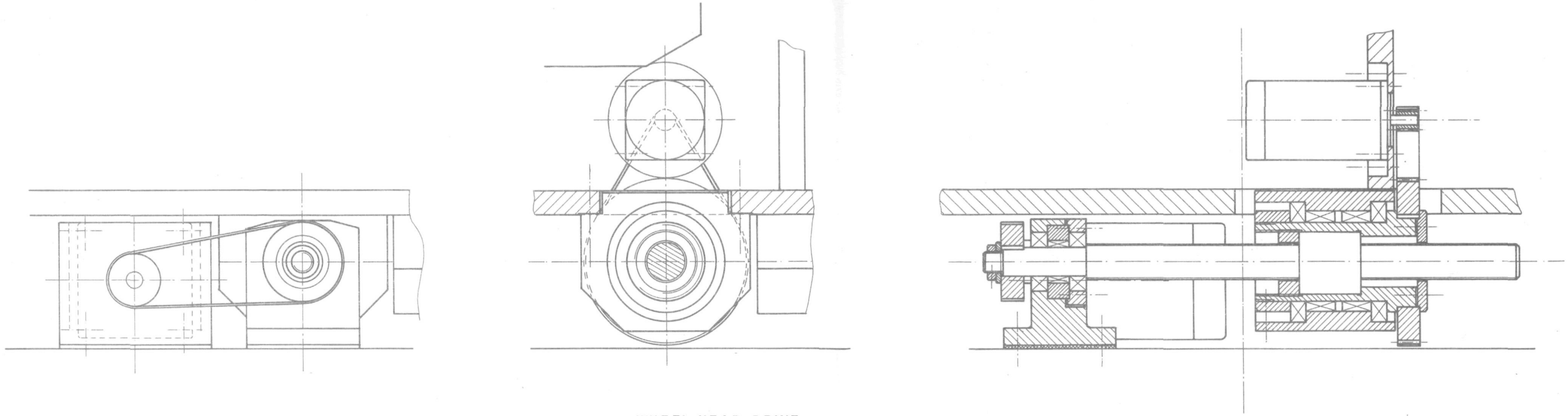

WHEEL HEAD DRIVE

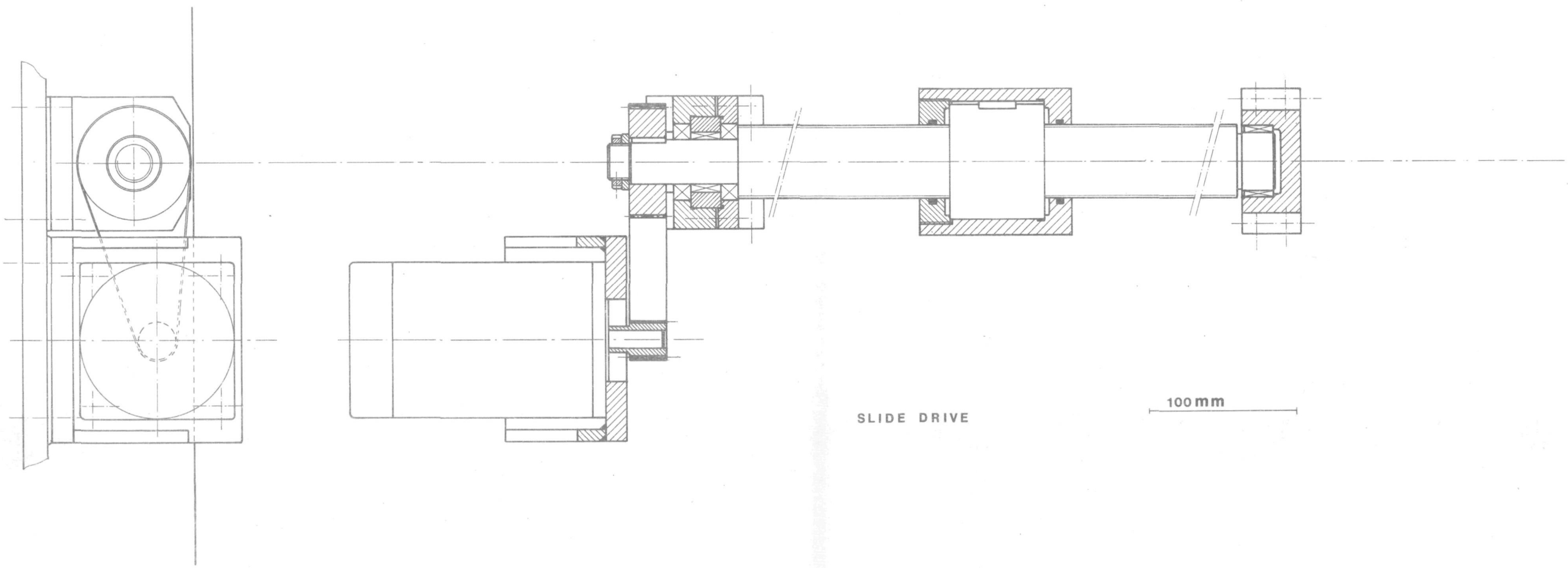

SLIDE DRIVE

DRAWING G: The drives of the wheel head and the slide.

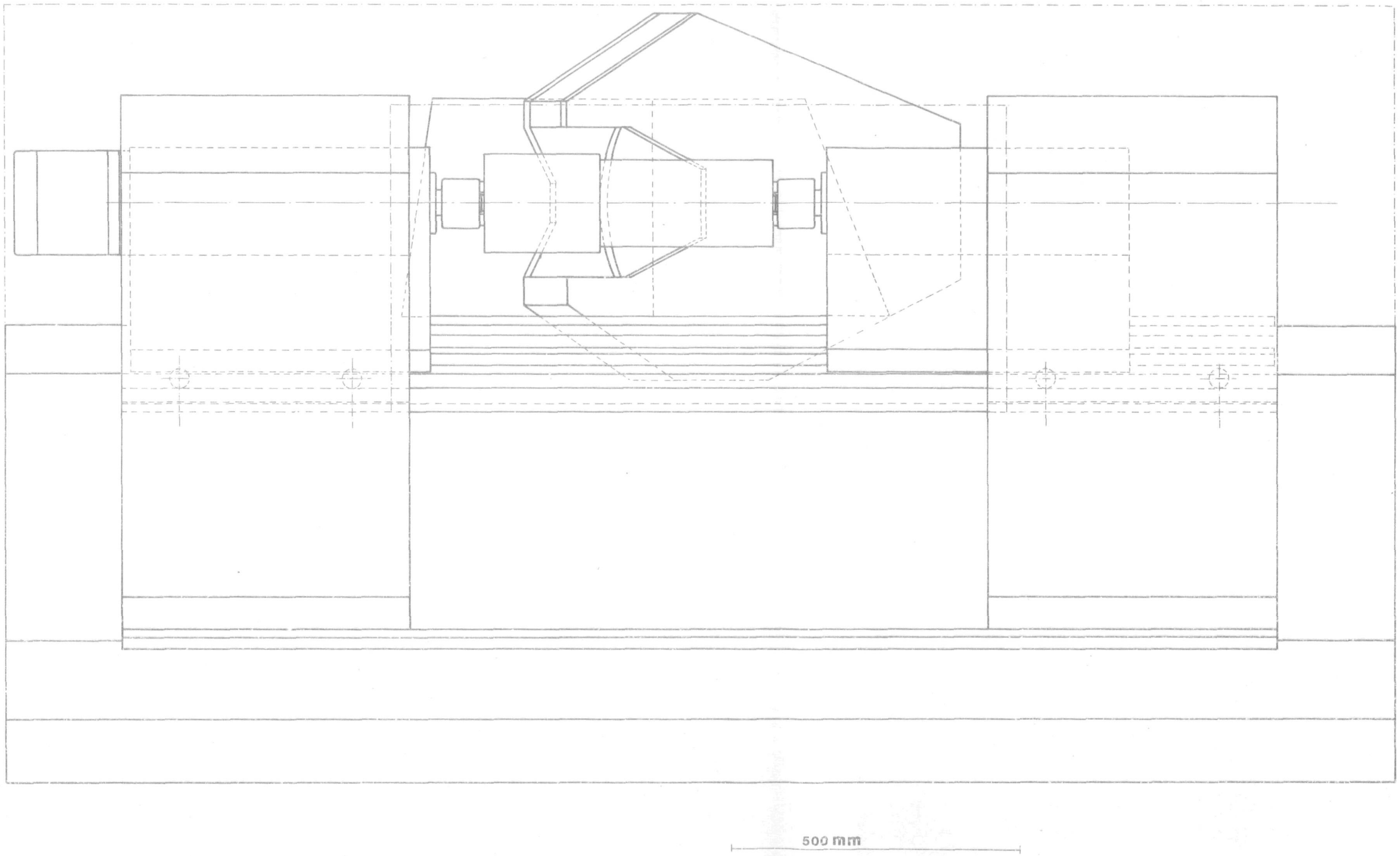

DRAWING H: Front view of the grinding machine.

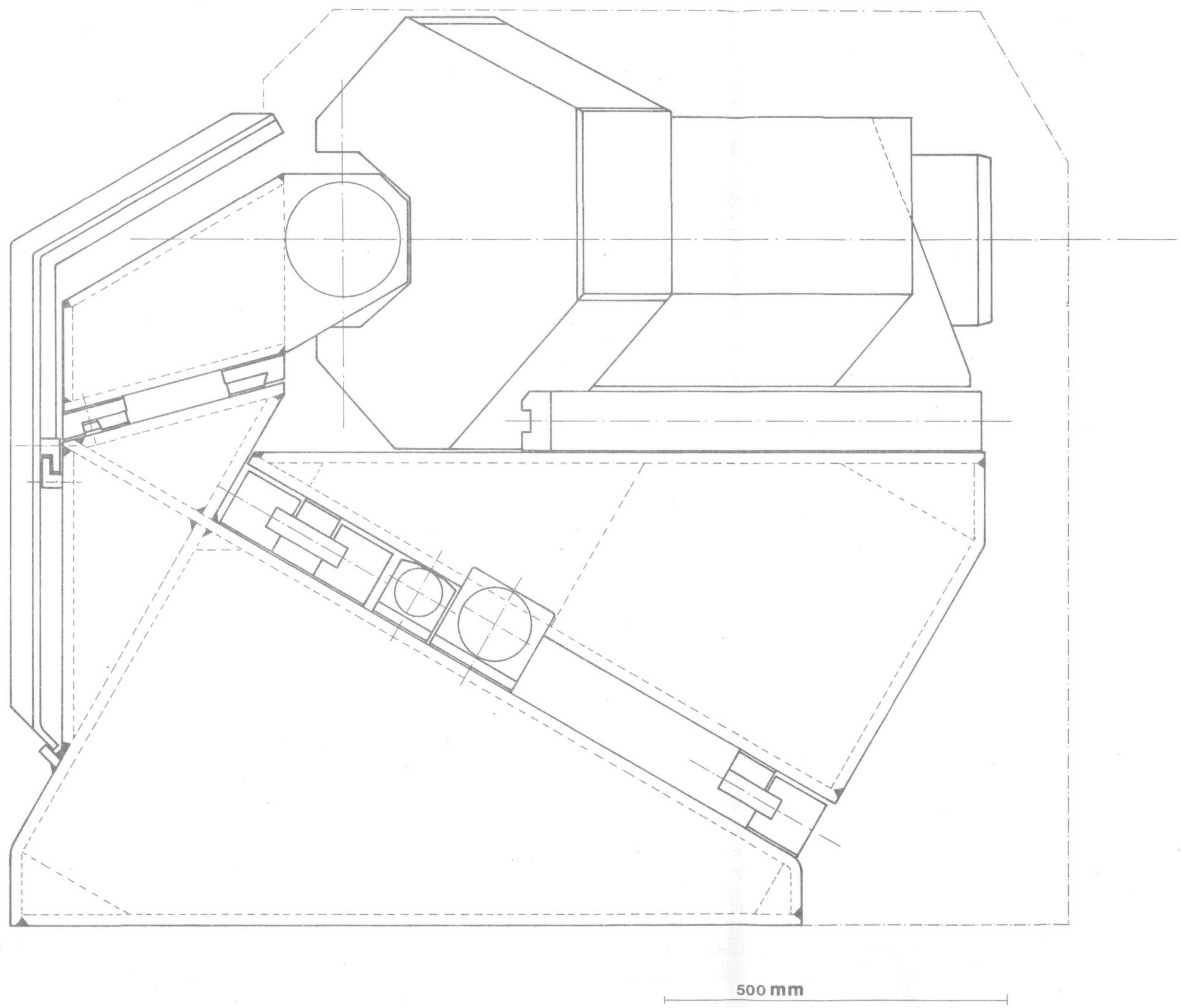

DRAWING I: Side view of the grinding machine.

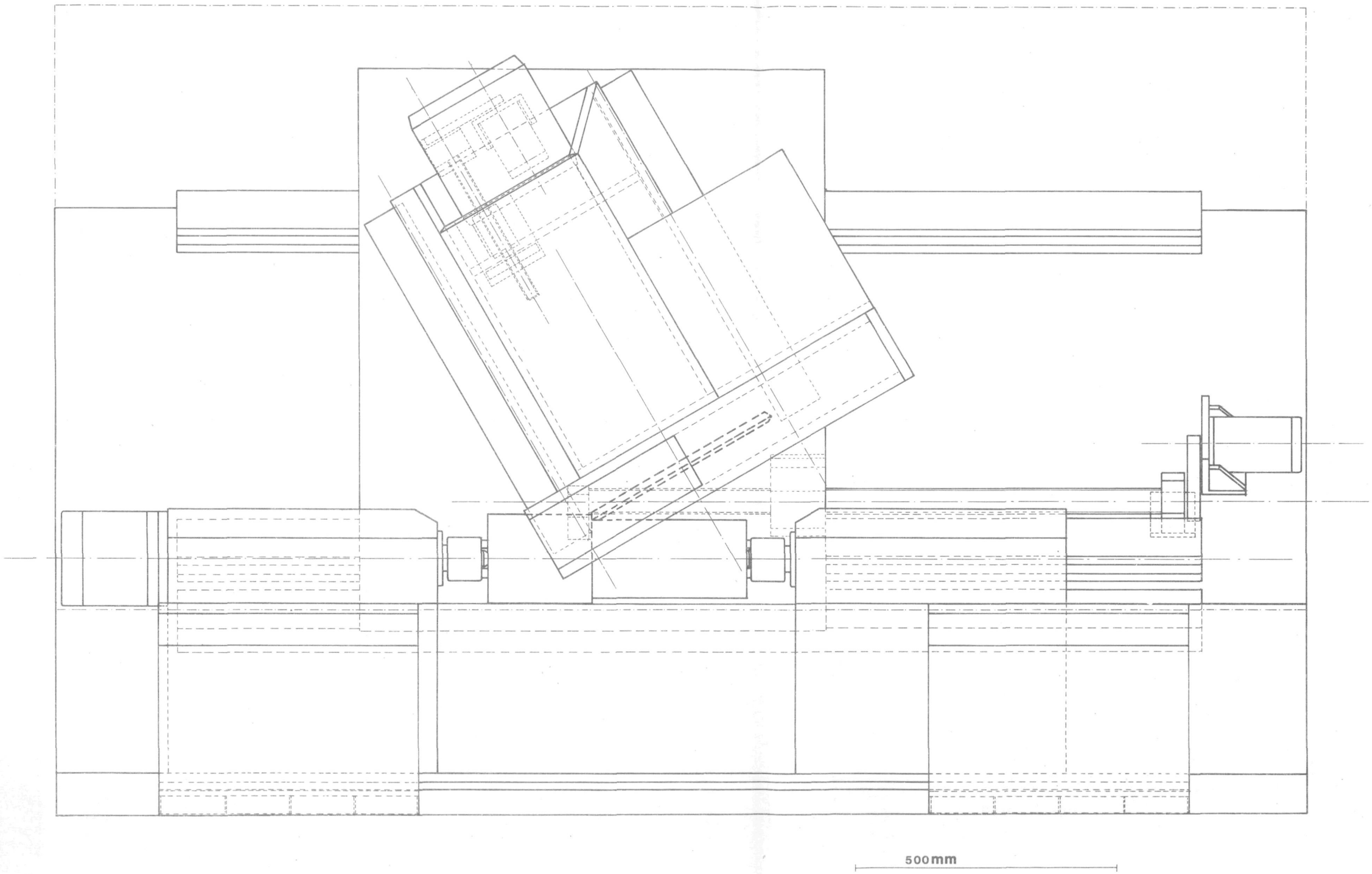

DRAWING J: Top view of the grinding machine.

13. CONCLUSION

In this thesis the main aspects of a design of a high speed cylindrical grinding machine are described. However, this design has to be regarded as a first step of the development of a grinding machine suited for industrial production.
In the first place a considerable part of the data concerning the grinding process and the dressing operation can only be determined by realizing these processes. These data will lead to a better understanding of the criteria for a final design. Secondly a study of the economics of the process has to be carried out. As it has been mentioned in the first chapter the design is based on a certain type of product. So it is necessary to know data concerning the various products of this type, the quantities of each product, the quantity of metal that has to be removed and so on. Based on these data and the data concerning the manufacture of the grinding machine a correct choice about the main dimensions and the power of the machine can be made.
The grinding machine, built according to the design described in this thesis, offers the possibility to study both the process itself and the economics of the process. This study may lead to a final design of a grinding machine that provides both a high metal removal rate and a high geometrical accuracy of the workpiece in one operation at reasonable cost.

Appendix

A. Deformation of the grinding spindle

The basis for the calculation of the dimensions of the grinding spindle and the stiffness of the spindle bearings is the deformation that is allowed with regard to the accuracy of the workpiece. In figure A.1 the forces applied to the grinding wheel and the grinding spindle are shown. As it has been considered in chapter 4.1 only the normal grinding force F_n is taken into account. This force causes the forces F_A and F_V in the bearings of the spindle. The values of these forces depend on the distance between the bearings b and the distance from the front bearing.

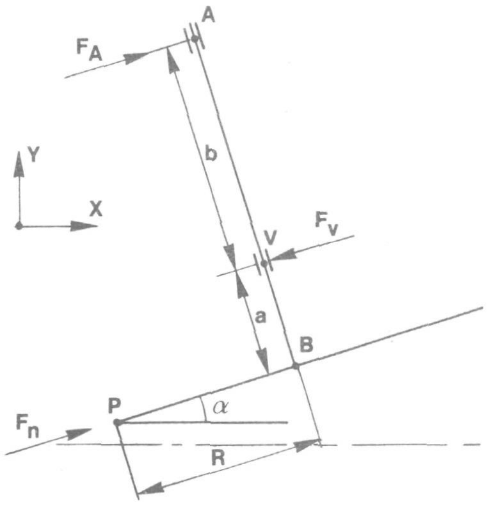

FIGURE A.1.

Grinding and bearing forces applied to the grinding spindle.

In figure A.2 the deformations of the grinding spindle and the spindle bearings are shown. These deformations result in a displacement of the point P of the grinding wheel in x-direction f_P^x and a displacement in y-direction f_P^y. From the demands concerning the accuracy of the workpiece it follows:

$f_P^x \leqslant 0.01$ mm and

$f_P^y \leqslant 0.005$ mm

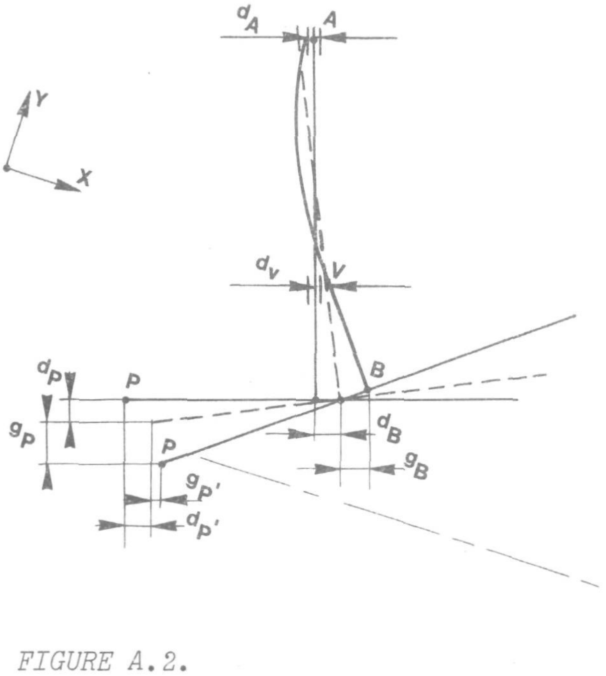

FIGURE A.2.

Deformation of the grinding spindle.

The displacement of P can be separated in two parts, one part represented by d_P and d_P', caused by the deformation of the bearings d_A and d_V and one part represented by g_P and g_P', caused by the deformation of the spindle. The deformation of the grinding wheel is not taken into account in the calculations. The value of d_P and d_P' can be calculated as follows:

The displacements at the bearings are:

$$d_A = \frac{F_A}{c_A} \text{ and } d_V = \frac{F_V}{c_V}$$

where c_A and c_V are the bearing stiffnesses. The linear displacement of the point B of the spindle:

$$d_B = (d_A + d_V) \cdot \frac{a + b}{b} - d_A$$

and the angular displacement in B:

$$\phi_B = \frac{d_A + d_V}{b}$$

So the displacements in x- and y-direction of the point P caused by deformations of the bearings are:

$$d_P{}^x = \frac{d_A + d_V}{b} \cdot R \cdot \sin\alpha + (\frac{a+b}{b} \cdot (d_V+d_A) - d_A) \cdot \cos\alpha \qquad (A.1.)$$

$$d_P{}^y = (\frac{a+b}{b} \cdot (d_V+d_A) - d_A) \cdot \sin\alpha - \frac{d_A + d_V}{b} \cdot R \cdot \cos\alpha \qquad (A.2.)$$

where R represents the radius of the grinding wheel and α the angle between the grinding spindle and the y-axis. The value of g_P, caused by the deformation of the spindle, is calculated as follows:
The linear displacement of the point B of the spindle:

$$g_B = \frac{F_A \cdot b^2 \cdot a}{3 \cdot E \cdot I} + \frac{F_n \cdot a^3}{3 \cdot E \cdot I}$$

and the angular displacement in B:

$$\phi^1{}_B = \frac{F_A \cdot b^2}{3 \cdot E \cdot I} + \frac{F_n \cdot a^2}{2 \cdot E \cdot I}$$

where E is the Young's modulus of the spindle material and I the moment of inertia of the spindle. The displacements in x- and y-direction of the point P, caused by deformation of the spindle, are:

$$g_P{}^x = (\frac{F_A \cdot b^2}{3 \cdot E \cdot I} + \frac{F_n \cdot a^2}{2 \cdot E \cdot I}) \cdot R \cdot \sin\alpha + (\frac{F_A \cdot b^2 \cdot a}{3 \cdot E \cdot I} + \frac{F_n \cdot a^3}{3 \cdot E \cdot I}) \cdot \cos\alpha \qquad (A.3.)$$

$$g_P{}^y = (\frac{F_A \cdot b^2 \cdot a}{3 \cdot E \cdot I} + \frac{F_n \cdot a^3}{3 \cdot E \cdot I}) \cdot \sin\alpha - (\frac{F_A \cdot b^2}{3 \cdot E \cdot I} + \frac{F_n \cdot a^2}{2 \cdot E \cdot I}) \cdot R \cdot \cos\alpha \qquad (A.4.)$$

From the equations A.1 to A.4 it follows:

$$f_P{}^x = F_n \cdot R\{\frac{a}{b^2 \cdot c_A} + (1+\frac{a}{b}) \cdot \frac{1}{b \cdot c_V} + \frac{a \cdot b}{3 \cdot E \cdot I} + \frac{a^2}{2 \cdot E \cdot I}\} \cdot \sin\alpha +$$

$$+ F_n \cdot \{\frac{a+b}{b} \cdot ((1+\frac{a}{b}) \cdot \frac{1}{c_V} + \frac{a}{b \cdot c_A}) - \frac{a}{b \cdot c_A} + \frac{a^2 \cdot b}{3 \cdot E \cdot I} + \frac{a^3}{3 \cdot E \cdot I}\} \cdot \cos\alpha$$

(A.5.)

$$f_P^{\,y} = F_n \cdot \{ \frac{a+b}{b} ((1+\frac{a}{b}) \cdot \frac{1}{c_V} + \frac{a}{b \cdot c_A}) - \frac{a}{b \cdot c_A} + \frac{a^2 \cdot b}{3 \cdot E \cdot I} + \frac{a^3}{3 \cdot E \cdot I} \} \cdot \sin\alpha +$$

$$- F_n \cdot R \cdot \{ \frac{a}{b^2 \cdot c_A} + (1+\frac{a}{b}) \cdot \frac{1}{b \cdot c_V} = \frac{a \cdot b}{3 \cdot E \cdot I} + \frac{a^2}{2 \cdot E \cdot I} \} \cdot \cos\alpha \qquad (A.6.)$$

The value of a is chosen as small as possible and equals 100 mm, while the demands concerning the accuracy of the workpiece are related to the maximum grinding forces, so F_n = 3000 N. By means of a computer program the optimum bearing distance b is calculated at different values of the spindle diameter D and the bearing stiffnesses c_A and c_V. Based on these calculations the following data are determined:

$$c_V = 150 \cdot 10^4 \text{ N/mm}$$

$$c_A = 75 \cdot 10^4 \text{ N/mm}$$

$$D = 120 \text{ mm}$$

$$b = 250 - 325 \text{ mm}$$

B. Calculation of the hydrostatic bearings

The grinding spindle is supported in two radial bearings and one axial bearing. As there is no load in axial direction the axial bearing only has to fix the position of the spindle. In the description of the control of the machine it is shown that the axial bearing is used as a measuring device for the detection of a load perpendicular to the plane of the grinding wheel. Consequently the demands for this bearing are related to this control system and will not be considered in this appendix. The design of the bearings is based on the following data:

stiffness of the front bearing	$c_V = 15 \cdot 10^8$ N/m
maximum load at the front bearing	$F_V = 4000$ N
stiffness of the rear bearing	$c_A = 7.5 \cdot 10^8$ N/m
maximum load at the rear bearing	$F_A = 1000$ N

The data concerning the stiffness of the bearings follow from the calculations of the spindle in the appendix A. From these calculations it also follows that the spindle diameter has to be at least 120 mm. As the influence of the diameter of the spindle at the rear bearing on the deformation of the spindle at the grinding wheel is very small, a smaller diameter of the spindle at the rear bearing can be chosen. One of the most important criteria for the bearings concerns the heat generation in the bearings. For this reason the oil-supply to the bearings will be realized with one pump for each bearing chamber. In figure B.1. the hydrostatic bearing is shown schematically. A system with four bearing chambers is chosen in order to reduce the influence of the direction of the load on the stiffness of the bearing that

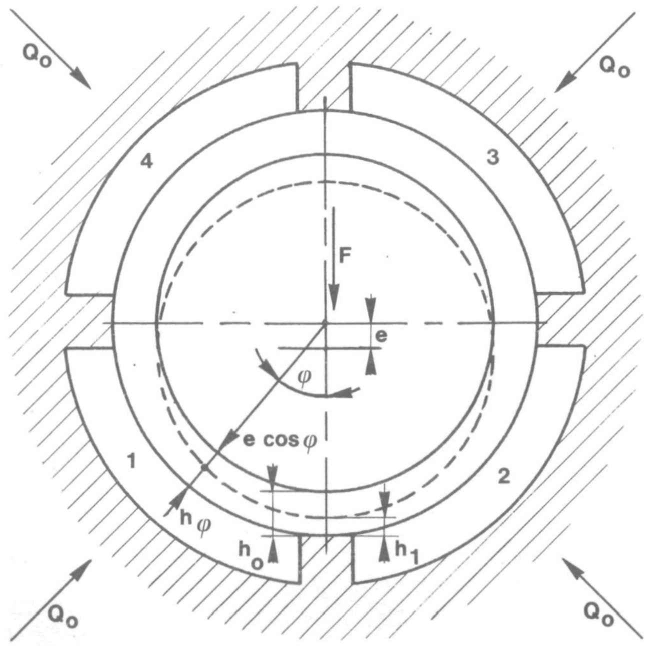

FIGURE B.1.

Schematic view of a hydrostatic bearing.

should appear at three chambers. On the other hand an increase of the number of chambers increases the friction in the bearings [28]. The calculations of the bearings are based on the following relation between the oil flow Q through a gap with a height h, a width b and a length l, caused by a pressure difference Δp:

$$Q = \frac{\Delta p \cdot h^3 \cdot b}{12 \cdot \eta \cdot 1} \qquad (B.1.)$$

where η is the viscosity of the oil. Besides the most unfavourable direction of the load is chosen, this means the direction towards the gap between two chambers. In each bearing chamber the oil flow that enters the bearing equals the flow that leaves the bearing. In chamber 1:

$$Q_0 = Q_1 + Q_{1-2} + Q_{2-4} \qquad (B.2.)$$

where Q_0 is the oil flow from the pump to the bearing chamber, Q_1 the oil flow that leaves the bearing chamber in axial direction and Q_{1-2} and Q_{1-4} the oil flows that leave the bearing chamber in tangential direction to the chambers 2 and 4. Because of the symmetry of the load $Q_{1-2} = 0$. According to the equation B.1.:

$$Q_1 = \frac{2 \cdot p_1}{12 \cdot \eta \cdot 1_a} \cdot \int_0^{\frac{\pi}{2}} \frac{D}{2} \cdot (h_o - e \cdot \cos\phi)^3 \cdot d\phi \qquad (B.3.)$$

where h_o is the height of the gap between the spindle and the bearing at a concentric position of the spindle, l_a the length of the bearing gap in axial direction, p_1 the pressure in chamber 1 and e the displacement of the spindle caused by a force F. From the equation B.3. it follows:

$$Q = \frac{p_1 \cdot D \cdot a}{12 \cdot \eta \cdot 1a} \qquad (B.4.)$$

with:

$$a = h_o^3 \cdot \frac{\pi}{2} - 3 \cdot h_o^2 \cdot e + 3\, h_o \cdot e^2 \cdot \frac{\pi}{4} - \frac{2}{3} \cdot e^3$$

As:

$$Q_{1-4} = \frac{(p_1 - p_4) \cdot L_e \cdot h_o^3}{12 \cdot \eta \cdot 1_t}$$

in which L_e is the length of the bearing and l_t the length of the gap that separates the chambers

$$Q_0 = \frac{p_1 \cdot D \cdot a}{12 \cdot \eta \cdot 1_a} + \frac{(p_1 - p_4) \cdot L_e \cdot h_o^3}{12 \cdot \eta \cdot 1_t} \qquad (B.5.)$$

In the same way:

$$Q_0 = \frac{p_4 \cdot D \cdot b}{12 \cdot \eta \cdot 1_a} + \frac{(p_1 - p_4) \cdot L_e \cdot h_o^3}{12 \cdot \eta \cdot 1_t} \qquad (B.6.)$$

with:

$$b = h_o^3 \cdot \frac{\pi}{2} + 3\, h_o^2 \cdot e + 3\, h_o \cdot e^2 \cdot \frac{\pi}{4} + \frac{2}{3} e^3$$

As the forces in the bearing have to be in equilibrium

$$F = (p_1 - p_4) \cdot D \cdot L_e \qquad (B.7.)$$

From the equations B.5., B.6. and B.7. it follows:

$$F\left(\frac{1}{L_e \cdot 12 \cdot \eta \cdot l_a} + \frac{h_o^3}{12 \cdot \eta \cdot l_t \cdot D} \cdot \frac{b+a}{a \cdot b}\right) = Q_0 \cdot \frac{b-a}{a \cdot b} \qquad \text{(B.8.)}$$

From this equation the relation between the force F and the displacement e can be calculated at various conditions both concerning the geometry of the bearing and the flow and the pressure of the oil.
The second requirement for the bearings concerns the heat generation in the bearings. This heat generation can be divided into two parts. One part concerns the energy dissipated as a result of the pressure drop in the bearing gaps. This power P_p, supplied by the pump, can be expressed by:

$$P_p = \frac{4 \cdot Q_0 - p_o}{\varepsilon} \qquad \text{(B.9.)}$$

in which p_o equals the average value of the pressures in the four bearing chambers and ε represents the efficiency of the pumps. According to the equation B.1.:

$$p = \frac{4 \cdot Q_0 \cdot 12 \cdot \eta \cdot l_a}{2 \cdot \pi \cdot D \cdot h_o^3}$$

and from this equation it follows:

$$P_p = \frac{24 \cdot \eta \cdot Q_0^2 \cdot l_a}{\pi \cdot D \cdot h_o^3 \cdot \varepsilon} \qquad \text{(B.10.)}$$

The second part of the heat generation is caused by the friction in the oil film in the gaps of the bearing. This power P_W can be expressed by:

$$P_W = F_W \cdot \eta \cdot \frac{V^2}{h_o} \qquad \text{(B.11.)}$$

In this equation F_W represents the area at which the friction appears and V the speed at the circumference of the spindle. The equation B.11 can be written as:

$$P_W = (2 \cdot \pi \cdot D \cdot l_a + 4 \cdot l_t\,(L_e - l_a)) \cdot \frac{\eta \cdot \omega^2 \cdot D^2}{4 \cdot h_o} \qquad \text{(B.12.)}$$

in which ω represents the speed of rotation of the spindle. The temperature rise ΔT of the oil from the inlet of the bearing to the outlet can be calculated from

$$\Delta T = \frac{P_p + P_W}{4 \cdot Q_0 \cdot \rho \cdot c_W} \qquad \text{(B.13.)}$$

in which ρ represents the density of the oil and c_W the specific heat of the oil.
The choice of the bearing parameters is based on the following considerations. At first the requirements concerning the stiffness of the bearing have to be met. This means that h_o has to be small while the values of D, l_a, L_c and l_t have to be large. On the other hand the requirements concerning the heat

generation lead to small values of D, l_a, L_e and l_t while h_o has to be large. Finally there are some limits like the minimum viscosity of the oil, the available pumpunits and the dimensions of the bearings with regard to the dimensions of the spindle. In order to find a compromise that results in a practical design a computerprogram has been drafted. Based on the results of the calculations according to this program the following data determine the front- and the rearbearing of the grinding spindle:

Frontbearing	Rearbearing
$Q_0 = 4.10^{-5}\ m^3/s$	$Q_0 = 3.10^{-5}\ m^3/s$
$h_o = 30.10^{-6}\ m$	$h_o = 30.10^{-6}\ m$
$l_a = 4.10^{-3}\ m$	$l_a = 4.10^{-3}\ m$
$l_t = 8.10^{-3}\ m$	$l_t = 8.10^{-3}\ m$
$L_e = 9.10^{-2}\ m$	$L_e = 6.10^{-2}\ m$
$D = 12.10^{-2}\ m$	$D = 8.10^{-2}\ m$
$\eta = 4{,}35.10^{-3}\ kg/m.s.$	$\eta = 4{,}35.10^{-3}\ kg/m.s.$

At these data and at a speed of 10.000 r.p.m. the following values of the stiffness, the pump pressure, the pump and friction power and the temperature rise of the oil are obtained:

Frontbearing	Rearbearing
$C_V = 1536.10^6\ N/m$	$C_A = 768.10^6\ N/m$
$p_o = 16.4\ .\ 10^5\ N/m^2$	$p_o = 18.5\ .\ 10^5\ N/m^2$
$P_p = 350\ W$	$P_p = 300\ W$
$P_w = 3300\ W$	$P_w = 850\ W$
$\Delta T = 13.8^o\ C$	$\Delta T = 5.8^o\ C$

C. Contact of the rotor circumferences

In chapter 5.1. it has been shown that the rotor circumferences do not touch each other mathematically. This means that the rotor circumferences have two lines in common. In figure C.1. this situation is shown. In this figure

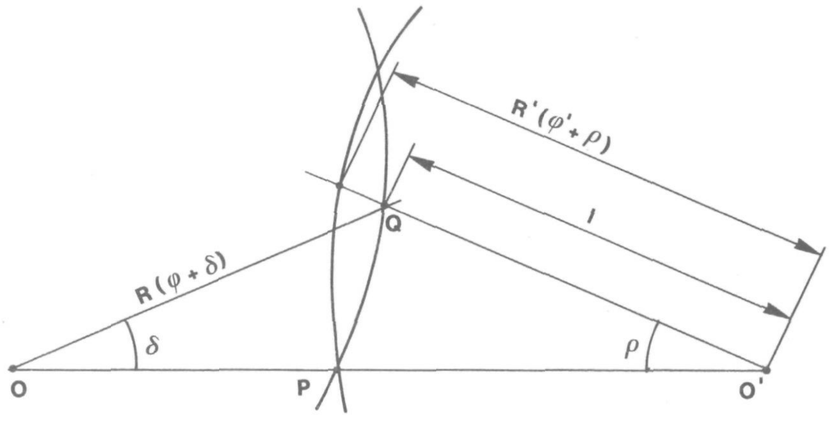

FIGURE C.1.

Relative position of the rotor circumferences.

the rotor circumferences have a point P at angles ϕ respectively ϕ' in common. If the rotor circumferences have a second point in common there must be an overlap of the two rotors in a point Q quite near the point P. In order to determine whether this overlap appears the following calculation is carried out. At a very small angle δ the value of $R(\phi + \delta)$ is calculated according to the equation 5.9 in chapter 5. From the value of $R(\phi + \delta)$ the value of the distance O'Q and the value of the angle ρ are calculated. The figure C.1. shows that an overlap of the rotor circumferences appears if the value of $R'(\phi' + \rho)$ exceeds the value of the distance O'Q. By means of a computer program these calculations are carried out at different values of the angles ϕ and ϕ' and for different values of δ. From these calculations it follows that the maximum width of the overlap, determined by the value of $x = R'(\phi + \rho) - 1$ does not exceed 0.0025 mm.

D. Leakage and mechanical losses in the hydraulic motor

D.1. Leakage

In the hydraulic motor leakage flows appear as a result of gaps between the rotors mutually and between the rotors and the housing. First the leakage at the place where the rotors touch each other will be calculated. The flow of oil through a gap is determined by the dimensions of this gap, the pressure drop from the inlet to the outlet of the gap and the viscosity of the oil. From the geometry of the rotors it follows that the gap between the rotor circumferences is identical with a gap between two cylinders with diameters that equal the average diameters of the rotors as far as the height of the gap is concerned. In figure D.1. this gap is

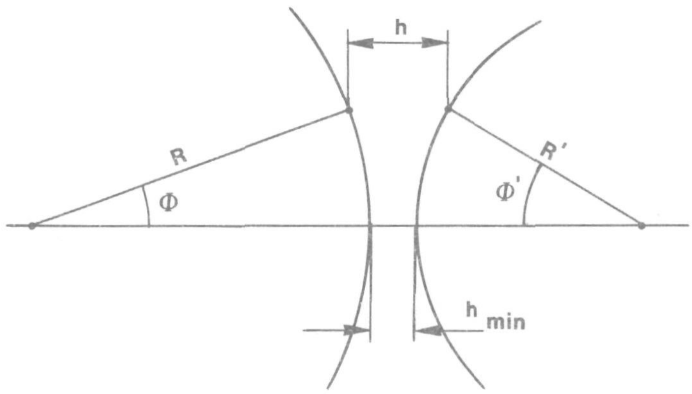

FIGURE D.1.

Gap between the rotor circumferences.

shown. According to this figure the value of the height of the gap h can be expressed by:

$$h = h_{min} + R \cdot (1 - \cos\phi) + R' \, (1 - \cos\phi') \qquad \text{D.1.}$$

As, according to the rotor geometry described in chapter 5, $2 \cdot \phi' = 3 \cdot \phi$ and $2 \cdot R = 3 \cdot R'$ the equation D.1. changes into:

$$h = h_{min} + R \cdot \left(\frac{5}{3} - \cos\phi - \frac{2}{3} \cdot \cos \frac{3 \cdot \phi}{2}\right) \qquad \text{D.2.}$$

It is assumed that the oil flow Q through the gap is determined by:

$$Q = \frac{h^3}{12 \cdot \eta} \cdot \frac{\delta p}{\delta \phi} - \omega \cdot R \cdot h \qquad \text{D.3.}$$

in which η represents the dynamic viscosity of the oil, p the pressure in the oil film and ω the angular velocity of the central rotor. The maximum value of Q appears at $\omega = 0$ and the maximum pressure drop from the start to the end of the gap $\Delta p = 350 \cdot 10^5$ N/m^2. From the equation D3 it follows:

$$Q = \frac{\Delta p}{12 \cdot \eta \cdot \int_{-\beta}^{+\beta} \frac{R}{h^3} \cdot d\phi} \qquad \text{D.4.}$$

in which the values $-\beta$ and $+\beta$ determine the values of ϕ at the start and the end of the gap. The solution of the equation D.4. is obtained by means of a computer program and leads to a leakage flow $Q = 2.95 \cdot 10^{-4}$ m^3/s per m width of the gap at a value of $h_{min} = 2.10^{-2}$mm and a viscosity of the oil $\eta = 0.087$ Ns/m^2. As the total width of the gap equals 0.144 m the leakage flow $Q_{L1} = 4.25 \cdot 10^{-5}$ m^3/s.
The second part of the leakage flow concerns the gap between the rotors and the housing. As the leakage at the rotor circumferences is relatively small, this part is neglected. The flow of oil Q_{L2} at the gaps between the side planes of the rotors and the housing is determined by the equation:

$$Q_{L2} = \frac{\Delta p \cdot b \cdot h^3}{12 \cdot \eta \cdot l} \qquad \text{D.5.}$$

In this equation b represents the width of the gap and l the length of the gap. As the average length of the gap is assumed to be 1.5 mm at a total width $b = 1.65$ m this part of the leakage flow $Q_{L2} = 5.76 \cdot 10^{-4}$ m^3/s at a gap height $h = 2.5 \cdot 10^{-2}$ mm, a viscosity of the oil $\eta = 0.087$ $N.s/m^2$ and at a pressure drop $\Delta p = 3.5 \cdot 10^7$ N/m^2. The choice of the values of h and l depends also on the heat generation in the oil film. The total leakage flow at maximum pressure $\underline{Q_L = 6 \cdot 18 \cdot 10^{-4} \ m^3/s.}$

D.2. Mechanical losses

The mechanical losses in the hydraulic motor concern the losses caused by friction in the bearings, the gear transmission and the oil films in the motor. The first two parts of the losses depend on a number of unknown factors like bearing pre-load, lubrication of the bearings and the gears, geometrical accuracy and so on. In this calculation only the friction losses in the oil films between the rotors and the housing are taken into account. As the friction losses at the circumferences of the rotors are very small if compared with the friction at the side planes of the rotors these losses are neglected. The power P_L generated in an oil film between the surfaces that move relative to each other can be determined by the following equation:

$$P_L = A_F \cdot \eta \cdot \frac{V^2}{h} \qquad \text{D.6.}$$

in which A_F represents the total area of the oil film and V the relative velocity of the two surfaces in question. From the dimensions of the rotors and the maximum speed of the rotors the value of P_L can be calculated. At the dimensions of the oil film mentioned in the first section of this appendix the friction power

$$\underline{P_L = 24.2 \text{ kW.}}$$

In the figure D.2. the total efficiency ε of the hydraulic motor as far as the losses calculated above are concerned is shown as a function of the speed of the motor n at maximum power.

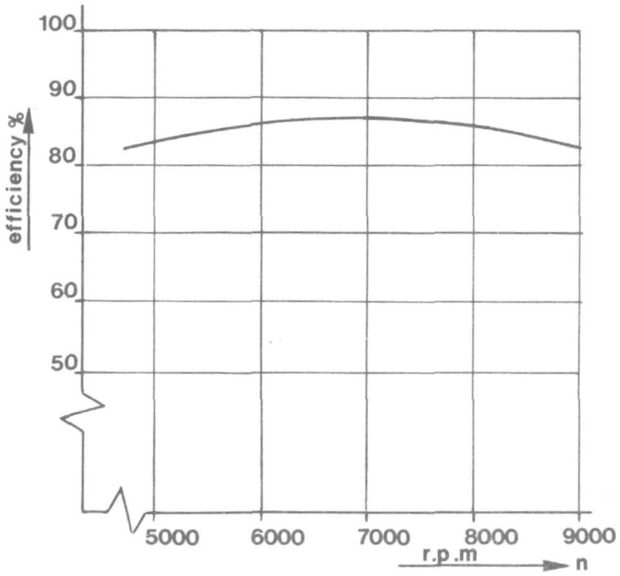

FIGURE D.2.

Efficiency of the hydraulic motor.

REFERENCES

[1] Ernst, W. — Erhöhte Schnittgeschwindigkeit beim Aussenrund-Einstechschleifen und ihr Einfluss auf das Schleifergebnis und die Wirtschaftlichkeit. Aachen, Dissertation T.H., 1965.

[2] Gühring, K. — Hochleistungsschleifen, eine Methode zur Leistungssteigerung der Schleifverfahren durch hohe Schnittgeschwindigkeit. Aachen, Dissertation T.H., 1967.

[3] Völler, R. — Sinnvolle Anwendung des Hochgeschwindigkeitsschleifens. Zeitschrift für industrielle Fertigung 64 (1974) no. 5, p. 259 - 264.

[4] Stewart, I.J. — Einfluss des Hochgeschwindigkeitsschleifens auf den Schleifvorgang. Fertigung 2 (1971) 2, p. 75 - 81.

[5] Shaw, M.C., Farmer, D.A. and Nakayama, A. — Mechanics of the abrasive cut-off operation. Paper no. 66-WA/Prod.-13 ASME, New York, 1966.

[6] Mueller, J.A. — Abrasive Machining - Cut off. ASTME paper MR 69 - 204.

[7] Storm, T. — Adaptive control in cut-off grinding. Proceedings of the 13th M.T.D.R.-Conference, Birmingham, 1970.

[8] What the future holds for grinding. Metalworking Production 118 (1974) p. 48 - 55.

[9] Research hots up to meet tomorrow's demands. Metalworking Production 118 (1974) p. 56 - 59.

[10] S.B. Baars — Doorslijpmachine. Internal report, University of Technology, section Machine tools, Delft, 1969.

[11] Rüggeberg, T. — High-speed and high-efficiency abrasive cutting. Proceedings of the International Grinding Conference, Pittsburg, Pennsylvania, april 1972, p. 524 - 537.

[12] Kaminskayia, V.V. Calculation and research on machine tool structures and foundations.
Proceedings of the 8th M.T.D.R.-Conference, Manchester, 1967.

[13] Paulsen, W.C. Finite Element Stress Analysis.
Machine Design 43 (1971),
nr. 24, p. 47 - 52
nr. 25, p. 146 - 150
nr. 26, p. 90 - 94.

[14] ASKA - User's Reference Manual.
I.S.D.-report nr. 73
Stuttgart, 1971.

[15] Pahlitzsch, G and Schmitt, R. Einfluss des Abrichtens mit diamantbestückten Rollen auf die Feingestalt der Schleifscheiben-Schneidfläche.
Werkstattstechnik, 58 (1968) nr. 1, p. 1 - 8.

[16] Pahlitzsch, G. and Schmitt, R. Wirkung von Korngrösse und -Konzentration beim Abrichten von Schleifscheiben mit diamantbestückten Rollen.
Werkstattstechnik, 59 (1969) nr. 4, p. 158 - 161.

[17] Klemm, W. Untersuchungsergebnisse bei der Anwendung von Diamant-Abrichtrollen.
Fertigungstechnik und Betrieb
19 (1969) nr. 11, p. 669 - 675.

[18] Scheidemann, H. Einfluss der durch Abrichten mit zylindrischen und profilierten Diamantrollen erzeugten Schleifscheiben-Schneidfläche auf den Schleifvorgang.
Braunschweig, Dissertation, T.U., 1973.

[19] Frank, H. Das Abrichten von Schleifscheiben mit Diamanten und der Einfluss auf das Schleifergebnis beim Aussenrund-Einstechschleifen.
Aachen, Dissertation, T.H., 1967.

[20] Schreitmüller, H.J. and Dederichs, M. Pneumatisches Messverfahren zur Ermittlung des Schleifscheibenverschleisses.
Industrie-Anzeiger 93 (1971)
nr. 68 p. 1733 - 1734.

[21] Opitz, H. and Langbein, R. Untersuchungen an Schutzhauben für Hochgeschwindigkeitsschleifmaschinen.
Industrie-Anzeiger 95 (1973)
nr. 17, p. 328 - 331.

[22] Krug, H. and Schoor, N. — Beeinflussung der Bruchgeschwindigkeit umlaufender Schleifscheiben durch die axialen Einspannkräfte.
Industrie-Anzeiger 96 (1976)
nr. 65, p. 1463 - 1467.

[23] Suzuki, I. and Wada, R. — Schleifscheibenbruch während der Rotation.
Werkstatt und Betrieb 105 (1072)
nr. 9, p. 643 - 647.

[24] Safety in High Speed Grinding.
Publication nr. M3071E of Cincinnati-Milacron, England.

[25] Frank, H. — Hochgeschwindigkeitsschleifen, Werkstückgüte und Zerspanleistung.
Publication of Guilleaume-Werk, Bonn-Beuel.

[26] Kortendieck, W. — Merkmale beim Schleifen mit erhöhter Umfangsgeschwindigkeit.
Werkstatt und Betrieb 104 (1971)
nr. 3, p. 157 - 163.

[27] Grinding fluids can break the air barrier.
Metalworking Production 118 (1974) nr. 1
p. 68 - 73.

[28] Opitz, H. — Aufbau und Auslegung hydrostatischer Lager und Führungen und konstruktive Gesichtspunkte bei der Gestaltung von Spindellagerungen mit Wälzlagern.
Bericht über die VDW-Konstrukteur-Arbeitstagung am 21. und 22. Februar 1969.

CURRICULUM VITAE

14 october 1939	born in Bennekom.
1951 - 1956	Marnix College, Ede.
1956	diploma H.B.S.-b.
1956 - 1964	University of Technology, Delft, mechanical engineering.
1964	diploma werktuigkundig ingenieur.
1964 up to the present	member of the scientific staff of the University of Technology, Delft.

STELLINGEN

1. Bij het vervaardigen van produkten dient aan spaanloze bewerkingen zoveel mogelijk de voorkeur te worden gegeven boven verspanende bewerkingen.

2. De losse kop van draai- en slijpmachines dient het werkstuk even nauwkeurig te ondersteunen als de vaste kop.

3. Een weloverwogen materiaalkeuze zal het gebruik van staal en gietijzer doen afnemen.

4. Alleen het onderzoek naar de toepasbaarheid van numerieke besturing kan reeds tot een aanzienlijke produktieverbetering leiden.

5. Het onderwerpen van de z.g. "contacten met derden" aan strenge normen zal de afstand tussen de Technische Hogescholen en het bedrijfsleven vergroten.

6. De benaming "sportief pookje" bij auto's is een verzachtende uitdrukking voor een minder goede oplossing van een aandrijfprobleem.

7. Evenmin als een onderneming bij het vertrek van een direkteur de produktie stopt of afremt dient het vertrek van een hoogleraar aanleiding te zijn het betreffende onderwijs te onderbreken.

T. Storm
Delft, 10 juni 1976